Kristin Roseth Aass

IL-32 and Multiple Myeloma Bone Disease

Master´s Thesis in Molecular Medicine,

Trondheim, November 2016

Supervisors: Therese Standal and Siv Helen Moen

Norwegian University of Science and Technology,

Faculty of Medicine

Department of Cancer Research and Molecular Medicine (IKM)

NTNU

Norwegian University of
Science and Technology

Abstract

Multiple myeloma is a malignancy of plasma cells characterized by multiple tumors in the bone marrow and progressive osteolytic bone disease. The bone lesions are caused by increased bone resorption by osteoclasts and decreased bone formation by osteoblasts. Recently, we found that myeloma cells obtained from bone marrow plasma had high copy number of IL-32, a novel interleukin that has not previously been related to multiple myeloma. Further investigation revealed that IL-32 was secreted by the myeloma cells bound to exosomes, indicating that the interleukin could influence the bone marrow microenvironment. Preliminary results from the group showed that rhIL-32 and even more potently, IL-32 in myeloma-derived exosomes, increased osteoclastogenesis, both *in vitro* and *in vivo*. Here, these findings were validated by treating primary monocytes with exosomes derived from IL-32 expressing- and IL-32 KO myeloma cells. Strikingly, number of osteoclasts in cultures was increased by treatment with IL-32-containing exosomes, while IL-32 depleted exosomes did not increase osteoclastogenesis, which support that IL-32 may act as an inducer of osteoclast differentiation. The influence of IL-32 on osteoblasts was not previously studied, and therefore addressed in this thesis. We evaluated the effects of IL-32 on osteoblast differentiation from primary mesenchymal stromal/stem cells (MSCs). Our results indicate that IL-32 alone has no effect on osteoblast differentiation or proliferation. IL-32 has previously been shown to upregulate CYP27B1[1], the enzyme that catalyze conversion of pro- to active vitamin D. We therefore hypothesized that IL-32 could influence osteoblasts by increasing CYP27B1 and thereby activate vitamin D-dependent signaling pathways in the cells. However, we found no clear evidence for effects of IL-32 in the presence of the pro form of vitamin D ($25(OH)D_3$), evaluated by extent of various parameters of osteogenic differentiation. There was a tendency for increased biosynthesis of the active form of vitamin D, $1,25(OH)_2D_3$ in response to IL-32, but an optimized protocol is needed to conclude on this matter. Furthermore, CYP27B1 mRNA was not upregulated in response to IL-32, but the mRNA detection levels were low, suggesting that CYP27B1 expression should be evaluated by other means. Finally, as our preliminary results showed that IL-32 is upregulated in myeloma cells in response to hypoxic conditions, we investigated the effects of hypoxia on MSCs. Interestingly, these cells were found to express IL-32, and the expression is increased by hypoxia and by stimulation with IL-32 itself, the latter suggesting an positive feedback loop between myeloma cells and MSCs in the bone marrow. Taken together, these findings

contribute to an increased understanding of the role of IL-32 in multiple myeloma bone disease. However, more research is required to conclude on the role of IL-32 in osteoblasts and MSCs, as well as determining the cellular mechanisms behind IL-32 promoted osteoclastogenesis.

Acknowledgement

This master's thesis was conducted at the Cancer-induced Bone Disease group at Centre of Molecular Inflammation Research (CEMIR) and Center for Myeloma Research, Department of Cancer Research and Molecular Medicine at the Norwegian University of Science and Technology.

First and foremost, I would like to thank my supervisor Therese Standal for the guidance, teaching and encouragement during the work of my thesis. She has in an extraordinary way included me in the research group and their projects, and introduced me to scientific thinking as well as improving my understanding of scientific processes.

I would like to thank my co-supervisor Siv Helen Moen for great help during the laboratory work. As I started in the lab relatively inexperienced, she has dedicated a lot of time demonstrating everything from pipetting to advanced experimental methods. I also want to thank her for the care and patience she has shown, the feedback when planning new experiments, and advices whenever I experienced problems.

Also, I would like to thank the post-docs at our group, Marita Westhrin and Muhammad Zahoor for answering all my questions, and kindly including me as part of the group. I am also grateful for the patience, help and advice from the senior engineers at our lab; Berit, Hanne and Glenn, their warm personalities, and for making the laboratory a nice place to work.

I would like to thank my family, which always have been a mainstay for me, and my friends, including my sister Ingrid, for making my life so meaningful and bright. Last, but not least I will thank my boyfriend and best friend, Robin, for his support and love. He has as a cancer researcher himself been a great inspiration for me, as well as a valuable helper and discussion partner during my master study.

Table of contents

Abstract 3

Acknowledgement 5

Abbreviations 11

Introduction 13

Multiple myeloma prevalence and diagnosis 13

B-cell transformation and disease progress 13

Treatment strategies 14

Genetics of multiple myeloma 15

Multiple myeloma and the microenvironment 17

Bone and bone remodeling 18

Osteoblasts 19

Osteoclasts 20

The bone disease of multiple myeloma 22

Treatment of myeloma bone disease 24

Interleukin 32 25

IL-32 in disease 26

Effect of IL-32 on bone cells 26

IL-32 in multiple myeloma 27

Vitamin D 29

Vitamin D and bone formation 30

Aims and hypotheses 33

Material and methods 35

Primary cells and cell lines 35

Culture conditions 35

Determining the effect of IL-32-containing exosomes on osteoclasts 36

Osteoclast isolation and differentiation 36

The principle of TRAP-staining 37

Determining the effect of IL-32-containing exosomes on osteoblasts 38

Gene knock-out by CRISPR/Cas 38

Principle of exosome isolation 38

Procedure for exosome isolation 39

Validate IL-32 knockout in JJN-3 clones by Western Blot 39

The principle of Western Blot 39
Reagents used in Western Blot 40
Procedure for Western Blot 41
Evaluate effects of rhIL-32 on mRNA gene expression in osteoblasts and MSCs by RT-qPCR 42
Quantitative Real Time- PCR 42
The principle of RNA isolation 43
Procedure for RNA-isolation 44
The principle of cDNA synthesis 44
The principle of Taqman assay 45
Procedure for TaqMan qPCR 47
Evaluate IL-32 effects on early osteoblast differentiation by measuring the activity of alkaline phosphatase (ALP) 48
Principle of ALP-assay 48
Procedure for ALP-assay 49
Evaluate IL-32 effecs on osteoblast proliferation using the CellTiter-Glo assay 50
Principle of CellTiter-Glo assay 50
Procedure for CTG-assay 51
Evaluate rhIL-32 effects on osteoblast mineralization by Alizarin Red-S Staining 51
The principle of Alizarin Red S-staining 51
Reagents used in ARS-staining 51
Procedure for ARS-staining 52
Evaluate the effect of IL-32 on CYP27B1-activity 52
The principle of ELISA 53
Statistics 55
Results 57
Part 1 57
Effect of IL-32-containing exosomes on osteoclast differentiation 57
Part 2 59
Effect of rhIL-32 and IL-32- containing exosomes on osteoblast differentiation 59
Effect of rhIL-32γ and rhIL-32α on osteoblast differentiation 59
Effect of rhIL-32γ and rhIL-32α on osteoblast proliferation 64
Effect of rhIL-32 on RANKL expression 64
Effect of IL-32-containing exosomes on osteoblast mineralization 66
IL-32 protein expression is absent in IL-32 KO B11 JJN-3 clone, while a truncated protein may be expressed by IL-32 KO D1 JJN-3 clone 68

Part 3 69
Effect of rhIL-32 on osteoblast differentiation when combined with 25(OH)D_3 69
Effect of rhIL-32 on osteoblast proliferation in the presence of 25(OH)D_3 73
Effects of rhIL-32 short-term treatment on osteoblast-specific gene expression in the presence of 25(OH)D_3 or 1,25(OH_2)D_3 74
Effect of rhIL-32 on CYP27B1 76
Effects of rhIL-32 on *CYP24A1* expression 78
Effect of rhIL-32 on RANKL in the presence of 25(OH)D_3 80
Effect of rhIL-32 combined with 25(OH)D_3 on late osteoblasts differentiation evaluated by extent of matrix mineralization 82
Effect of 48 hours stimulation with rhIL-32 and 25(OH)D_3 on osteoblasts 85
The role of dexamethasone in osteoblast differentiation experiments with vitamin D 87
Part 3 89
Effect of hypoxia on bone marrow mesenchymal stromal cells 89
Discussion 93
IL-32 in myeloma cell-derived exosomes promote *in vitro* osteoclast differentiation 93
Exosomes from myeloma cells may promote *in vitro* osteoblast differentiation 95
IL-32 had no apparent effect on osteoblast differentiation 95
IL-32 does not increase RANKL in MSCs or osteoblasts 96
Osteoblasts are more responsive to IL-32 when combining with 25(OH)D_3, but there is currently not evidence for a inhibitory role of IL-32 through vitamin D metabolism 96
Osteogenic markers are sensitive to experimental conditions and technical variations in laboratory procedures 97
CYP27B1 expression was not induced by rhIL-32 in osteoblasts, but may transiently be upregulated in MSCs 98
1,25$(OH)_2D_3$ inhibitory actions as well as CYP27B1 expression and enzymatic activity may be primarily associated with later stages of osteoblast differentiation 99
Dexamethasone was required for 1,25$(OH)_2D_3$ dependent inhibition of mineralization 100
1,25$(OH)_2D_3$ biosynthesis was negatively associated to osteogenic markers but not dependently of rhIL-32 101
Bone marrow mesenchymal stromal cells express IL-32 and the expression is increased by IL-32 and by hypoxia 102
CYP27B1 expression in MSCs may be increased by hypoxia 103
Conclusion 104

References **107**

Appendices **121**

Abbreviations

APRIL: A Proliferation-Inducing Ligand

BAFF: B-cell Activating Factor belonging to the TNF-Family

BMP-2: Bone morphogenic protein-2

DMSO: Dimethyl Sulfoxide

EDTA: ethylenediamine tetraacetic acid

IGF-1: Insulin-like growth factor

IL-1β: Interleukin-1β

IL-2: Interleukin 2

IL-18: Interleukin 18

IL-6: Interleukin 6

LPS: lipopolysaccharide

M-CSF: Macrophage Colony Stimulating fFctor

MAPK: Mitogen Activated Proten Kinase

MIP-1 α: Macrophage Inflammatory Protein 1 α ,

M-CFS: Macrophage colony stimulating factor

NK4: Natural Killer Transcript 4

NF-κB: Nuclear Factor 'kappa-light-chain-enhancer' of Activated B-cells

PI3K : Phosphatidylinositol-4,5-bisphosphate 3-kinase

Poly(I:C): Polyinosinic–polycytidylic acid

SDF-1α: Stromal Cell-derived Factor

S1P: Sphingosine-1-Phosphate

TGF- β: Transforming growt factor-β

TNF-α: Tumor Necrosis Factor -α

VEGF: Vascular Endothelial Growth Factor

Wnt: Wingless

Introduction

Multiple myeloma prevalence and diagnosis

Multiple myeloma is a neoplasm of plasma cells, which is terminally, differentiated B-lymphocytes. These monoclonal (M) antibody producing malignant cells establish in the bone marrow and remodels the microenvironment to a suitable niche for tumorigenesis[2]. Multiple myeloma is the second most common blood cancer and is still considered as an incurable disease although new treatment strategies have improved the overall survival time[3,4]. The main diagnostic criteria for multiple myeloma are presence of M-protein in serum or urine, and at least 10 % clonal plasma cells in the bone marrow[5]. In 2014, 371 new cases of myeloma were reported in Norway, of these, 188 were men and 183 were women[6]. Almost all incidences concern individuals older than 60 years, while only 2 % of the diagnosed cases were people younger than 40 years[7]. On a global basis, myeloma is responsible for 1 in 100 cancer incidences[8].

B-cell transformation and disease progress

B-cells are part of the adaptive immune system, which maintains information from earlier infections. The "immunological memory" is created when T cells present an antigen from an infecting agent to B cells, which then differentiate to plasma cells in a process called "affinity maturation". The terminally differentiated cells are able to produce large amounts of antibodies in which the paratope matches the epitope of the previously internalized and presented antigen. This enables the immune system to activate an enhanced and more effective response on second exposure to the pathogen[9].

The transformation of plasma cells to malignant cells is a result of genetic alterations accumulating over time[10]. Multiple myeloma is therefore described by distinct clinical stages, with an increasing severity correlated with the number of mutations (see **Figure 1**)[10]. It was earlier thought that myeloma could occur *de novo*, but this theory is more or less rejected as a consequence of new findings showing that myeloma consistently develops from a

premalignant stage called *monoclonal gammopathy of undetermined significance* (MGUS)[11]. MGUS is characterized by an increased population of plasma cells in the BM and detectable amount of the characteristic M protein in serum[11]. Approximately 1 % of MGUS cases are predicted to progress into the next phase, smouldering multiple myeloma, which is also asymptomatic, but characterized by a heavier tumor load in the BM[10]. Later stages are defined as multiple myeloma and are associated with features like bone disease, elevated calcium levels in blood, increased level of M-protein, decreased level of blood cells, renal dysfunction and peripheral neural damage[10]. Plasma cell leukemia is the last, definite stage of disease, defined by the presence of circulating plasma cells (>20 %) in peripheral tissues and associated with poor survival prospects[10]. The stepwise transformation to symptomatic myeloma is often seen in relation to the Darwinian evolution model, where the selective pressure leads to a repertoire of several clonal lines in each disease phase[12]. The development of genetically distinct clones occur in a branched system, in which one branch of subclones soon or later will acquire the genetic features required to enter the next level of disease. This heterogeneity of subclones, both within one patient and between patients, complicates the therapeutic strategies for multiple myeloma, in which challenges include high risk of relapse and drug resistance[13].

Treatment strategies

The therapeutic picture of myeloma provide great challenges regarding drug resistance and relapse, but the current approach using combinations of the proteasome inhibitor Bortezomib and the immunomodulatory drugs (IMiDs) Thalidomide and Lenalidomide, have improved survival time for patients radically[14]. The initial choice of treatment strategy is generally dependent on age[15]. Autologous stem cell transplantation improves the overall prognosis, but is usually only performed in younger patients (<65yr)[15]. Eventually, bone marrow microenvironmental- and subclone heterogeneity-mediated refractory relapse occur in nearly all patients[14]. However, there is heavy investigation on new treatment regimens to overcome the recurring drug resistance, including new proteasome inhibitors and IMiDs, pathway-targeted therapies, epigenetic agents, and humanized monoclonal antibodies[3].

Genetics of multiple myeloma

The genetic changes in multiple myeloma can be divided into *primary events* responsible for immortalization of plasma cells, and *secondary events*, which promote progression of disease[10] (**Figure 1**). Depending on the initiating primary event, myeloma can be divided into the hyperdiploidy- and non-hyperdiploidy form, the prevalence of the two forms being approximately equally distributed[13,16]. Non-hyperdiploid myeloma is caused by translocation errors during class shift recombination (CSR)[13]. CSR is a crucial part of the B-cell affinity maturation where the activation-induced deaminase (AID) mediate double strand breaks in the immunoglobulin loci[13]. Somatic hypermutation of the immunoglobulin heavy chain locus (IGH@) at 14q32 in B-cells is an important mechanism for creating antibody diversity[13]. In non-hyperdiploid myeloma the double strand breaks are not repaired locally, and instead the IGH@ locus is translocated to another chromosome, usually 4, 6, 11, 16 or 20, resulting in juxtaposition of the Ig enhancer to one of various oncogenes[2,10]. Hyperdiploidy myeloma involves triplication of the odd numbered chromosomes and is associated with better prognosis[10]. A typical IGH@ translocation-event places cyclin-D genes under enhancement of the Ig-loci, but also hyperdiploidy is associated with increased cyclin D expression, leading to cell cycle progress past the G1/S phase checkpoint[10]. The fact that cyclin D1 is consistently deregulated in both the hyperdiploid and non-hyperdiploid group, suggests that aberrancies in the D-type cyclin pathway are a crucial event in early myeloma pathogenesis[11].

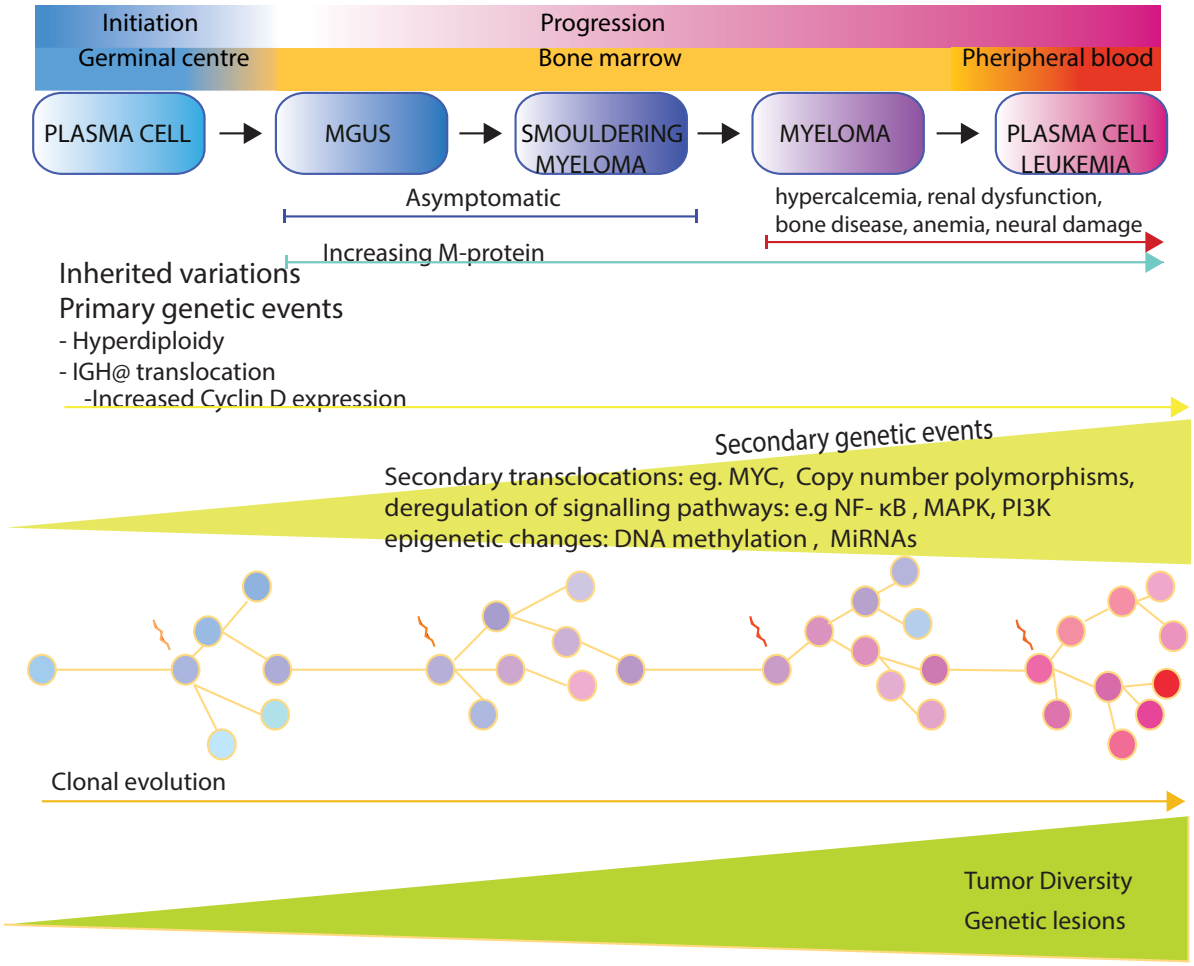

Figure 1: Stages of multiple myeloma and key events in disease progression. Multiple myeloma is a malignancy of plasma cells, which evolves by a step-wise transformation of plasma cells, the different stages characterized by increasing symptoms and severity of disease. Primary genetic events are responsible for the initiation of plasma cell transformation, resulting in the asymptomatic condition MGUS. Further on secondary genetic events leads to disease progression and clonal propagation. Multiple myeloma is characterized by metastasis at multiple sites in the bone marrow and severe symptoms, including bone disease. The final stage is defined as *plasma cell leukemia* as myeloma cells are spread to extramedullary sites, circulating at high levels in the blood. Information in figure is taken from articles[13,17].

Secondary genetic events contribute to disease progression in the later stages of myeloma and includes deregulation of signaling pathways as NF-κB, PI3K and MAPK, key transcription factors as MYC as well as copy number polymorphisms and epigenetic changes, and are, in contrast to primary genetic events, not associated with CSR errors[10] (**Figure 1)**.

Multiple myeloma and the microenvironment

Unlike solid cancers, which metastasize at distinct sites, myeloma cells home at multiple sites in the bone marrow, allowing for a close interaction with the microenvironment [2,18]. For that reason, the bone marrow of myeloma patients shows differential cellular composition and tissue architecture compared to healthy individuals[2]. The bone marrow microenvironment is composed of a heterogeneous population of cells, including hematopoietic stem cells, endothelial cells, immune cells, erythrocytes, bone marrow stromal cells and bone remodeling cells. The self-renewing mesenchymal stem cells are part of the stromal cell population as well as precursors for other stromal cells, including osteoblasts and osteocytes, adipocytes, chondrocytes, and fibroblasts[2]. Myeloma cells interact with cells of the microenvironment, both by cell-to-cell contact via adhesion molecules and by secreting soluble factors, thereby modulating these cells to promote tumor survival and growth through extensive bi-directional cell signaling[2,11]. A great repertoire of growth factors contribute to myeloma pathogenicity and drug resistance, including IL-6, IGF-1, VEGF, IL1ß, SDF-1α, TNF-α, APRIL, BAFF, MIP-1α , as well as Wnt and Notch family members; and new agents are continuously added to the list as the myeloma research field expand[18].

Bone marrow mesenchymal stromal and stem cells sampled from a myeloma patients exhibit abnormal features, both with regard to genetic profile and cytokine production, functioning as supporters of proliferation, apoptotic resistance as well as migration and invasiveness of the myeloma cells[2]. MSCs from myeloma bone marrow were shown to transfer tumorigenic factors in exosomes to the myeloma cells which enhanced tumor growth and tumor homing to the bone marrow in animal models, whereas healthy donor-derived MSC exosomes exerted anti-tumorigenic effects both in vitro and in vivo[19].

The osteoclasts and osteoblasts are strongly affected by the presence of myeloma cells in the bone marrow. Uncoupling of bone remodeling by osteoclast activation and osteoblast inhibition results in a destructive bone disease (further discussed in the section “The bone disease of multiple myeloma”)[20,21].

Bone and bone remodeling

There are two types of bone, cortical- and trabecular bone which compose 80 % and 20 % of the adult human skeleton, respectively[22]. Cortical bone is dense and solid tissue forming the outer layer of all bones, while trabecular bone is soft, porous bone in the bone marrow compartment[22] (see **Figure 2**).

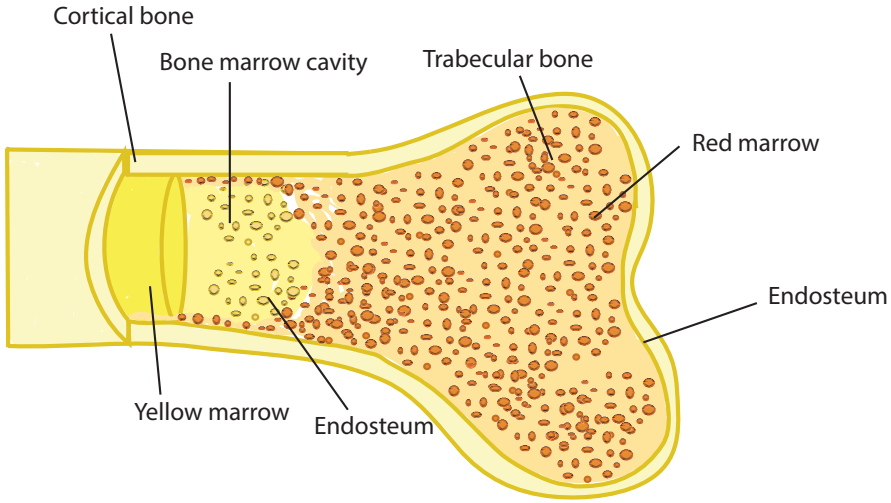

Figure 2: Bone anatomy: Anatomy of the epiphysis- the end of a long bone. The cortical bone is the compact and highly resistant layer covering all bones. The trabecular bone, a soft, porous structure with high surface to mass ratio is found beneath the cortical bone, and is highly represented at the epiphyseal ends[22]. Bone remodeling occurs mainly on the endosteum, the interface between the trabecular or cortical bone and the bone marrow[22]. The red marrow is the site of hematopoiesis and is mainly located in flat bones and the epiphyseal ends while the yellow marrow consists of mainly adipocyte tissue and is found in the medullary cavity of the bone shafts [23].

Bone serves important physiological functions including structural support and protection of vital organs and bone marrow, attachment for skeletal muscles, as well as reservoir for calcium and phosphate, maintaining the mineral balance in serum[24]. Bone remodeling is a constant and routinely process that allows for architectural adaption of bone, as well as renewal of possibly damaged bone matrix[25]. Remodeling of bone is also important to maintain calcium homeostasis, involving hormonal regulation by PTH and vitamin D[24]. The bone remodeling process is initiated by recruitment and activation of mononuclear preosteoclast which migrate to active bone surface areas were they fuse and differentiate into mature, multinucleate osteoclast under the influence of osteoclastogenic factors like RANKL and M-CSF[22,26]. The reversal phase represent the transition between bone resorption and formation, where mononuclear cells at the bone surface recruit osteoblasts to the resorption cavities[24]. This coordinated action is referred to as "coupling"[27]. Correct coupling is essential to balance the two processes; that mean, to replace the resorbed bone with an equivalent of synthesized bone[27]. In addition to the systemic regulation of bone remodeling, several local regulation

mechanisms have been pointed out the latest decade. Other "coupling factors" includes osteoclast derived signals, growth factors, surface proteins and bone topographic changes[28].

Osteoblasts

Osteoblasts are the major bone producing cells, located at the endosteum, which is the interface between the trabecular bone and the bone marrow[23]. In normal, healthy bone osteoblast compromise 4-6 % of the total cell repertoire of the bone marrow. They differentiate from mesenchymal stem cells in a stepwise process, driven forward by expression of different genes which in turn are closely regulated by pro-osteogenic pathways, including BMP and Wnt[29]. As a general criterion, expression of the transcription factors RUNX2, Dlx5 and Osterix is required for commitment to the osteoprogenitor lineage[26].

RUNX2 is considered as the master gene of osteoblast differentiation, upregulating a set of genes including Collagen I, alkaline phosphatase (ALP) and *BGLAP*[26]. The pivotal role of RUNX2 in osteogenic development is supported by the fact that *RUNX2*-knockout mice are completely devoid of osteoblasts[26]. However, overexpression of RUNX2 in osteoblasts inhibited further maturation and lead to osteopenia, indicating that RUNX2 is important in early stages of osteogenic differentiation, but not necessary, or even inhibitory for the later stages of differentiation[30]. After the first osteogenic differentiation phase, a proliferation phase follows, where the pre-osteoblastic cells show ALP activity[26]. The transition to mature osteoblast involves increased expression of Osterix and production of osteocalcin, bone sialoprotein, osteopontin and collagen type I, as well as cell morphological changes towards the characteristic cuboidal shape[26].

The Wnt-family consists of at least 19 secreted glycoproteins that bind to cell surface receptors and activate different signaling pathways[31]. These proteins bind to both the Frizzled receptor and LRP-5/6 coreceptors stabilizing β-catenin, which accumulates and then translocate to the nucleus, activating target genes[31]. The canonical Wnt/β catenin pathway is considered as an important driver of osteogenic differentiation[32]. The importance of this pathway was first pointed out by clinical and *in vitro* studies, showing that knockout mutations of Wnt receptor LRP5 were associated with osteoporosis[32]. Knockout of the Wnt canonical pathway component β-catenin resulted in absence of the late osteoblastic marker gene Osterix, however, early osteogenic differentiation was not inhibited, indicating that Wnt-

pathway signaling is required primarily in the later stages of osteoblast maturation[33]. In addition to promotion of osteoblastgenesis, the Wnt-pathway exhibit inhibitory effects on osteoclastogenesis via upregulation of the RANKL decoy receptor OPG[33].

The Bone Morphogenetic Proteins (BMPs) belongs to TGF-β-superfamily and different isoforms, including BMP-2, 4, 5, 6 and 7, are shown to be important in osteoblastic differentiation, likely through the upregulation of RUNX2 and Osterix[29]. Their role in bone formation was first identified through the ability to induce ectopic bone formation in mice[34]. Among the BMPs, BMP-2 is the most frequently studied in relation to MSC osteogenic differentiation and is a prominently used stimulator of bone formation in clinical applications[35].

The bone formation by osteoblasts can be seen as a two-step process. In the first step the osteoblast deposit osteoid, which is an organic extracellular matrix composed of collagen I and small quantities of specialized proteins as osteocalcin and ostepontin[26]. In the next step the osteoblasts produce inorganic mineralization compounds, importantly hydroxyapatite, catalyzing the mineralization of the bone matrix[26,36]. The bone minerals constitute approximately 60 % of the cortical bone, providing rigidity, while water and organic material compose the remaining 40 % in equal proportions, conferring the proper balance between stiffness and flexibility[37]. In the final stage, mature osteoblasts are destined to different fates; some die by apoptosis or become quiescent bone lining cells, while other subpopulations show cytoplasmic processes towards the bone matrix[26]. These cells, soon completely embedded in the osteoid, undergo morphological and cellular changes to become osteocytes[29]. Osteocytes are mechanosensing cells that communicate with each other and the surroundings, converting mechanical signals into chemical signals that regulate osteoblasts as well as osteoclasts and thereby directing the total bone turnover[25].

Osteoclasts

Osteoclasts, the bone resorptive cells, are large multinucleate cells originating from mononuclear cells of the monocyte/macrophage lineage[38]. RANKL and M-CSF are critical cytokines for osteoclastogenesis, promoting the activation of several transcription factor which direct the osteoclast specific gene expression[22]. Osteoclast precursors initially circulate

in blood, but when encountering activated resorption sites, they fuse to form multinucleated cells at sizes up to 100 μm [24,39]. The pre-osteoclast express receptors on their cell surface that enables them to bind to peptides on the bone matrix[22]. The usual localization of osteoclasts is within bone resorption pits called lacunae on the bone surface[22]. The osteoclasts secrete acidifying hydrogen ions that degrade the mineral component of the bone, and the enzyme cathepsin K which then digest the remaining collagenous matrix [40,41].

The OPG/RANKL/RANK system is an important regulator of osteoclastgenesis and bone remodeling in general. The RANK ligand and its decoy receptor osteoprotegerin (OPG) are both members of the TNF receptor-ligand superfamily[42]. RANKL is expressed on immature osteoblasts and other stromal cells in response to circulating factors as PTH, glucocorticoids and $1,25(OH)_2D_3$, as well as local cytokine signaling[43-45]. By binding to RANK on the osteoclastic precursors, RANKL induces differentiation, activation and survival of the osteoclasts[45]. Stromal cells also produce OPG, which binds to RANKL and inhibits its effect on osteoclastgenesis[46]. The control of bone resorption is therefore dependent on the OPG/RANKL ratio in stromal/osteoblastic cells. The finding that a large repertoire of hormones and cytokines exert their effect through the OPG/RANKL/RANK system led to the introduction of the "convergence hypothesis" which suggest that all pro-resportive and anti-resorptive signals; physiological as well as pathological, are detected by the osteoblastic lineage and that the total outcome determine their OPG/RANKL ratio, and thereby the level of bone resportion [47,48].

The bone disease of multiple myeloma

The bone disease, a hallmark of multiple myeloma, is characterized by increased osteoclastgenesis and decreased osteoblastogenesis[49]. Approximately 80% of patients diagnosed with myeloma show skeletal aberrations, though the extent of skeletal involvement vary from single osteolytic lesions or osteoporosis, to extensive osteolysis, skeletal pain and pathological fractures[50]. Furthermore, while other cancers that metastasize in bone, as breast and prostate cancer, are associated with both osteoblastic and osteolytic lesions, myeloma lesions are purely osteolytic, located in areas near tumor foci[49]. The decrease, or in some cases absence of osteoblast activity is thus a distinctive feature related to myelomatous bone metastasis[51].

An extensive number of studies emphasize the central role of bone disease in multiple myeloma pathogenesis. It is commonly accepted that reduced bone density in form of osteolytic lesions and interactions with the cells involved in the bone remodeling are important for the myeloma cell survival and proliferation; - in myeloma patients the degree of osteolysis has been shown to be an important indicator of disease severity[36,52]. Furthermore, low level of bone disease in patients is associated with an improved event-free survival[53]. Also, investigation of already established drugs, such as thalidomide, lenalidomide and bortezomib has shown that these treatments affect osteoclast and osteoblast activity[51,54,55], suggesting that interference with the bone remodeling cells count for some of the inhibitory effect exhibited by these cytostatics. Bone disease and osteoclast-osteoblast interactions are therefore important study objects and treatment targets for multiple myeloma.

In myeloma multifactorial mechanisms act to increase osteoclastgenesis[49] (see **Figure 3**). The unbalanced RANKL:OPG ratio counts to a great extent for the increased osteoclast differantiation. This ratio is not only distorted by the myeloma cells, but also by other microenvironmental cells; for example co-cultivation with myeloma cells resulted in upregulation of RANKL and downregulation of OPG in MSCs[56]. Myeloma cells also stimulate osteoclastic activity by producing soluble factors as RANKL, MIP-1α, Il-3, SDF-1α and GDF15 [56-60]. Syndecan-1, a proteoglycan produced by the myeloma cells, influence the bone formation by sequestering the RANKL antagonist OPG, as well as conditioning the local environment with osteoclast promoting factors[61]. Other factors associated with bone remodeling, including IL-17, IL-6, TSP-1 and TNF-α are found at higher concentrations in

bone marrow and/or blood of myeloma patients, but their role in bone disease is not fully elucidated[62-64].

Inhibition of osteoblast maturation is a central mechanism in myeloma bone destruction. Immature osteoblasts express high levels of RANKL; stalling of the bone synthesizing cells in the osteoprogenitor phase is therefore a central contribution to increased osteoclastgenesis [65,66]. Also IL-6 and SDF-1 are upregulated in immature osteogenic cells and may be promoters of lytic bone resorption locally[67,68]. Myeloma cells inhibit osteoblast differentiation and function through a diverse set of mechanisms. The myeloma cells interact directly with osteoblasts via adhesion molecules to inhibit the actions of the transcription factor *RUNX2* and decrease bone matrix production[69]. Furthermore, factors produced by the myeloma cells and the myeloma-microenvironmental cells inhibit osteoblast differentiation. Many of these are interact with the Wnt-pathway and thereby inhibit commitment of the osteoprogenitor cells to later maturation stages. Wnt-inhibitors produced by the myeloma cells include sclerostin, sFRP-2 and -3, which bind to the Frizzled receptor and the LRP-5/6 antagonists DKK1[70-72](**Figure 3)**. Also other soluble factors produced by the myeloma cells, including hepatocyte growth factor (HGF), IL-3 and IL-7, have been shown to inhibit osteoblasts through various mechanisms[69,72].

Myeloma cells interact with various lineages of hemapoietic cells to enhance osteoclastgenesis and thereby tumor growth. The recruitment of monocytes and macrophages to focal lesions and the production of Il-8 by these cells lead to increased osteoclastgenesis[73]. T-lymphocytes are known to support bone resorption by production of RANKL and IL-3, while dendritic cells seem to infiltrate myeloma-tumors, producing significant amounts of RANKL and other osteoclast promoting factors[74-76].

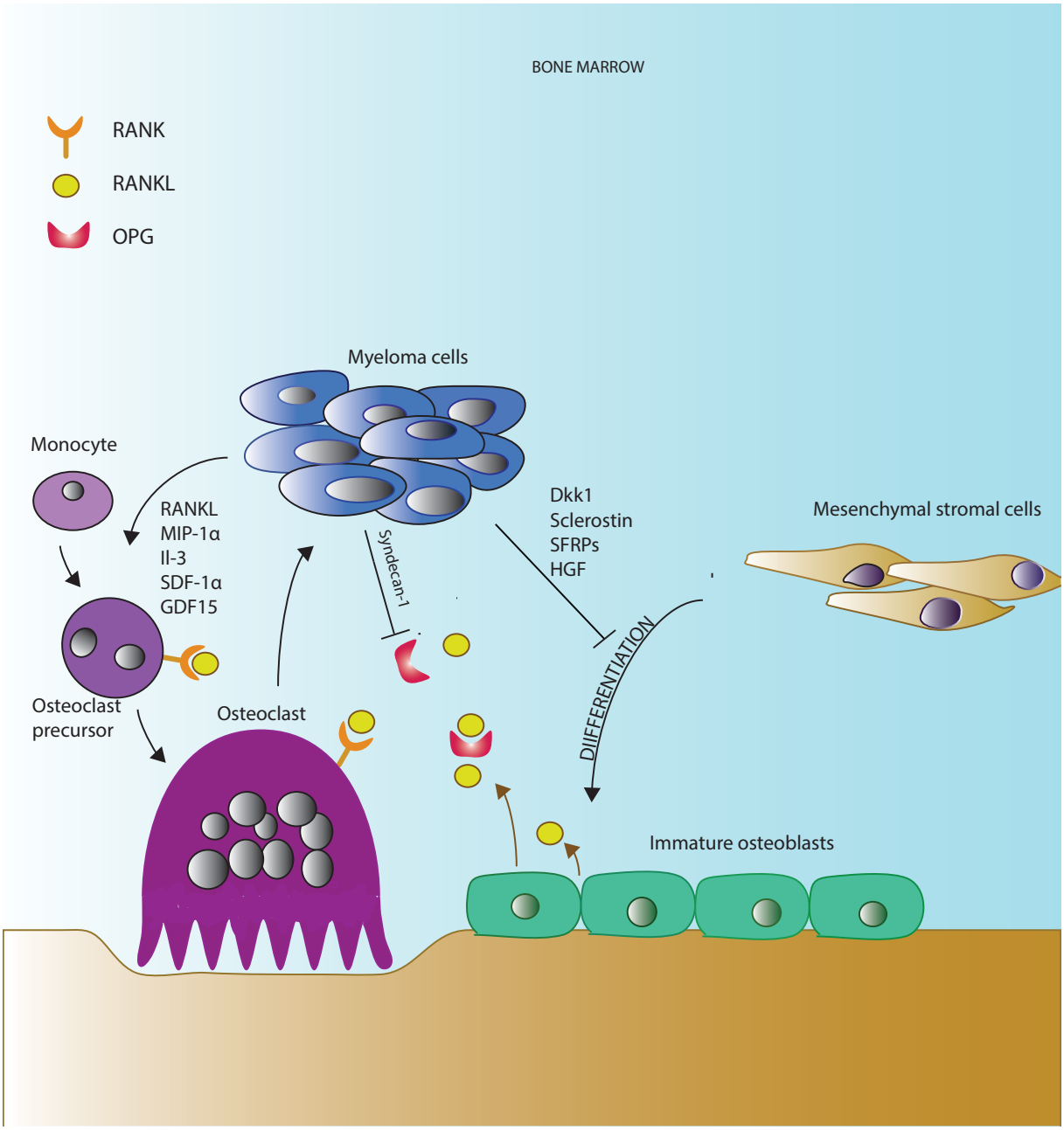

Figure 3: Mechanisms of myeloma bone disease. The myeloma cells modulates the bone marrow microenvironment by secreting factors that induce osteoclastogenesis and inhibit osteoblast differentiation, resulting in osteolytic lesions and progressive bone disease. Information presented in figure is taken from articles[51,60,70,72]

Treatment of myeloma bone disease

From the early eighties biphosphanates have been a cornerstone in treatment of myeloma bone disease[77]. The biphosphanates bind to mineralized bone matrix with high avidity, there they target the osteoclasts by interfering with intracellular processes[20]. For example the nitrogen-biphosphanate zoledronic acid inhibits the activity of a key enzyme in the

mevalonate pathway[78]. Osteoclasts recruitment and formation are reduced, and the cells die from apoptosis[78,79].

RANKL is also a potent target in MM bone disease, and in animal models use of recombinant OPG or RANKL-fc fusion protein inhibited MM-induced osteolysis [80,81]. The RANKL-antibody denosumab has until now shown less potency, but extensive clinical trials is now ongoing where zoledronic acid and denosumab are compared in as treatments in newly diagnosed myeloma patients[82,83].

In addition to inhibition of osteoclasts, treatment can also be directed towards activation of the osteoblastic lineage. The Wnt-pathway, which is essential for osteoblast formation is inhibited by different factors secreted by the myeloma cells. This pathway can therefore be activated indirectly by using neutralizing agents against Wnt-inhibitors, for example DKK1[84]. Further on, the Wnt pathway can also be activated directly through Wnt3a signaling or treatment with lithium chloride[85,86]. In addition to their bone forming activity, osteoblasts also has shown inhibitory effects on myeloma cell survival, therefore representing an important target, both with regard to treating the bone disease and MM in general[87,88].

Interleukin 32

IL-32 is categorized as an inflammatory cytokine, although it has no sequence homology to the other known cytokine families[89]. IL-32 was originally known as NK4, a transcript from natural killer cells[90], but was not characterized as an inflammatory mediator before 2005[89]. IL-32 is produced by a set of immune cells, and is induced by a other cytokines, such as IFN-γ, IL-2 and IL-18[91]. IL-32 itself was shown to induce the production of TNF-α and other pro-inflammatory factors through NF-kB and p38 MAP kinase dependent pathways[89]. However, the mechanisms of IL-32 seems, by some means, to differ from other interleukins, Netea Mihai G et al. (2006) found that a repertoire of Toll-like receptors, which usually induce production of inflammatory cytokines, did not induce IL-32 in pheripheral blood mononuclear cells, while expression was highly induced by bacterial exposure[92].

In humans, IL-32 is localized at chromosome 16p13.3, and there is also found gene versions with some sequence similarity in both equine, bovine, ovine and swine genome[89]. Rodents do not express IL-32[93]. The IL-32 gene contains 8 exons and the ~ 25 kDa protein was originally found to exist as four splice variants; IL-32α, IL-32β, IL-32δ and IL-32γ[89]. However, today in all 9 splice variants of IL-32 have been characterized[94,95]. IL-32γ considered as the most biologically active form[96,97].

IL-32 in disease

IL-32 has demonstrated both inhibitory and activating roles on tumor growth. For example IL-32 was shown to promote breast cancer and gastric cancer growth and invasiveness, while it may exhibit an inhibitory role against colon cancer and melanoma[98-101]. However, the results are not consistent for IL-32 regarding the latter cancer types, demonstrating the complex role of IL-32 in disease. Recently, it was shown that IL-32 alpha induced migration in melanoma cells via ERK1/2 pathway activation and that IL-32 over-expression in colorectal cancers increased metastasis[102,103]. IL-32 may also be involved in regulation of glycolysis in hypoxic conditions, shown in the context of breast cancer[104].

Also, IL-32 plays a role in inflammatory disorders and infections; increased IL-32 expression was demonstrated in response to inflammatory bowel disease, influenza A infection and autoimmune disorders such as rheumatoid arthritis (RA)[105-107].

Effect of IL-32 on bone cells

Kim et al. (2010) showed that IL-32, in the presence of RANKL, induce osteoclast differentiation from monocytes and bone resorption *in vitro*[107]. However, when treating monocytes with IL-32 only, osteoclast formation was still increased, but the cells appeared to be in an inactive state, shown by low resorptive activity on bone disks[107]. Also, in the same study, they demonstrated that IL-32 increased RANKL expression and decreased OPG expression in rheumatoid arthritis fibroblast-like synviocytes, resulting in an enhanced RANKL:OPG ratio. Based on their preliminary findings of the effect of IL-32 on osteoclasts, Kim et al. (2012) focused on the mechanism of action, and found that IL-32 was particularly important in the fusion stage of osteoclast differentiation[108]. In another study, IL-32, in

synergy with IL-17, was able to induce osteoclastgenesis without RANKL, but resorption pit formation was not observed[96].

IL-32 has also been linked to vitamin D antimicrobial-pathways in monocytes and macrophages[1]. CYP27B1 is a hydroxylase that generate the active metabolite of vitamin D. When stimulated with IL-32, monocytes showed increased expression of CYP27B1, as well as conversion of inactive vitamin D to the active form[1]. The vitamin D receptor was also upregulated, indicating that the antimicrobial response resulting from IL-32 may be mediated by active vitamin D[1]. Further supporting this hypothesis, the IL-32 induced immune response in primary macrophages was inhibited by insufficiency of pro-vitamin D, indicating that the effector functions of IL-32 are completely dependent on vitamin D[1].

In a recent article by Eun-Ju et al. (2015) IL-32 was pointed out as a positive inducer of osteoblast differentiation[109]. Stimulation of calvarial mouse preosteoblasts with exogenous IL-32γ promoted rapid osteogenic differentiation and matrix maturation, shown by increased ALP activity and enhanced mineralization after 2 weeks[109]. Further investigation revealed that one mechanism responsible for the increased osteoblastgenesis was IL-32 suppression of Wnt-inhibitor DKK1[109]. Stimulation with IL-32γ also resulted in reduced abundance of DKK1 in human osteoblasts[109].

Bone marrow stromal cells also express IL-32, shown in the human stromal cell lines HS-5 and HS-27a in the context of myelodysplastic syndromes[110]. In a more recent study, IL-32 produced by bone marrow stromal cells significantly induced apoptosis of bone marrow myelodysplastic cells[111].

IL-32 in multiple myeloma

Although both positively and negatively associated to many cancers, IL-32 has not previously been studied in relation to multiple myeloma. Interestingly, by assessing primary myeloma cells from BM aspirates with NanoString analysis we found by that IL-32 is highly expressed by the primary myeloma cells compared with macrophages, the latter an IL-32 expressing cell type (**Figure 4A**) (Zahoor et al, manuscript in preparation). Further on, IL-32 mRNA was expressed in a subgroup of patient plasma cells, and in some cell lines (**Figure 4B**). Also, IL-

32 expression in both cell lines and primary cells was increased by hypoxia (**Figure 5**). We found IL-32γ in conditioned media assessed by ELISA (data not shown), indicating that IL-32 is secreted by the myeloma cells. Furthermore, when staining primary cells for IL-32, the protein appeared to be located in exosomes. This was further supported by detection of IL-32 in the isolated exosome fraction after ultracentrifugation. The finding that IL-32 was secreted from the myeloma cells suggested direct influence on the bone marrow microenvironment, and therefore we were interested in the effect on osteoclasts and osteoblasts. Exosomes from cell lines expressing IL-32 were endocytosed by PBMCs and induced osteoclastogenesis in these cultures, as well as in the calvaria of a myeloma-mouse hybrid model. In the mouse model, exosomes derived form myeloma cells cultured in hypoxia induced more osteoclastogenesis than exosomes derived from myeloma cells cultured in normoxia. Also, recombinant IL-32 induced osteoclast differentiation both *in vitro* and *in vivo* (Zahoor et al, manuscript in preparation). Further on, we wanted to investigate if IL-32 had an effect on osteoblasts, which became the main study objective of this master's project.

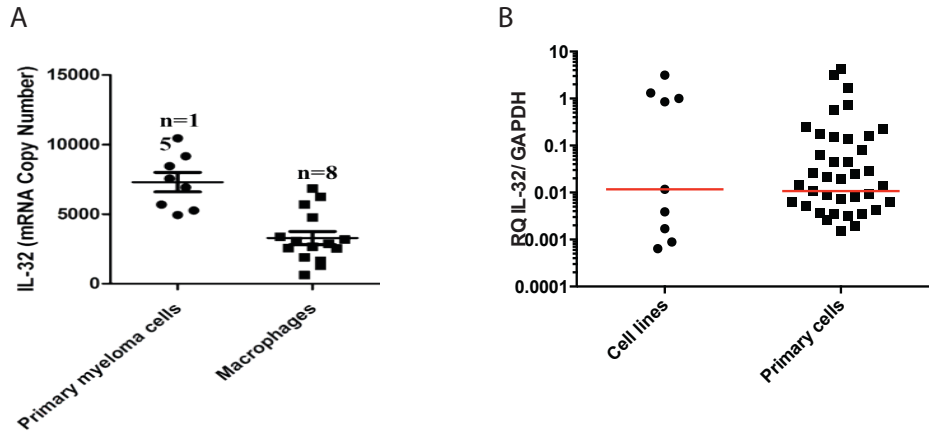

Figure 4: Preliminary results for IL-32 expression in primary myeloma cells . A) mRNA copy number of IL-32 in Primary myeloma cells and macrophages assessed by NanoString. **B)** mRNA expression of IL-32 in cell lines and primary cells rimary myeloma cells showed a more stable expression of IL-32 than myeloma cell lines, although a subgroup of IL-32 expressing cells assessed by RT-qPCR (Zahoor et al. manuscript in preparation).

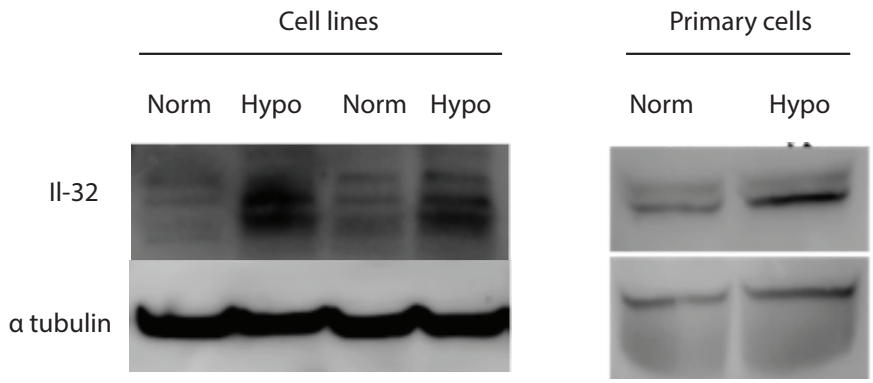

Figure 5: Myeloma primary cells and cell lines were cultured in hypoxic (hypo) conditions (2 % O_2) for 24 hours. Hypoxia increased IL-32 expression in both primary cells and cell lines (Zahoor et al. manuscript in preparation)

Vitamin D

The biologically active form of vitamin D, 1α,25 dihydroxyvitamin D_3 (1,25-$(OH)_2D_3$) is generated in a stepwise process[112] (**Figure 6**). Initially, vitamin D_3 is synthesized in the skin as pre vitamin D (cholecalciferol) upon UVB exposure or alternatively, dietary vitamin D is absorbed from the intestine[112]. In the liver, c-25 hydroxylation by p450 2-hydroxylase enzymes, including CYP24R1 and CYP27A1, generate the inactive metabolite 25-hydroxyvitamin D_3 ($25(OH)D_3$) which is the main circulating form of vitamin D[113,114]. Subsequent hydroxylation at the 1α position by 25-Hydroxyvitamin D_3 1-alpha-hydroxylase (CYP27B1) in the kidneys generates the active metabolite of vitamin D, which then can bind to the vitamin D receptor (VDR) to activate gene transcription and regulate the mineral ion balance[112,113]. Besides the major $25(OH)D_3$ metabolism in renal cells, also other cell types, including MSCs, osteoblasts and different immune cells express CYP27B1 and are thereby able to generate the active vitamin D metabolite[115,116]. Finally, the degradation of $25(OH)D_3$ and $1,25(OH)_2D_3$ are facilitated by 25-hydroxyvitamin D-24-hydroxylase (CYP24A1), which catalyze the conversion into 24-hydroxylated products[117].

Vitamin D and bone formation

$1,25(OH)_2D_3$ is frequently used in treatment of bone disease to improve bone mineralization and maintain a positive calcium balance. CYP27B1 knockout mice showed defective bone mineralization, further emphasizing the importance of correct physiological levels of 1,25-$(OH)_2D_3$ [112]. Although its necessity in bone mineralization is commonly accepted, the complete mechanism behind is still not elucidated[113]. It is well accepted that $1,25(OH)_2D_3$ through VDR signaling regulates mineral ion homeostasis and thereby influence bone formation, however, the presence of CYP27B1 and VDR in osteoblast and chondrocytes, and the activating effect of $1,25(OH)_2D_3$ on osteoblast differentiation are evidences for a more potent role of vitamin D on osteoblast bone synthesis than indicated by the classical view[113].

The effect of vitamin D on osteoblasts has been exploited in many studies, but the results are contradictory, suggesting that the impact of vitamin D vary depending on the species examined and the maturation stage of the osteoblasts[113]. In mice, $1,25(OH)_2D_3$ seem to exert inhibitory effects on osteoblast differentiation and activity[118,119]. In rats, active vitamin D decreased ALP and collagen I mRNA levels in preosteoblasts, while the same markers were upregulated by vitamin D in late stage cultures[120]. Finally, in human osteoblast- and MSC-cultures, stimulation with either the $25(OH)_2D_3$ form or the active $1,25(OH)_2D_3$ form induced mineralization and osteoblast differentiation[113]. Also, $1,25(OH)D_3$ has been shown to increase expression of *RUNX2* and collagen I in human osteoblasts[121].

Incubation with the $25(OH)D_3$- substrate showed that osteoblasts express significant amounts of CYP27B1 and that this enzyme produce sufficient levels of the active $1,25(OH)_2D_3$ to increase osteoblast activity, including mineralization and ALP activity[122]. Besides its obviously positive effects on human osteoblast bone formation, $1,25(OH)_2D_3$ also seem to restrict over-mineralization by negative feedback signaling, for example CYP27B1 was lower in MSCs from individuals with elevated levels of $1,25(OH)_2D_3$[115]. Further supporting this regulative role, $1,25(OH)_2D_3$ induces inhibitors of the mineralization process in human osteoblasts, including activin A, osteocalcin and osteopontin[112,123].

Not only osteoblast are influenced by vitamin D, there is also extensive evidence for 1,25 $(OH)_2D_3$ as promoter of osteoclast differentiation[45]. RANKL is upregulated on osteoblasts by the active metabolite vitamin D, which in turn activate osteoclasts[124]. Paradoxically $1,25(OH)_2D_3$ is used in osteoporosis therapy to increase bone density by inhibiting bone resorption[45]. These contradictory actions are not fully explained, but one mechanism in which $1,25(OH)_2D_3$ restricts osteoclastic bone resorption is by inhibition of osteoclast precursor migration from blood to bone[125].

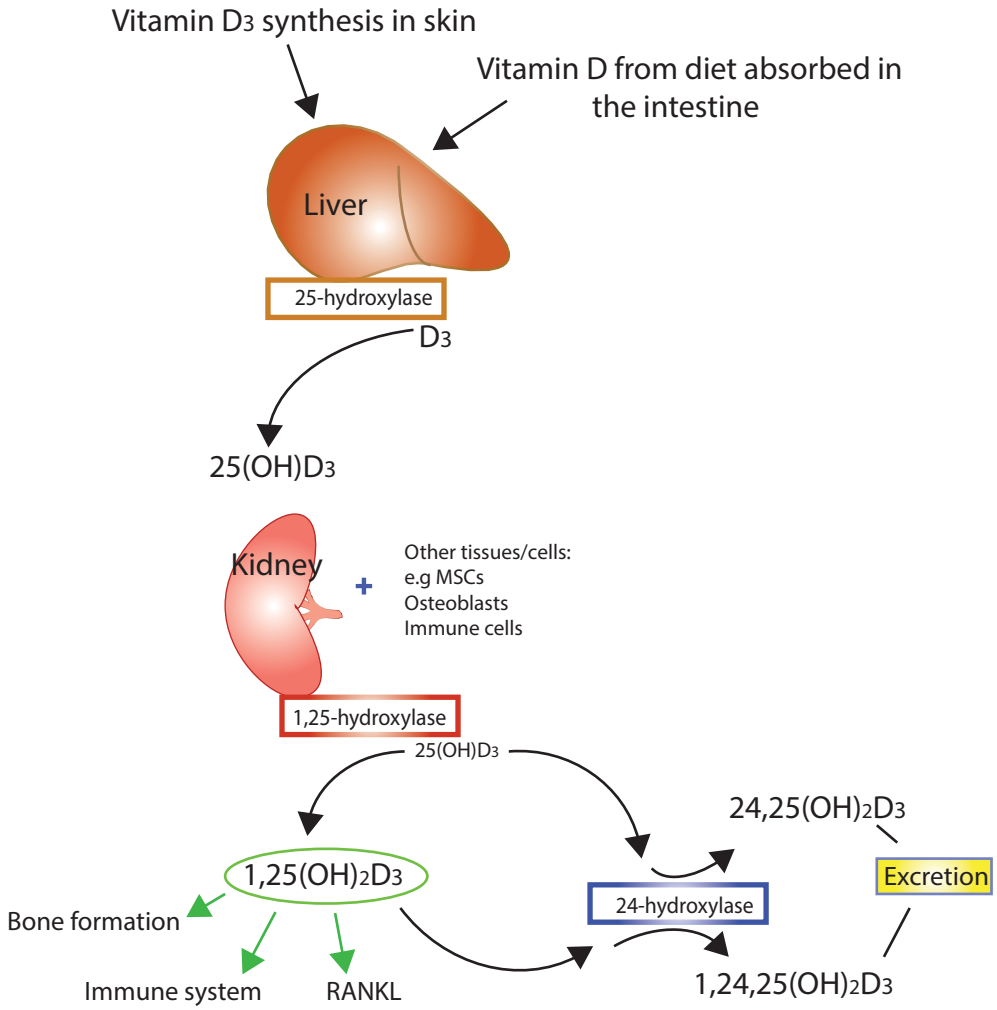

Figure 6: Vitamin D metabolism[126]. Vitamin D is initially synthesized in the skin or originates from dietary sources absorbed from the intestine. In the liver 25-hydroxylase generate the pro form of vitamin D, $25(OH)D_3$, which is further hydroxylated at the 1α-position in the kidney or in other 1,25 hydroxylate expressing cells, generating active vitamin D, $1,25(OH)_2D_3$. The active form of vitamin D influence various processes in the body including bone formation and immunologic responses. RANKL is also induced by vitamin D. 24-hydroxylase initiates the degradation of both the active and pro-form of vitamin D by generating 24-hydroxylated products that can be excreted.

Aims and hypotheses

The main aim of the project was to investigate how IL-32 from myeloma cells affects the bone marrow microenvironment, more specifically osteoblasts and osteoclasts.

IL-32 is a relatively uncharacterized cytokine and has not yet been described in relation to multiple myeloma. We found that IL-32 is expressed by primary myeloma cells, and recombinant IL-32 as well as IL-32 in myeloma-derived exosomes increased osteoclast differentiation both *in vitro* and *in vivo*. As IL-32 clearly influences the bone resorptive cells, we wanted to investigate a possible effect of IL-32 in the bone forming cells, osteoblasts, which are the main study objects of this thesis.

The main objectives were:

1. **To investigate the effect of IL-32 containing exosomes on osteoclast differentiation.** To validate that the exosome-induced osteoclastogenesis previously demonstrated were due to IL-32, the gene was knocked out in JJN-3 myeloma cells, and exosomes from IL-32 knockout and wild-type were treated to primary monocytes. The osteoclast differentiation in these cultures where then evaluated by number of osteoclasts. My contribution to these experiments was to confirm the results generated by Zahoor et al. by counting the osteoclasts.

2. **To examine the effect of rhIL-32 and IL-32 containing exosomes on osteoblast differentiation and proliferation.** As both rhIL-32 and Il-32 containing exosomes had an effect on osteoclast differentiation, we wanted to investigate the effect on osteoblasts differentiation and function. The level of osteoblast differentiation was to be evaluated by well-established parameters for osteoblast differentiation in various maturation stages, including alkaline phosphatase (ALP)-assay, *RUNX2*, Osterix and osteocalcin gene expression, as well as Alizarin Red-S staining of mineralization. The evaluation of osteoblast responses to IL-32 would also include osteoblast proliferation and RANKL expression.

3. **To clarify if IL-32 plays a role in vitamin D metabolism in MSCs and osteoblasts.** The active form of vitamin D, $1,25(OH)_2D_3$, is a major player in systemic regulation

of bone metabolism. Furthermore, recent years investigation have revealed that $1,25(OH)_2D_3$ is generated by bone cells locally and thereby also directly influence bone remodelling. However there are contradictory results whether its impact is negative or positive on the cellular level. IL-32 has previously been linked to vitamin D metabolism in a study by Montoya et al. (2014) were monocytes stimulated with IL-32 showed increased expression of CYP27B1 as well as conversion of inactive vitamin D to the active form[1]. We therefore hypothesized that IL-32 could upregulate CYP27B1 in osteoblasts, and thereby indirectly affect the cells through increased 1,25(OH)2D3. Whether $1,25(OH)_2D_3$ plays an inhibitory or activating role on osteoblasts in our hMSC system was not known. The hypothesis was to be evaluated by measuring CYP27B1 expression and -enzyme activity and by extent of the same parameters as in objective 2

4. **Examine the effect of hypoxia on MSCs**

   As IL-32 expression by bone marrow stromal cells was demonstrated in the context of myelodysplasmic syndromes[111], we wanted to investigate whether IL-32 was expressed by MSCs in our system. As our preliminary results showed that IL-32 was increased in myeloma cells in hypoxia, we also wanted to examine expression of IL-32 in MSCs cultured in hypoxia.

Material and methods

A table with information about the reagents used, including manufacturer and catalogue numbers, is provided in Appendix 7.

Primary cells and cell lines

Primary human bone marrow-derived mesenchymal stromal cells (MSCs) from male healthy donors were obtained from Lonza. Three different donors; 19, 23 and 24 (lot # 0000307219, # 0000446319 and # 0000451491) were used. The myeloma cell line JJN-3 was a gift from J.Ball (University of Birmingham, United Kingdom). Peripheral blood mononuclear cells were isolated from serum obtained from the Blood Bank, St. Olavs Hospital.

Culture conditions

MSCs were cultured in mesenchymal stem cell growth media (MSCGM, Lonza) according to manufacturer's instructions, at 37˚C in a humidified atmosphere containing 5 % CO_2. The cells were passaged maximum seven times. To differentiate the hMSC in osteogenic direction, modified MSCGM with L-ascorbic acid (0.05 mM; Sigma-Aldrich), dexamethasone (10^{-8} M, Sigma-Aldrich) and β-glycerophosphate (10 mM; Sigma-Aldrich), hereafter referred to as differentiation- or diff-media, were introduced to cells at confluence. The differentiation media was replenished every 3-4 day. For IL-32 experiments recombinant human (rh)IL-32γ (R&D Systems) and rhIL-32α (R&D Systems) were supplemented in media at different concentrations (details provided in Results). For vitamin D and IL-32 experiments 25(OH)D_3 (Sigma Aldrich) and 1,25$(OH)_2$ D_3 (Sigma Aldrich) reconstituted in etanol and DMSO respectively were combined with rhIL-32 γ.

The JJN-3 cells, IL-32 KO and WT, were cultured at 37˚C in a humidified atmosphere containing 5 % CO_2, in RPMI 1640 medium (Sigma Aldrich) supplemented with glutamine (100 µg/ml, Sigma Aldrich), gentamicin/gensumycin (20 µg/mL, Sanofi) and 10% fetal calf serum (Gibco/Invitrogen). The cells were split twice a week.

The primary monocytes were cultured at 37˚C in a humidified atmosphere containing 5 % CO_2, in osteoclast differentiation medium (α-MEM, Thermo Fisher) containing 10% FCS and 1% penicillin/streptomycin (Invitrogen), supplemented with 30 ng/ml M-CSF, 10 ng/ml RANKL and 1 ng/ml TGF-β (all Peprotech). Media was replenished every 3-4 days.

Determining the effect of IL-32-containing exosomes on osteoclasts

Zahoor et al. previously demonstrated positive effect of IL-32-containing exosomes on osteoclast differentiation. To validate that the effect was due to IL-32 in the exosomes, the exosome-fraction was isolated from IL-32 knockout and mock wild-type JJN-3 cells (knock-out procedure further described in Appendix 3) and used to stimulate primary monocytes. Several validation experiments were performed to obtain sufficient biological replicates for publishing, and my contribution was to count the number of osteoclasts in cultures of terminated experiments performed by M. Zahoor.

Osteoclast isolation and differentiation

Peripheral blood mononuclear cells (PBMCs) were isolated from EDTA-blood (buffycoat) of normal healthy donors using a Ficoll gradient. Monocytes were then isolated using adherence or CD14+ isolation. The cells were then seeded in 96-well plates (8000 cells/well) and cultured in α-MEM media with various supplements: for preosteoclast experiments cells were treated with and M-CSF (1ng/ml), recombinant IL-32 (25 ng/mL) and exosomes (5 µL exosomes/150µLmedium), with or without RANKL (50 ng/ml) directly after seeding, for 5-6 days. For post-osteoclast experiments cells were first differentiated into preosteoclast in OC-differentiation medium containing M-CSF, RANKL and TGF-β (concentrations as previously reported) for 5 days (depending on the donor) until the first binuclear cells appeared. Subsequently the preosteoclasts were treated for 3 days with recombinant IL-32 and exosomes (5 µL exosomes/150µLmedium), with or without RANKL (50 ng/ml) and M-CSF (1ng/ml). The osteoclast differentiation was evaluated by staining of tartrate resistant acid phosphatase (TRAP)-staining with subsequent counting of TRAP-positive cells. The principle of TRAP is described below, while complete principles and protocols for PBMC isolation and CD14+ - and adherence monocyte isolation are presented in Appendix 1 as these are not part of the main methods of this project.

The principle of TRAP-staining

Tartrate resistant acid phosphatase (TRAP) is a metalloenzyme involved in bone resporption and highly expressed in osteoclasts. It is considered as an important histochemical marker for these cells[127]. However, the more recent years TRAP expression has been demonstrated in other cells, including dendritic cells and macrophages[128]. TRAP staining is still one of the most commonly used histochemical assays for osteoclast detection[129]. TRAP staining of osteoclasts was in this case performed using Leukocyte Acid Phosphatase Kit (Sigma Aldrich), which employs napthol AS- BI phosphate and fast Garnet GBC salt. When napthol AS-BI phosphate is hydrolyzed by TRAP it combine with the diazoniom salt in an reaction called *azo coupling* that forms stable maroon dye deposits at sites of enzymatic activity[130,131] As the name emphasizes TRAP is resistant to tartrate acid inhibition and this property is exploited in the staining assay. By adding tartrate the staining of other cell types expressing tartrate sensitive acid phosphatases is avoided. However, also monocytes and macrophages express TRAP to some extent, thus a second criteria should be used when counting osteoclasts among the TRAP positive cells. In the current study only cells with three or more nuclei where counted. **Figure 7** shows a cropped version of an imaged osteoclast well, demonstrating which cells that where marked and thereby counted. The protocol for TRAP-staining can be found in Appendix 1.

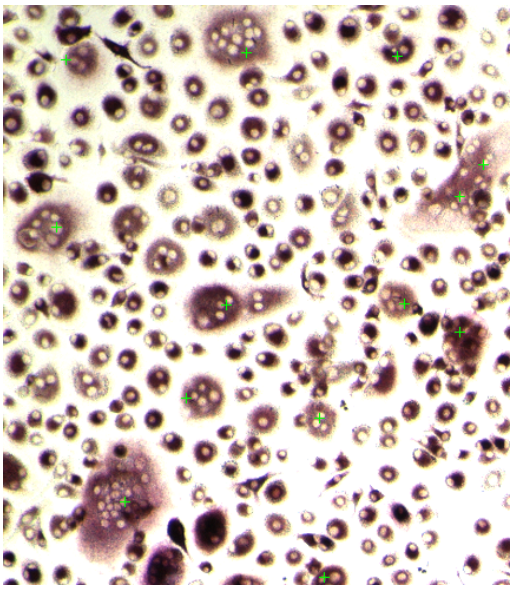

Figure 7: Counting of TRAP-positive, polynuclear osteoclasts. Imaging of stained cells was performed using EVOS FL Auto Cell Imaging System (Thermo Fisher) and the cells were counted manually using the program NIS Elements Microscope Imaging Software (Nikon Instruments). The counting was performed without knowledge of experimental setup, and criteria for osteoclasts were TRAP stained cells with three or more nuclei.

Determining the effect of IL-32-containing exosomes on osteoblasts

Gene knock-out by CRISPR/Cas

To evaluate the role of IL-32-containing exosomes on osteoclasts and osteoblasts, the IL-32 gene was knocked out in the well-established myeloma cell line JJN-3. The knock-out was performed by M. Zahoor using the gene interference system CRISPR-Cas, generating two knockout (KO) lines, designated B11 and D1. JJN-3 cells without IL-32 knockout were exposed to the same protocol conditions and used as "mock" control (designated wild-type (WT) in further sections). Description of knock-out procedure and the principles of CRISPR/Cas can be found in Appendix 3.

Following IL-32 knock-out and selection of IL-32 negative cells, clonal propagation of successfully transfected clones and wild-type was performed. When sufficient cell numbers were obtained, the clones were cultured at high density for 48 hours in media containing exosome depleted FCS followed by exosome isolation by ultrasentrifugation. The exosome-fraction was reconstituted in PBS and treated to MSCs cultures during osteogenic differentiation, 20 µL/ 600 µL differentiation medium. Media were replenished every 3-4 day, each time supplementing with freshly thawed exosomes.

Principle of exosome isolation

EVs can be divided into three major population based on size and origin; apoptotic bodies, shedding vesicles and exosomes, the latter being the smallest, 40-100 nm in diameter and of endocytic origin[132]. Differential centrifugation is the most common method for isolation of exosomes. By performing successive rounds of centrifugation with increasing force and duration, cells and particles sediment in a stepwise manner, dependent on size and density[132]. The different components in the cell culture media are separated by sedimentation in the following order; cells, apoptotic bodies and cell debris, shedding vesicles and exosomes. There are several biases concerning differential centrifugation. First, the different types of EVs show nearly similar sedimentation properties, with overlapping dimensions and densities, so the exosome population may be dispersed with other vesicular particles. Also the yield

may be reduced by co-sedimentation of exosomes with larger particles in early centrifugation step. Finally, the choice of centrifuge rotors is also a determinant of total exosome yield[132].

Procedure for exosome isolation

JJN-3 knockout cell lines and wildtype were cultured in a density of 0.8 million cells/mL for 48 hours in media with 10 % exosome depleted FCS (exosome depletion of FCS were achieved through ultracentrifugation at 120000×g for 16 hours). Culture media were harvested and cells removed by centrifugation at 112×g for 8 min. The supernatant was centrifuged again at 448×g, for 8 min, followed by high-speed centrifugation (8500×g) for 20 min using Thermo Scientific™ Sorvall™ (Thermofisher) to remove dead cell and debris. The exosome media were then filtrated with 0.20 µm filter to remove residual cell particles. The next centrifugation step was performed at Beckman Coulter ultracentrifuge 120000×g for 70 min. The pellet, now containing exosomes, was washed by resuspending in 400 µL sterile PBS, followed by a second ultracentrifugation. The purified exosomes (from 50 mL media) were resuspended in 200 µL differentiation media or PBS (the latter for osteoclast stimulation), and then sterile filtrated with 0.20 µm filter. The exosomes were stored at -80 ˚C prior to use in stimulation experiments

Validate IL-32 knockout in JJN-3 clones by Western Blot

I performed western blot on lysates from the two IL-32 KO clones B11 and D1 and the WT to validate the knock out of IL-32.

The principle of Western Blot

Western blotting, also known as immunoblotting is a well-established method for protein analysis and allows for detection of a single protein among many proteins present in a sample[133]. Western blot combine separation of proteins by polyacrylamide gel electrophoresis and antibody mediated detection of the protein of interest. The first step in protein analysis is protein extraction. For cell cultures, the most common method for lysis is resuspending the cell pellet in a buffer containing a detergent. To be able to compare protein levels between samples it is important to load equal amounts of protein from each sample. In this case the

protein quantitation was performed using the colorimetric Bradford assay, which is based on reaction between positively charged amino acids and Comassie Blue[134].

To separate proteins based on molecular weight by migration towards the positive anode, the native charges must be masked by an anionic detergent, in this case lithium dodecyl sulfate, which cover the proteins and gives them an overall negative charge. By including the reducing agent DTT, the secondary and tertiary structures are disrupted[135]. The polyacrylamide gel consist of crosslinked monomers and polymers in which smaller proteins easy travel through the pores while larger proteins are retarded, resulting in size dependent separation. To enable immunodetection, the proteins are first transferred from the gel onto a nitrocellulose membrane by electroblotting. The immunodetection is usually performed in two steps: first binding to a primary antibody specific for the target protein, and then detection by adding an secondary antibody conjugated to an enzyme, fluorophore or isotope. Horseradish peroxidase is commonly used for detection, generating a chemiluminescent signal when adding a peroxide substrate[135]. To recognize the target protein the bands are compared to the ladder with proteins of known weights[134]. To adjust for protein loading differences, another protein, usually from a housekeeping gene, is detected at the same membrane and used for normalization[136].

Reagents used in Western Blot

Tween- Tris buffered saline (T-TBS) was prepared by adding 500 mL of 1 M Tris HCl (pH 7.5), 300 mL 5 M NaCl and 100 mL 10% Tween 20, and water up to 10 L. Lysisbuffer was prepared by combining NP40 (1 %), 50 mM NaCl, 50 mM Tris-HCl and glycerol (10 %) Complete™, Mini, EDTA-free Protease Inhibitor Cocktail (Sigma Aldrich), 50 mM NaF and 1mM Na3VO4 (Sigma Aldrich). 0.1 M DTT sample buffer was prepared by diluting 1M DTT solution (PanReach AppliChem) in NuPAGE® LDS Sample Buffer (4X) (ThermoFisher). SeaBlue and Magic Mark ladders were purchased from Invitrogen. 5% and 1 % BSA/Tween-Tris Buffered Saline (T-TBS) solutions were prepared by diluting BSA (Sigma Aldrich) in T-TBS. Goat Polyclonal Human IL-32 Antibody was purchased from R&D Systems and diluted 1:1000 in 1 % BSA/T-TBS, while Polyclonal Rabbit Anti-goat Immunoglobulins /HRP) was purchased from Dako and diluted 1:2000 in 5 % BSA/T-TBS. Mouse monoclonal GAPDH antibody (Abcam) was diluted 1:40 000 in 5 % BSA/T-TBS. Polyclonal goat anti-mouse antibody/HRP (Thermo Fisher) was diluted 1:5000 in T-TBS. Super Signal® West Femto

from Thermo Fisher was prepared shortly before use, combining equal proportions of Super Signal peroxide buffer and Luminol Enhancer Solution.

Procedure for Western Blot

JJN-3 IL-32 KO cell lines and WT were cultured in standard conditions using 10 % FCS in RPMI 1640. From each cell line, 3×10^6 cells were harvested and lysed by adding 120 µl lysisbuffer to the pellet. The reconstituted pellet were vortexed followed by incubation on ice for 30 min. The mix were centrifugated at 13000×g in 15 min, to separate cell debris and protein. The protein content of each supernatant was evaluated using Bradford reagent (Sigma Aldrich) and BSA (Sigma Aldrich) standards (starting at 2 mg/ml, 1:2 dilutions) as reference. Bradford reagent combined with sample (2 µl) or BSA (1:2 dilutions, starting at 10 µl) were prepared in a 96-well plate and the absorbance measured at 595 nm using BioRad microplate. To obtain the same protein concentration in all samples they were diluted in lysisbuffer using measured protein levels as reference. Samples were prepared for gel electrophoresis by adding 5 µl 10% DTT in NuPAGE® LDS sample buffer to 15 µl sample, followed by heating to 70°C for 10 min and a brief centrifugation. 3.5 µl of SeeBlu and 2.5 µl of Magic Mark ladders were 18 µl of each sample were loaded to the lanes in a NuPAGE 10mm×10well 4-16 % Bis-Tris gel (Invitrogen) mounted in a X Cell Sure Lock™ (Invitrogen) The gel was run in MES SDS running buffer (Invitrogen) at program 1 at Power Ease 500 (Invitrogen): Step 1: 30 min, 80 V, step 2: 30 min, 150 V, step 3: 3 h, 180 V (all 120mA). The run was terminated after 80 min and the gel were blotted onto a nitrocellulose membrane (iBLOT® 2NC mini stacks membrane , Invitrogen) The blotted membrane were then blocked for 1 h using 5 % BSA/T-TBS as blocking buffer and incubated over night with goat polyclonal human IL-32 antibody (R&D systems). Following removal of primary antibody, the membrane were washed 3×5 min with T-TBS before incubation with secondary antibody (polyclonal rabbit anti goat) conjugated to horseradish peroxidase (HRP) for 1 hour. The membrane were washed thoroughly (5 × 5 min) with T-TBS before bands were visualized by chemiluminescence using 2 mL Super Signal® West Femto. The membrane was transferred to a plastic film before imaged on Licor Odyssey FC (LI-COR Biosciences, NE, USA). To adjust for differences in protein concentration between samples, GAPDH was used as internal loading control protein, by detection on the same membrane. The membrane was incubated in 60 minutes with Mouse monoclonal GAPDH antibody and washed 3×5 min with T-TBS,

before incubated with secondary antibody (goat anti-mouse /HRP). The chemiluminescent signal was detected by adding Super Signal® Femto and imaged on Licor Odyssey.

Evaluate effects of rhIL-32 on mRNA gene expression in osteoblasts and MSCs by RT-qPCR

Expression of genes involved in osteoblast differentiation, as well as genes involved in the vitamin D metabolism was measured by RT-qPCR. Also expression of IL-32 in MSCs was evaluated. The procedure of RT-qPCR can be divided into RNA isolation, followed by cDNA synthesis and finally, the polymerase chain reaction, where amplification and quantification of the mRNA of interest are performed.

Quantitative Real Time- PCR

Quantitative real time PCR (qPCR) is a technique that quantifies the expression of genes in "real time", which means to measure the gene expression directly during the polymerase chain reaction, using fluorescent probes or dyes[137]. Reverse transcription (RT)- qPCR is a variant of PCR that exploit the ability of an enzyme called reverse transcriptase to transcribe RNA to complementary DNA (cDNA), which then are used as template in the qPCR reaction, In conformity with traditional PCR, real time PCR can be divided into three phases, an exponential phase where the product is doubled for every cycle, the linear phase where the reaction slows down and both the reaction components as well as the products are decreasing, and a plateau phase where the reaction is completely finished[138]. The PCR based technique allows for relative quantification of gene expression in different samples. The term relative quantitation refers to the quantification of differences in mRNA levels between multiple samples[138]. The results are expressed as a fold-change or fold-difference in expression levels across the samples, relative to the levels in a reference sample and normalized by expression levels of an endogenous control gene[138]. The endogenous control should not differ between the samples, thus highly and constitutively expressed genes are used, such as housekeeping and maintenance genes[139]. In this case Glyceraldehyde-3-phosphate dehydrogenase (GAPDH) was used as endogenous control, but for hypoxia experiments GAPDH was unfavorable as internal control because it is itself upregulated in hypoxic conditions[140]. Instead, the TATAA-box binding protein (TBP) was used for normalization in these experiments. In the

quantitative RT-qPCR experiments in this thesis, the comparative C_t method ($\Delta\Delta C_t$ method) was used to calculate fold differences (RQ) between samples. The concept for calculating RQ by the C_t-method is described in Appendix 5. The C_t (threshold cycle) value describes the intersection between the amplification curve and the threshold line[138]. The threshold is set to a level where the target amplification is significantly above the background signal[138]. Thus, the C_t -value reported for each well is a measure of when the target is amplified to a significantly high level. The more target available in the sample, the earlier the amount of amplicon reach a significant level, and the lower the C_t-value[138]. If a C_t value is high (between 34-40) it implies that the level of target RNA in that sample is very low, giving a less precise result, and a reduced ability to detect low-fold changes[138]. In this case we performed two-step real time PCR, where cDNA synthesis and the PCR reaction was performed in separated steps, further described in the following sections.

The principle of RNA isolation

The general steps of RNA isolation include lysis of cells, inactivation of RNases and then separation of the nucleic acid from cell debris[141]. A successful RNA isolation should produce a pure RNA sample, free from contaminants, including proteins, carbohydrates, lipids and importantly, DNA. There are many different methods available for nucleic acid extraction, but the most common in commercial kits is solid-phase extraction[141]. This extraction method is based on using spin columns, containing a solid phase that absorbs the nucleic acids, while other substances can be washed away[141]. In this case, we used High Pure RNA isolation Kit (Roshe) in which the column solid phase material was glass fiber fleece. The initial lysis of the sample was performed using a reagent that contains a detergent and and the salt guanidine hydrochloride which lyses the sample, inactivates RNases and facilitate binding of the RNA to the solid phase of the column[142]. Guanidine hydrochloride is a chaotropic agent that disrupts the hydrogen bonds between the nucleic acids and water and thereby aids RNA absorbance to the glass fiber fleece[143]. It also contributes to denaturation of proteins, including nucleases, by disrupting hydrophobic interactions in the tertiary structure[143]. Afterwards, lysis buffer and cell debris is removed by centrifugation, DNase is added to the filter to digest DNA present in the sample. While the RNA is retained in the column, DNA fragments and other contaminating substances are removed by repeated wash-centrifugation

steps using different wash buffers. Finally the purified RNA is eluted from the filter by adding a low salt-buffer[142].

Procedure for RNA-isolation

The cells were seeded in 6 wells-plate, 80 000 cells/well. When confluent (after 1-2 days) the cells were stimulated (each individual treatment are specified in Results) and cultured under these conditions until termination of experiments (6 hours-14 days). The cells were harvested using a cell scraper and centrifuged (5 min, 4˚C, 800×g), the pellets stored at -80 ˚C until RNA isolation.

For RNA isolation, High Pure RNA Isolation Kit (Roshe Applied Science) was used, all reagents provided. Cells were resuspended in 400 µL lysis buffer and 200 µL PBS. The sample was transferred to a glass fleece filter tube placed in a collection tube and centrifuged at 8000×g for 15 s. The flowthrough liquid was discarded and the collection tube and the filter tube again combined. 10 µl DNase were diluted in 90 µL DNase Incubation Buffer (100 µL per sample) and added onto the filter in the upper tube, followed by 15 min incubation in RT. 500 µl Wash buffer I were added to the filter tube and centrifuged at 8000×g for 15 s. Flowthrough were discarded and collection tube combined with filter tube. The step were repeated, this time using 500 µL of Wash buffer II. Next, 200 µL Wash Buffer II was added and the columns centrifuged at 13 000×g to ensure removal of all buffer. The collection tube was discarded and the filter tube placed in a 1.5 mL eppendorf tube. 40 µl elution buffer was added to the filter tube and the assembly centrifuged for 1 min at 8000×g. The RNA was immediately placed on ice, then concentration and quality of the eluted RNA measured on NanoDrop® ND-1000 Spectrophotometer (Thermo Scientific). Later the RNA were stored at -80 ˚C or taken directly to reverse transcription.

The principle of cDNA synthesis

Complementary DNA (cDNA) was synthesized from total RNA using the High Capacity RNA-to-cDNA kit (Applied Biosystems). The isolated RNA is not suited as a template for the DNA polymerase used in the PCR reaction, RNA must therefore be converted to complementary DNA. This action is performed by an enzyme; *revers transcriptase* (RT),

which is originally found in retroviruses. In the optimal temperature range, incubated in a buffer providing the correct conditions, and with the presence of deoxyribonucleotides and primers revers transcriptase is able synthesize DNA from a RNA template[144]. First the DNA is synthesized as a part of a RNA:DNA hybrid, followed by degradation of the RNA strand by RNase H or the enzyme itself[144]. Then the remaining ssDNA is used as template to synthesize double stranded cDNA[144].

Procedure for cDNA synthesis

The reagents for reverse transcription were left to thaw on ice before RT reaction mix was prepared by using the volume of components described in **Table 1**. The samples were diluted according to the sample with the lowest concentration using RNase free water to obtain a final volume of 9uL. The RT-reaction mix was aliquoted into PCR tubes, and briefly centrifuged before reverse transcription of RNA to cDNA was performed on a thermal cycler (2720 Thermal Cycler, Applied Biosystems), programmed to cycle at 37 °C for 60 min, at 95°C for 5 min, and 4°C until reaction termination.

Table 1: Volume of components included in the reverse transcriptase reaction

Component	Volume/Reaction	
	+RT	-RT
2×RT Buffer	10 µl	10 µl
20×RT Enzyme Mix	1 µl	-
Nuclease-free H_2O	9 µl	10 µl
Sample		
Total per reaction	20 µl	20 µl

The principle of Taqman assay

Taqman assay is a well-established and reliable application for analysis of gene expression in real time PCR. In addition to the two PCR primers, the application includes the sequence specific TaqMan® probe, which is designed with a fluorescent molecule at its 5'end and a quencher at its 3'end[145]. The quencher is in reality a long wavelength fluorophore that accepts and thereby quenches the energy transferred from the short-wavelength fluorophore, preventing it from emitting light. This energy transfer is called Fluorescence resonance

energy transfer (FRET), and is only present when the fluorophores are in close proximity[145]. The main steps of the TaqMan reaction are presented in **Figure 8**. Following the denaturation step of the PCR reaction where the cDNA strands separates, the TaqMan® probe anneal to the internal sequence of the target cDNA. During synthesis of the new strand the probe is cleaved by the 5' nuclease activity of the Taq-polymerase[133]. As a result of cleavage the fluorescent reporter molecule is separated from the quencher, disrupting FRET and thereby producing a fluorescent signal proportional to the amount of product amplified[145].

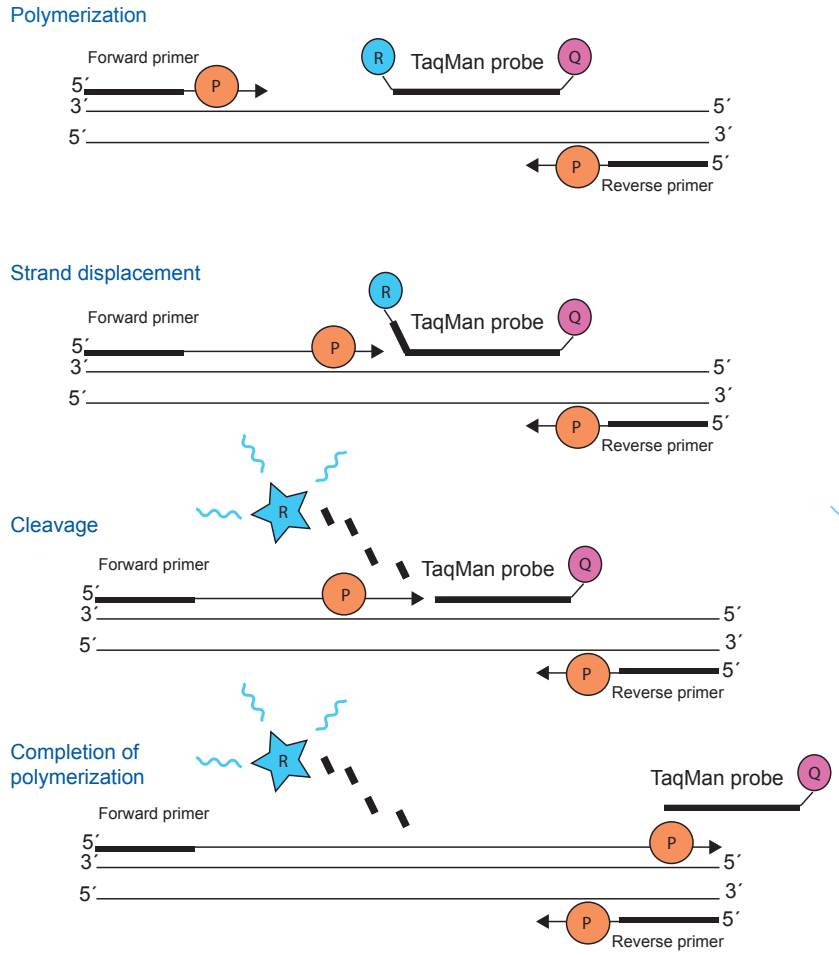

Figure 8: The principle of TaqMan Assay. Following denaturation of the dsDNA strand and annealing of the TaqMan probe, the Taq DNA polymerase synthesize new strand from the primers specific for the target gene. The nonflourescent quencher molecule on the 3'end of the TaqMan probe quenches the signal from the fluorescent dye on the 5'end. During polymerization the DNA polymerase displaces and cleaves the TaqMan probe by its 5'nuclease activity. The dye is separated from the quencher releasing a fluorescent signal. Information presented in figure is taken from Thermo Fisher, TaqMan® Chemistry vs. SYBR® Chemistry for Real-Time PCR[145].

The probe and primers used in the Taqman-assay is specific for the gene of interest, while the master mix provided by the manufacturer contain the rest of the unspecific ingredients needed, including dNTPs, passive reference dye, thermostable hot start DNA polymerase and other buffer components[145]. In the current project TaqMan® Universal PCR Master Mix was used, which includes AmpliTaq Gold® DNA polymerase, ROX internal passive reference dye for normalization of the reporter dye, and AmpErase®UNG, and dNTPs with dUTP. The reason for including dUTPs instead of dTTPs is to make carry-over contamination from previous PCR amplifications prone to degradation by the uracil DNA-glycolsylase UNG[146]. The temperature cycling in each round of PCR are necessary for correct timing of the uracil-cleavage, the polymerase activation, template denaturation and extension (presented in **Table 2**).

Table 2: Thermal cycling conditions for the RT-qPCR reaction, using TaqMan Gene Expression Master Mix Protocol [147]. Adapted from table 2, TaqMan® Gene Expression Master Mix, Protocol, 2007, (Applied Biosystems).

Steps	AmpErase®UNG incubation to cleave uracil containing PCR products	AmpliTaq Gold® DNA polymerase activation and deactivation of UNG	PCR reaction (40 cycles)	
			Denaturation of cDNA template	Annealing of primers and extension of template by DNA polymerase
Time	2 min	10 min	15 sec	1 min
Temperature	50 °C	95 °C	95 °C	60 °C

Procedure for TaqMan qPCR

cDNA was diluted with sterile ion free water to 1-2 ng cDNA/ µl. Taqman probe and mastermix was prepared in tubes (according to **table 3**) for each target gene, and adjusted with water to obtain 20 µl per well when combined with sample. All components for reaction was prepared in a 96-well PCR plate (MicroAmp®, Thermo Fisher) and sealed with transparent adhesive film (MicroAmp) Thermo Fisher) before centrifuged at 1500 rpm in 2 minutes to spin down contents and eliminate air bubbles. The plate was then run on StepOne Plus Real Time PCR machine (Applied Biosystems), programmed at 2 hours run, comparative Ct-method, Taqman reaction. The cycle parameters were 50 °C for 2 min, 95 °C for 10 min,

95 °C for 15 sec and 60 °C for 1 min (**Table 2**)[148]. The gene expression was quantified by the comparative CT method using StepOne Software™[148].

Table 2: Components and volumes of the TaqMan qPCR (Applied Biosystems).

Component	Volume/reaction
TaqMan Universal PCR Master Mix	10 µl
TaqMan probe	1 µl
cDNA template + H_2O	9 µl
Total per reaction	20 µl

Evaluate IL-32 effects on early osteoblast differentiation by measuring the activity of alkaline phosphatase (ALP)

Principle of ALP-assay

Alkaline phosphatases is a group of several tissue-spesific isoenzymes that hydrolyze phosphate in alkaline environment, producing an organic radical and inorganic phosphate in which one of the forms, bone-specific alkaline phosphatase (BAP) is being highly expressed in (trabecular) bone[149,150]. The enzyme, which is expressed on the cell membrane of osteoblasts as well as matrix vesicles budding from these cells, is known to play an important role in bone mineralization, although the mechanism behind is not completely understood[149]. Alkaline phosphatase is in medical research considered as an important biochemical marker of osteoblastic activity, and can be detected trough various substrate signal amplification assays[151]. Enzyme-Labeled Fluorescence (ELF) substrate (ELF® 97 Endogenous Phosphatase Kit, Thermo Fischer) can be used to detect ALP activity. When hydrolyzed by ALP the substrate produces a yellow-green fluorescent precipitate that emit light at 530 nm. In order to adjust the ALP assay results for differences in cell number the amount of DNA in each sample can be measured using SYBRGreen (Molecular Probes), a fluorescent dye that binds specifically to double stranded DNA and emit light in proportion to the DNA concentration[72,152].

Procedure for ALP-assay

The ELF 97 Endogenous Phosphatase detection Kit (Molecular probes, Eugene, OR) was used to quantify alkaline phosphatase (ALP) activity. MSCs were seeded in 96 wells plates at density 2500 cells/well and stimulated to osteogenic differentiation (200 ul/well) in combination with different concentrations of rhIL-32 alpha and rhIL-32 gamma, and the pro and active form of vitamin D (concentrations in reported in Results). Media were replenished every 3-4 day (-100 µl, + 100 µl). At day 5 and day 7 the cells were fixated by adding 100 µl 4 % paraformaldehyde (PFA) to each well, incubating for 10 minutes at room temperature. To permabilize the cells they were incubated for 15 minutes with 200 µl 0.2 % Tween in phosphate-buffered saline (PBS) per well. Rinsing of the cells were repeated twice with 0.90 % natrium chloride, the last time leaving the plate in water for 10 minutes. The ELF substrate was diluted 1:20 in substrate buffer and 50 µl was added to each well and left for 5 minutes. The amount of fluorescence was measured using the ELF function (355 nm excitation filter and 535 nm emission filter) on Walla Victor3^{TM} 1420 Multilabel Counter (Perkin Elmer).

To quantify the DNA in each sample, the substrate was removed and the plate was rinsed in PBS. Later the cells were lysed in 1xSSC/100 µg/ml proteinase K buffer, 150 µl per well, using the pipette to gently loosen the cells from the bottom of the wells. A salmon sperm DNA standard curve was made by diluting 100 µg/ml 1xSSC/100 µg/ml proteinase K buffer 1:2. Triplets of 150 µl were added to a separate 96-well plate. Both plates were incubated at 56 $°C$ for 60-90 minutes. Sybrgreen (Molecular Probes) was diluted in water 1:500, and 10 µl were added to each well. The fluorescence was measured using the multilabel counter Walla Victor™ 1420.

Evaluate IL-32 effecs on osteoblast proliferation using the CellTiter-Glo assay

Proliferation of MSC derived osteoblast in response to rhIL-32 and rhIL-32/vitamin D stimulation was evaluated by measuring ATP levels in cultures by CellTiter-Glo (CTG).

Principle of CellTiter-Glo assay

CellTiter-Glo ®(CTG) Luminescent Cell Viability Assay (Promega) was used to evaluate proliferation of osteoblast after stimulation with IL-32. In the CTG-assay the number of viable cells in culture is quantified by measuring the level of adenosine 5`triphosphate (ATP) present in each sample[153]. ATP is the principal carrier of energy in cells, and can therefore be used as an indicator of metabolically active cells[153,154]. By adding single reagent (CellTiter-Glo® Reagent) to each well, the cells are lysed and a luminescent signal is generated[153]. The reagent contains a thermostable luciferase that catalyzes the mono-oxygenation of luciferin when ATP is present together with Mg^{2+} and molecular oxygen[153] (**Figure 9**). The luminescent signal created in this reaction is proportional to the amount of ATP present, which again is directly proportional to the number of viable cells. The luminescent signal has in general a half-life greater than five hours[153].

Figure 9: The principle of Cell-titer Glo[153] Luciferase mono-oxygenates luciferin in the presence of ATP, Mg^{2+} and O_2 and a luminescent signal generated.

Reagents used in CTG-assay

The CellTiter-Glo® Luminescent Cell Viability Assay was purchased from Promega (Madison, Wisconsin). CellTiter-Glo® Reagent was prepared by adding CellTiter-Glo® buffer to CellTiter-Glo® substrate, and stored at - 20°C.

Procedure for CTG-assay

MSCs were seeded in 96-well plates at a density of 2500 or 5000 cells/well and cultured in MSCGM to confluence. The media were then changed to osteoblast differentiation media included rhIL-32 and pro- and active vitamin D (concentrations specified in Results). Media were replenished if the experiment exceeded 3 days. At day 3, 5 or 7 after stimulation, 100 µl of CellTiter-Glo® Reagent was added to each well. The plate was covered in aluminum foil and incubated on a shaker at 300 rpm for 10 min The luminescence was then measured at using the luminometer function on Walla Victor™ 1420 multilabel counter (Perkin Elmer).

Evaluate rhIL-32 effects on osteoblast mineralization by Alizarin Red-S Staining

The principle of Alizarin Red S-staining

Alizarin Red S (ARS) staining is a well-described method for evaluation of calcium-rich deposits in cell cultures[155]. The Alizarin red S dye absorbs to the calcium portion of the mineral compound hydroxyapatite ($Ca_{10}(PO_4)_6(OH)_2$ which is the main inorganic component of bone[155,156]. Whether ARS interact with Ca^{2+} to form a salt or a chelate is not fully elucidated- the colored precipitate may contain both[156]. The ability of ARS to assay mineralization through calcium is an advantage compared to other methods that are based on measuring inorganic phosphate, which is highly present in cells and culture media[155]. ARS allows both qualitative and quantitative evaluation of mineralization; the mineral distribution can be observed directly from color precipitates in each well, then the dye can be extracted from the monolayer and quantified by spectrophotometry.

Reagents used in ARS-staining

Cetylpyridinium chloride (CPC) and Alizarin Red S were purchased from Sigma Aldrich. ARS was reconstituted in distilled water to obtain a concentration of 40 mM. pH was adjusted to 4.2 using NaOH. 10 % CPC sodium-phosphate buffer were prepared by reconstituting CPC in a sodium phosphate buffer which was adjusted to pH 7 by adding NaOH.

Procedure for ARS-staining

MSCs were seeded at a density of 15 000 cells/well in 24-wel plates and cultured in MSCGM (600µl/well) for 1-2 days. At ~ 80 % confluence, the cells were then stimulated in osteogenic direction using differentiation media (600µl/well) with different concentrations rhIL-32 and the pro and active form of vitamin D (for details, se Results). Media were replenished every 3-4 day by removing 200-250 µl and adding 300-400 µl. At day 14, 15, 16 or 21 the experiment were terminated by removing media and fixating cells on ice using 4 % PFA, 250 µl/well, incubating for 10 min. Following removal of PFA, the cells were carefully washed twice, first with PBS (300 µl/well), then with (500µl/well) physiological salt water (NaCl, 0.9 %). Staining of cells was performed by adding 250 µl 40 mM Alizarin- Red S to each well and incubating on a shaker for 30 min (60 rpm). The wells were then washed carefully with physiological salt water, 500 µl/well. The wash step was in total repeated 5 times, followed by incubation with 300 µl PBS for 15 min. Finally, the PBS were removed stained wells were photographed using a system camera mounted on a microscope.

The wells were kept in the fridge and later dye extraction were performed by adding 300 µl 10% CPC diluted in sodium-phosphate buffer (pH 7) and incubate on a shaker (70 rpm) for 60 min. Standard curve were prepared by using stock solution of Alizarin Red-S (40 mM), starting at 800 µM and diluting 1:2 in 10% CPC/sodium-phosphate buffer. Following incubation the samples were diluted 1:2 or 1:10 depending on the color intensity. Samples and standard curve were aliquoted on a 96-well plate (100 µl/well) and absorbance were measured using iMark™ Microplate Absorbance Reader from BioRad. The concentration of each sample was calculated from the absorbance values using the standard curve as reference.

Evaluate the effect of IL-32 on CYP27B1-activity

To obtain a quantitative measure of CYP27B1 activity in IL-32 stimulated osteoblasts the amount of biosynthesized 1,25 $(OH)_2$ D_3 in media was measured. The cells were seeded out in 24 wells plate at a density of 15000 cells/well. Two days later, when confluent, cells where stimulated with IL-32 and pro Vitamin D. The media was renewed every 3-4 day (-200 ul/+ 400 µl). The media were harvested from each well at day 15, and spun down once (5 min, 800×g) to remove cell debris and the supernatant was stored at -80 ˚C. The $1,25(OH)_2D_3$ EIA kit from (Immunodiagnostic Systems) was used to determine the level of biosynthesized 1,25

$(OH)_2$ D_3 in the supernatant. Because the $25(OH)D_3$ metabolite is circulating in the body at significantly higher levels than $1,25(OH)_2D_3$, and also is present in higher levels in $25(OH)D_3$ supplemented media, like in this case, there is risk for unspecific binding in the ELISA. [157]. Thus, a preliminary purification step where $1,25(OH)_2D_3$ is specifically isolated is recommended. For the ELISA kit from IDS this challenge is solved by including an immunoextraction of $1,25(OH)_2D_3$. Following the initial purification, $1,25(OH)_2D_3$ is quantified by a enzyme immunoassay based on competitive ELISA principles. The protocols for immunoextraction and ELISA are shown in Appendix 2, while the main steps of the 1,25D EIA are illustrated in **Figure 10**.

The principle of ELISA

ELISA (enzyme-linked immunosorbent assay) is an analytical technique where a solute of interest are immobilized to a solid surface and then detected by adding an enzyme-conjugated antibody and incubated with a substrate, producing a measurable signal[133]. Because the structural and chemical properties of the analyte as well as the nature of the sample solution itself vary, many different types of ELISA have been developed[158]. Direct, indirect, sandwich and competitive ELISA are the most common approaches, all frequently offered in commercial kits. In this case we used a competitive ELISA. The term competitive refers to the incubation step where sample antigens compete with assay provided antigens for the primary antibody binding sites[158] as illustrated in **Figure 10**. The add-in antigens are complexed with an antibody-enzyme conjugate, so when a substrate is added, the signal produced will be proportional to the number add-in's bound[158]. Therefore, in a competitive ELISA the absorbance is inversely correlated with the amount of antigen present in the sample; the higher concentration of analyte, the lower absorbance[158].

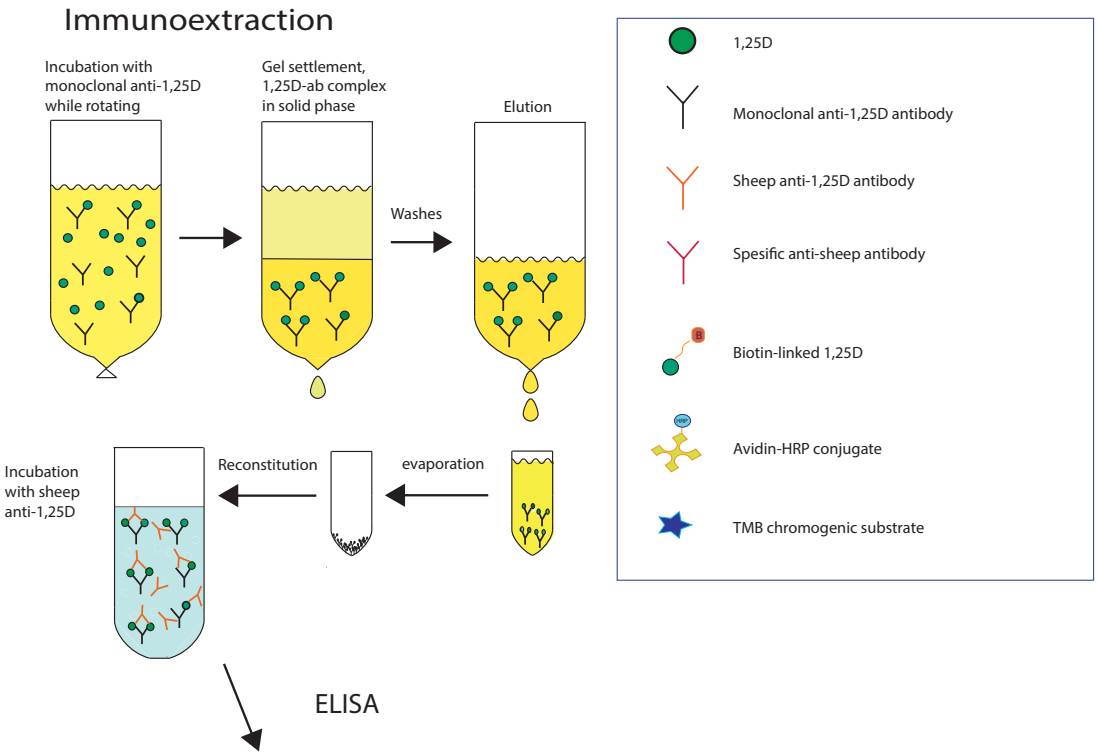

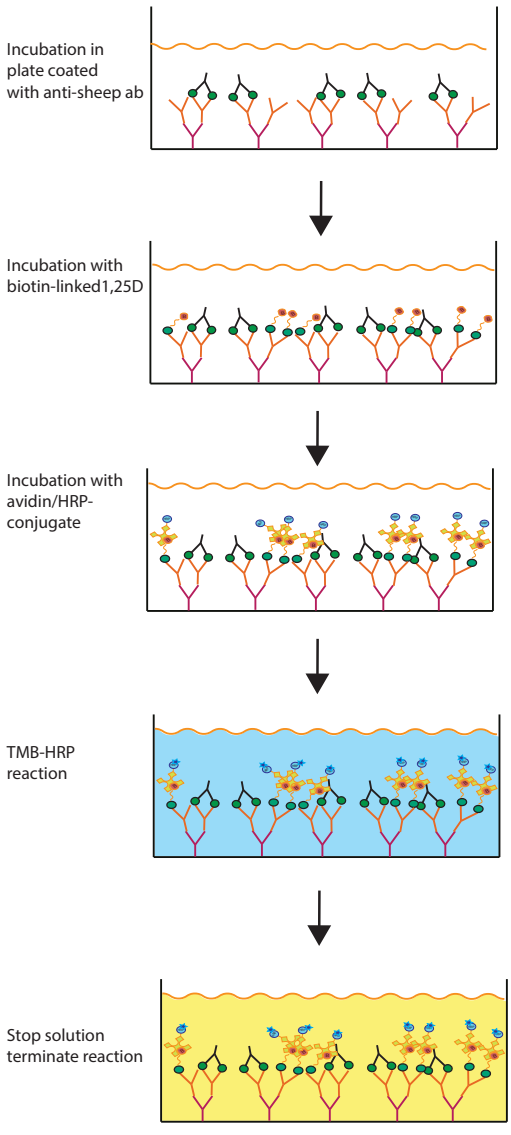

Figure 10: 1,25 dihydroxyvitamin D ELISA: The main steps of the 1,25 dihydroxyvitamin ELISA. including immunoextraction and detection assay. In the 1,25 dihydroxyvitamin D EIA from IDS, samples is immunoextracted to remove potential cross-reactants, as for example $25(OH)_2D_3$. In the immunoextraction step the samples are incubated with a solid phase monoclonal antibody specific for $1,25(OH)_2D_3$. The gel that forms contain $1,25(OH)_2D_3$. Following repeated washes of the gel the purified $1,25(OH)_2D_3$ is eluted and excess liquid is then removed by evaporation. The reconstituted eluates and calibrators are then incubated overnight with a sheep antibody specific for $1,25(OH)_2D_3$ Then the samples are transferred to a plate coated with specific anti-sheep antibodies. Following incubation, biotin-linked $1,25(OH)_2D_3$ is added, binding to the leftover antibodies. The egg-white protein avidin binds with high affinity to the vitamin biotin, an property which is frequently exploited in ELISA[133]. In the current assay avidin conjugated to the

enzyme horseradish peroxidase is used. The binding is selectively against complexed biotin. When adding the chromogenic substrate 3,3',5,5'-Tetramethylbenzidine (TMB), color is developed, intensity correlated to the number of enzyme-labeled avidin-molecules bound. The level of $1,25(OH)_2D_3$ is determined through binding of the antigen in a competitive manner. Although the biotin linked-$1,25(OH)_2D_3$ is added in a later step, it indirectly competes with the sample $1,25(OH)_2D_3$ for binding to the sheep anti-1,25D. Because it's the 1,25D biotin that is linked to the enzyme through avidin, the presence of these complexes determines the color intensity in each well. In this assay the absorbance is therefore inversely correlated with the amount of $1,25(OH)_2D_3$ present in the sample.

Statistics

Statistical analysis were performed using GraphPad Prism 5, using unpaired two sided Student's t-test, one-way ANOVA combined with Dunnett's test or two-way ANOVA with Bonferroni post hoc test. Results were considered statistically significant when $p<0.05$, designated with *. In cases of three biological replicates (N=3) the results were normalized and presented as relative measures.

Results

The current thesis focuses on the role of IL-32 in myeloma bone disease. Initially we demonstrated that exosomes isolated from IL-32 expressing myeloma cells increased osteoclastogenesis while IL-32 depleted exosomes from myeloma IL-32 KO cells resulted in reduced number of osteoclasts in primary monocyte cultures. The major study objective was the effects of IL-32 on osteoblasts. Although some results indicate that IL-32 in combination with vitamin D may play a role in regulation of osteoblast differentiation and function, particularly in later maturation stages, we overall found no clear evidence for IL-32 exerting an effect on osteoblasts, neither alone nor in combination with $25(OH)D_3$. Exosomes from IL-32 D1 KO and IL-32 WT myeloma cells did not induce differential effects on mineralization when treated to osteoblasts. However, as we found the D1-clone used in the osteoblast assay to express a truncated version of IL-32, at the moment no conclusion can be made. Interestingly, we found that MSCs also express IL-32 and that the expression is increased by hypoxia and by IL-32 itself.

Part 1

Effect of IL-32-containing exosomes on osteoclast differentiation

Induction of osteoclastogenesis by recombinant IL-32 and by exosomes from IL-32 expressing cell lines was already shown by our group (Zahoor et al. manuscript in preparation). To clarify if the effect of exosomes was mediated by IL-32 we generated IL-32 myeloma knock-out cells using CRISPR/Cas. We then compared the effect of the two knock-out clones B11 and D1 to wild-type, on osteoclast differentiation. Primary monocytes obtained from the Blood Bank, St.Olavs Hospital, were isolated and differentiated in osteoclast differentiation media, with IL-32 KO and WT exosomes either from the monocyte stage (day 0) or from preosteoclast stage (day 5) and designated preosteoclast-experiments or post-osteoclast experiments respectively. To examine if the lack of effect on osteoclast differentiation was related to the loss of IL-32, the IL-32 KO osteoclast cultures were treated with rhIL-32.

For preosteoclast experiments osteoclast number were significantly higher in samples treated with IL-32 containing exosomes from JJN-3 WT compared to IL-32 depleted exosomes from JJN-3 IL-32 KO B11 cells (**Figure 11**) Also when adding RANKL, osteoclast number was significantly different between the respective exosome treatments. There was however an uncertainty in the results as the RANKL control was low and IL-32 KO B11 was poorly rescued by RANKL.

For post-osteoclast experiments (**Figure 12**) both the B11 and D1 IL-32 KO clones were used. Although not significant, a reduction in osteoclasts were found in cultures treated with IL-32 KO B11 derived exosomes. However, when comparing the B11 and WT treatments combined with RANKL there was a significant difference in osteoclast numbers**.** The low-osteoclast phenotype in B11 IL-32 KO exosome treated cultures was partly rescued to WT-osteoclast level by adding IL-32γ, and completely rescued by adding a combination of IL-32 and RANKL. No reduction in osteoclast numbers were observed for IL-32 KO D1-exosome treated cultures compared to WT-exosome treated cultures, and there were no effect of RANKL.

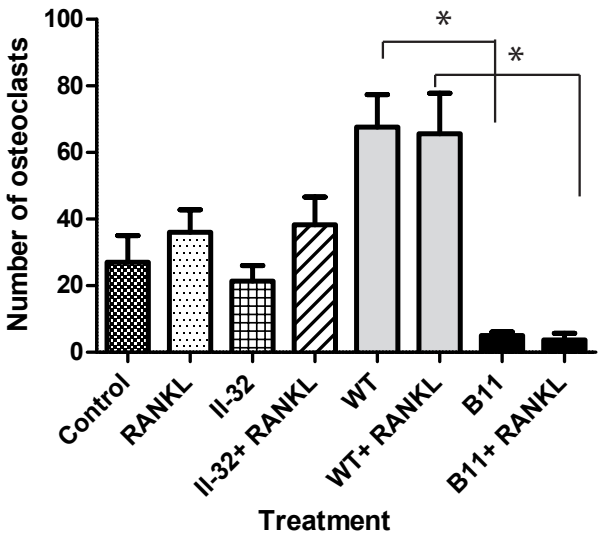

Figure 11: Preosteoclast-experiment: Number of preosteoclasts in cultures treated with IL-32 WT derived and IL-32 KO derived exosomes. Primary monocytes were seeded 8000 cells/well in 96-well plates and differentiated for 5-6 days with modified differentiation media, containing only MCS-F (30 ng/mL), including 5 ul exosomes/150 ul medium, with or without rhIL-32γ (25 ng/mL) and RANKL (50 ng/mL). The osteoclast differentiation was evaluated by TRAP-staining and subsequent counting of TRAP-positive, multinucleate osteoclasts. The data is presented as the mean+SEM of technical replicates. The results shown are from one representative experiment out of two (the other shown in Appendix 1). * indicates $p<0.05$ (unpaired two-sided Student's t-test)

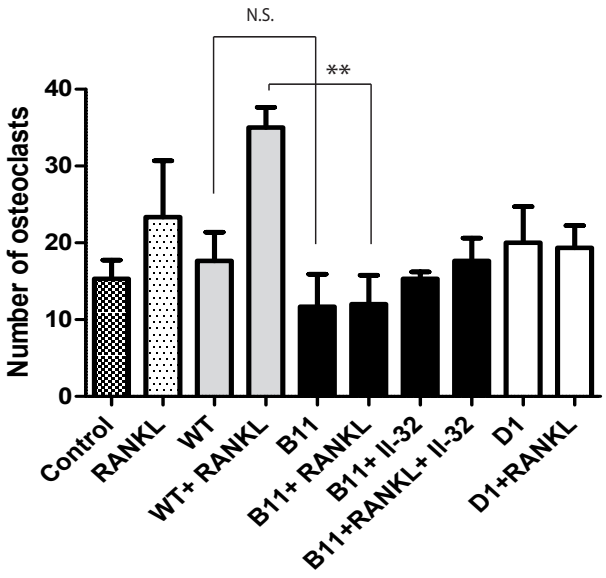

Figure 12: Post-osteoclast experiment: Total number of osteoclasts in cultures treated with IL-32 WT derived and IL-32 KO derived exosomes. Primary monocytes were seeded 8000cells/well in 96-well plates and differentiated into preosteoclasts with MCS-F (30 ng/mL) TGF-β (1ng/mL) and RANKL (10 ng/mL) before treated with 5 µL exosomes/150 ul medium, with or without rhIL-32γ (25 ng/mL) and RANKL (50 ng/mL). After 3 days the osteoclast differentiation was evaluated by TRAP-staining and subsequent counting of TRAP-positive, multinucleate osteoclasts. Data is presented as the mean+SEM of technical replicates. The experiment is one representative out of 3 independent experiments (the others shown in (Appendix 1). N.S. indicates $p>0.05$, ** indicates $p< 0.01$ (unpaired two-sided Student's t-test).

Part 2

Effect of rhIL-32 and IL-32- containing exosomes on osteoblast differentiation

Effect of rhIL-32γ and rhIL-32α on osteoblast differentiation

As preliminary data by Zahoor et al. showed that IL-32 alone increased osteoclastogenesis, the initial approach when turning our attention to osteoblasts was to treat the cells with different rhIL-32 isoforms and thereby evaluate the isolated effect of the cytokine on osteoblast differentiation. We searched current literature for optimal treatment concentrations of IL-32. In preliminary osteoclast experiments 25 ng/mL of IL-32 was the most effective in inducing osteoclastogenesis (Zahoor et al., manuscript in preparation) while in another study, mean±SD level of IL-32 γ measured in synovial fluid of rheumatoid arthritis patients was ∼5 ng/mL, while in osteoclast differentiation experiments in the same study, the concentration of 50 ng/mL were used to induce osteoclastogenesis[107]. We found no specific data on IL-32

concentration in the bone marrow, but the level of other cytokines, for example IL-3, were measured in the range of 0-10 ng/mL in bone marrow of multiple myeloma patients[159]. On this basis we chose to use concentrations of IL-32 in the range of 5ng/mL to 100 ng/mL. We employed the IL-32 isoforms γ and α in our stimulation experiments, as IL-32α is the main intracellular form[94] and IL-32 γ is characterized as a secreted form, and the isoform we suspected to be the secreted by the myeloma cells[160]. In most experiments we used osteoblasts cultured in differentiation media only (in figures designated "diff") as main control, MSCs cultured in MSCGM (basal) medium as negative control and osteoblasts differentiated in presence of BMP-2 as positive control.

First we evaluated the gene expression of RUNX2, which is a key transcription factor for osteogenic development, upregulated in early stages of osteoblast differentiation. Confluent MSCs were differentiated in osteogenic direction with osteoblast differentiation media with or without 5 ng/mL or 100 ng/mL rhIL-32 α and rhIL-32 γ for 3, 6 and 14 days (**Figure 13**). Then gene expression was evaluated by RT-qPCR. There were no significant differences in RUNX2 expression in any of the IL-32 treated samples compared to the control at day 3 (**Figure 13A**), neither at day 6 (**Figure 13B**). RUNX2 gene expression was also measured at day 7 (not shown), confirming the lack of differences between IL-32 treatment and control. As expected for an early osteogenic marker gene, *RUNX2* was detected at lower folds at day 14 (**Figure 13C**). At this time point also the BMP-2 control was low, indicating that there was in general decreasing levels of RUNX2 at this maturation stage. The low mRNA concentration may account for deviations in the data, as there was unexpectedly high RUNX2 expression in the sample treated with 100 ng/mL rhIL-32α. Alternatively it could indicate that IL-32α halts the osteoblasts in an immature stage.

We also evaluated the gene expression of Osterix, a transcription factor for late osteoblast differentiation[161], at day 7 and day 14 However, Osterix mRNA was not detected in any samples except the BMP-2 control, so the data are not presented.

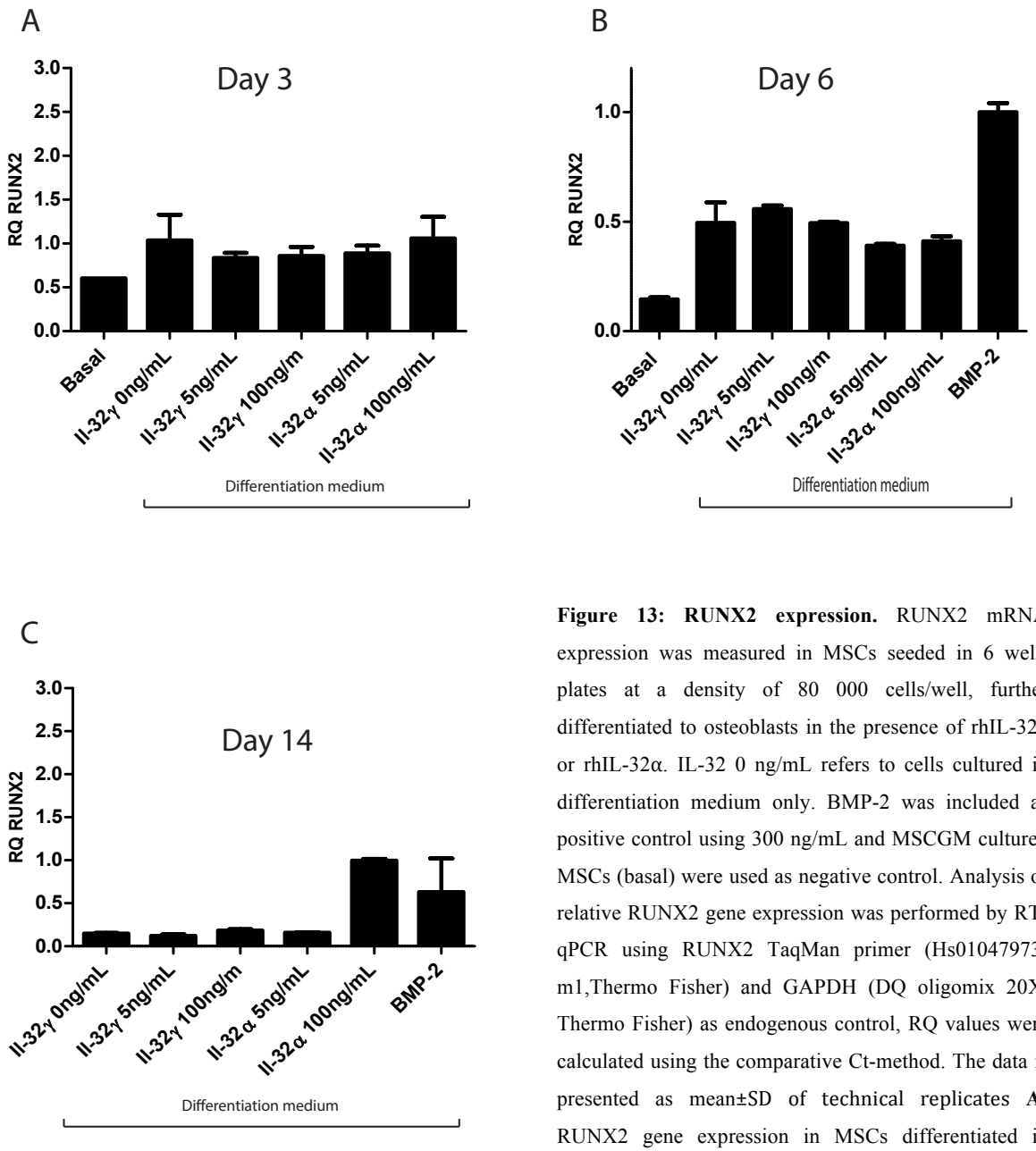

Figure 13: RUNX2 expression. RUNX2 mRNA expression was measured in MSCs seeded in 6 well-plates at a density of 80 000 cells/well, further differentiated to osteoblasts in the presence of rhIL-32γ or rhIL-32α. IL-32 0 ng/mL refers to cells cultured in differentiation medium only. BMP-2 was included as positive control using 300 ng/mL and MSCGM cultured MSCs (basal) were used as negative control. Analysis of relative RUNX2 gene expression was performed by RT-qPCR using RUNX2 TaqMan primer (Hs01047973-m1,Thermo Fisher) and GAPDH (DQ oligomix 20X, Thermo Fisher) as endogenous control, RQ values were calculated using the comparative Ct-method. The data is presented as mean±SD of technical replicates **A)** RUNX2 gene expression in MSCs differentiated in osteogenic direction for 3 days **B)** RUNX2 gene expression MSCs differentiated in osteogenic direction for 6 days **C)** RUNX2 gene expression in MSCs differentiated in osteogenic direction for 14 days.

To evaluate early osteoblast differentiation we also measured the activity of ALP, a phosphate hydrolytic enzyme involved in early bone formation events. MSCs were differentiated in osteogenic direction in the presence of IL-32γ or IL-32α. We tested the interleukin isoform at various concentrations to evaluate dose dependent responses. There was no effect of IL-32α (**Figure 14A**) or IL-32γ (**Figure 14B**) at day 5 for any of the concentrations tested; ranging

from 5 ng/mL to 100 ng/mL. ALP-activity for each sample was presented without adjustment for amount of DNA (see Material and Methods, ALP-assay) as we encountered problems with the protocol for DNA quantitation in the early experiments.

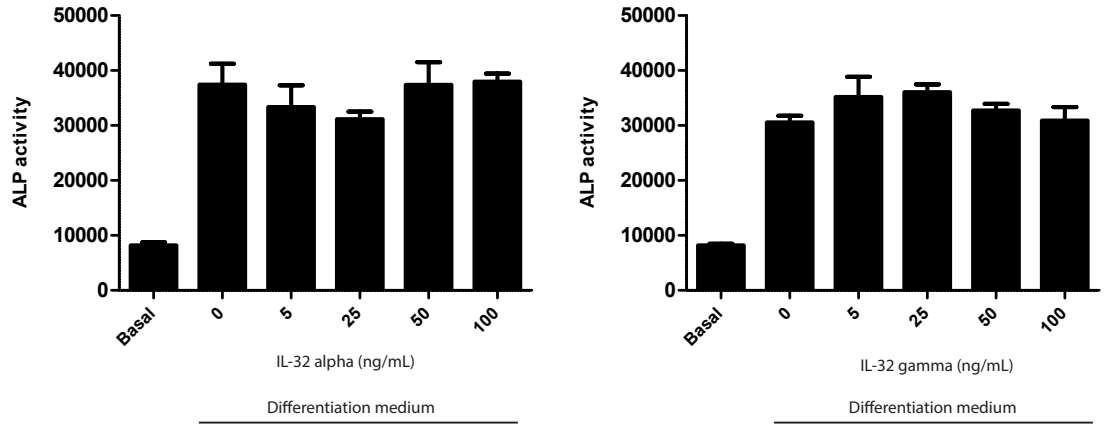

Figure 14: ALP-activity in preosteoblasts treated with rhIL-32. MSCs were seeded 5000 cells/well in 96-well plates and the day after differentiated in osteogenic direction in the presence of rhIL-32γ or rhIL-32α (concentrations indicated in figure). MSCGM (basal)-cultured cells were included as negative control. ALP-activity was measured after 5 days treatment, using ALP-assay. Data is reported as mean ± SEM of technical replicates. N.S. differences (comparing concentrations of rhIL-32 using one-way ANOVA, and Dunnett's test). The experiment shown is one representative out of two independent experiments (the other is shown in Appendix 5). **A)** ALP-activity in osteoblasts treated with rhIL-32α. **B)** ALP-activity in osteoblasts treated with rhIL-32γ.

Further on we evaluated mineralization in late osteoblasts by ARS-staining. The formation of bone takes place in a two-step process where osteoblasts synthesize organic matrix followed by mineral deposition to strengthen the elastic matrix[26]. The main mineral component hydroxyapatite can be measured by ARS-staining of the calcium proportion, and was therefore a parameter of mature osteoblast activity in our *in vitro* cultures.

The MSCs were differentiated in osteogenic direction for 15 and 21 days in the presence of rhIL-32γ or rhIL-32α. There were high levels of mineralization both at day 15 (**Figure 15A and B**) and at day 21 (**Figure 15C and D**), indicating that there is no effect of the two IL-32 isoforms on bone matrix mineralization.

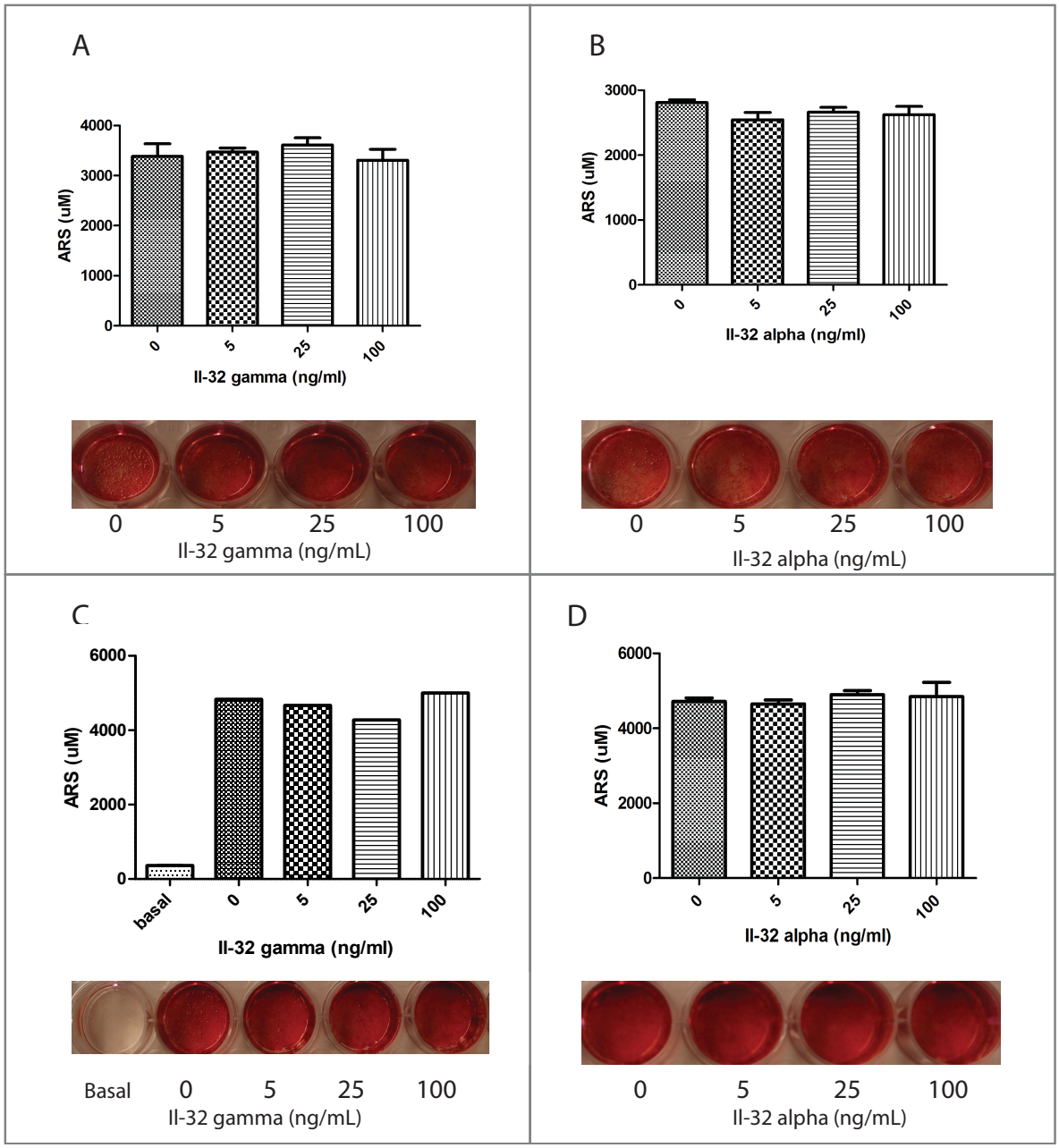

Figure 15: Mineralization in osteoblast after treatment with rhIL-32. MSCs were seeded 15000 cells/well in 24-well plates and cultured for two days before differentiated into osteoblasts in differentiation medium in the presence of rhIL-32γ or rhIL-32α (concentrations as indicated in figure). Mineralization was visualized by ARS-staining at day 15 and 21, followed by extraction of ARS from the monolayer and quantitation of color intensity. Concentration of ARS (uM) was determined by using an ARS standard curve. Data is reported as mean± SEM of technical replicates. **A)** Mineralization at day 15 in osteoblasts differentiated in the presence of rhIL-32γ. **B)** Mineralization at day 15 in osteoblasts differentiated in the presence of rhIL-32α. **C)** Mineralization at day 21 in osteoblasts differentiated in the presence of rhIL-32γ. Undifferentiated MSCGM cultured MSCs (Basal) were included as negative control. **D)** Mineralization at day 21 in osteoblasts differentiated in the presence of rhIL-32α.

Effect of rhIL-32γ and rhIL-32α on osteoblast proliferation

As inflammatory cytokines are known to both inhibit and promote cell proliferation[162], we wanted to assess the effect of IL-32 on MSC proliferation. An indirect way of measuring cell proliferation is to quantify the number of viable cells in cultures initially seeded at the same cell density. We measured cell viability in MSCs differentiated with rhIL-32 for 3 days, using the CTG assay that measures the level of ATP, which is a marker of metabolic active cells. No effect of proliferation was seen in MSCs treated with differentiation media in the presence of 0-100 ng/mL rhIL-32γ or rhIL-32α for 3 days (**Figure 16**).

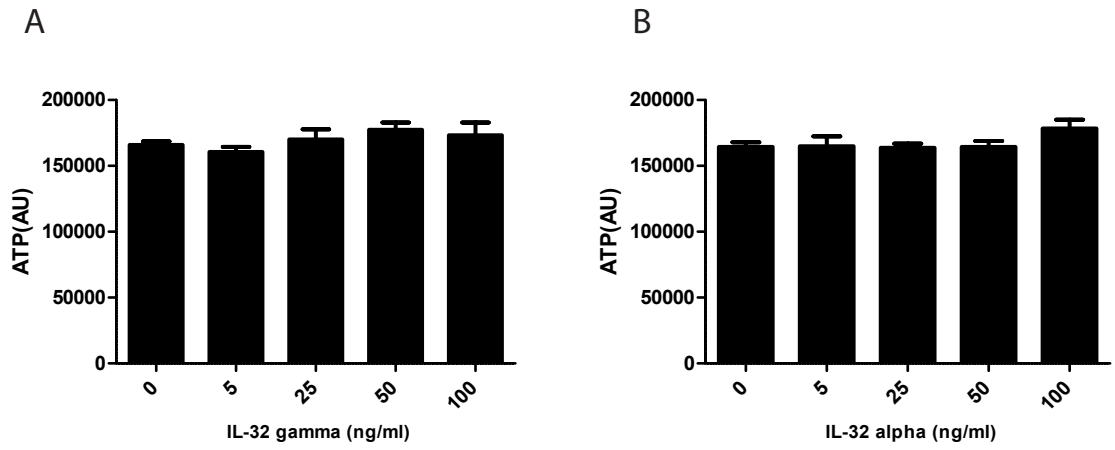

Figure 16: Proliferation of MSCs differentiatied in osteogenic direction for 3 days. Cells were seeded in 96-well plates at a density of 2500 cells/well, and the day after treated with differentiation media combined with rhIL-32α and rhIL-32γ at concentrations indicated. After 3 days the level of proliferation was evaluated by measuring ATP levels in each well by CTG assay. Data is reported as mean±SEM. (N.S using one-way ANOVA and Dunnett's test) **A)** Cell proliferation quantified by ATP level for cells treated with rhIL-32 γ. **B)** Cell proliferation quantified by ATP level for cells treated with rhIL-32 α.

Effect of rhIL-32 on RANKL expression

RANKL is an important inducer of osteoclast differentiation. We wanted to investigate if the rhIL-32 dependent increase in osteoclastogenesis shown in our *in vivo* mice experiments could be related to RANKL expression on osteoblasts. We therefore evaluated RANKL expression in early osteoblasts treated with the IL-32 isoforms γ and α (**Figure 17**). We also treated with parathyroid hormone (PTH), Poly(I:C) and LPS, the last two being a viral dsRNA analogue and a component from the membrane of gram negative bacteria, respectively[163]. All

are known to be potent promoters of RANKL[163,164] expression and therefore were used as positive controls.

Our previous experiences on RANKL predicted low levels and poor detection in qPCR. As expected RANKL mRNA levels were low, with Ct values> 35 for all samples except Poly (I:C) and LPS treated samples (**Figure 17**). The PTH control did not induce RANKL, indicating technical problems in the stimulation protocol. There were no significant differences between differentiation control (IL-32 0 ng/mL) and rhIL-32 treated samples, using one-way ANOVA. As also Ct-values were high and the difference in RANKL expression low, except for positive controls, no conclusions can be drawn from these results. However, rhIL-32 did not exert any RANKL inducing effect compared to the positive controls.

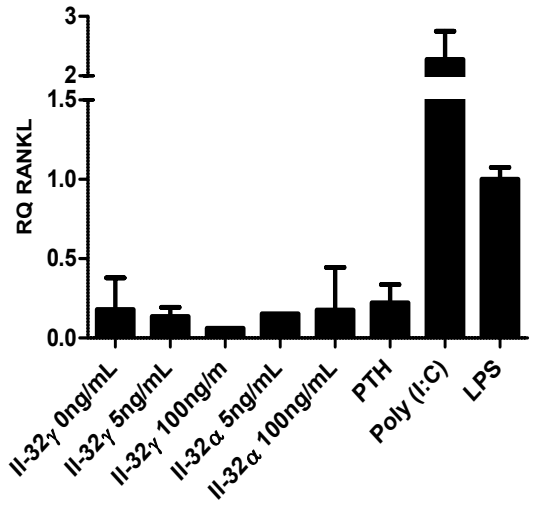

Figure 17: RANKL expression in MSC differentiated in osteogenic direction for 3 days. MSCs were seeded 80 000 cells/well in 6-well plates and differentiated in 3 days in the presence of rhIL-32 gamma or rhIL-32 alpha in concentrations 5 ng/mL and 100 ng/mL. As control cell treated with differentiation media only (IL-32 0 ng/mL) was included. PTH (10 nm), Poly (I:C) (5 µg/mL) and LPS (1 µg/mL) were used as positive controls. RANKL gene expression was measured by RT-qPCR using RANKL (TNFS11) and GAPDH (endogenous control) TaqMAN primers (Hs00243522_m1 and GAPDH DQ oligomix 20X, both Thermo Fisher). RQ values were calculated using the comparative Ct-method. Data is reported as mean RQ of technical replicates ±SD. N.S. comparing IL-32 0 ng/mL to IL-32 5 ng/mL and 100 ng/mL, one-way ANOVA.

Effect of IL-32-containing exosomes on osteoblast mineralization

As osteoclastogenesis was increased by stimulation with exosomes derived from IL-32 expressing myeloma cells, but not by IL-32-depleted exosomes from KO, we wanted to investigate whether there also was a difference between exosome treatments on osteoblast mineralization. We employed the same experimental approach as in the osteoclast experiments previously presented, using exosomes isolated from myeloma JJN-3 IL-32 KO D1 and JJN-3 "WT" clones. The JJN-3 cells designated WT had gone though the same knock-out procedure and clonal selection as the IL-32 KO, except that the IL-32 gene was not knocked-out and thereby the IL-32 expressing phenotype conserved. JJN-3 KO D1 and WT clones were cultured in exosome depleted media and exosomes isolated as described in Material and Methods. We used Bradford assay to measure the protein concentration in the exosome samples to ensure that there were exosomes present. (**Figure 18**). The exosomes isolated from the D1 IL-32 KO clone had significantly less protein, accounting for the lack of IL-32 in the exosome protein repertoire or alternatively a change in quantity of exosomes isolated .

Further on, we used the isolated exosomes to stimulate MSCs during osteogenic differentiation for a time period of 15 days. New exosomes was supplemented at each media renewal (every 3-4 day). In compliance with our previous IL-32 experiments we combined $25(OH)D_3$ treatment to exosomes from each clone to look for potentiating effects. Mineralization was visualized and quantified by ARS-staining (**Figure 19**).

In contrast to osteoclast experiments there were no difference between IL-32-containing exosomes and IL-32-depleted exosomes when evaluating the effect on osteoblasts (**Figure 19**). There was no differential efficiency in mineralization between WT-exosome- and D1-exosome- treated osteoblasts (unpaired two-sided Student´s T-test). Also there were equal mineralization between the exosome treatments when combining with $25(OH)D_3$. Although the IL-32 protein proportion of the exsome fraction did not seem to exert any residual effect, the exosome-treated cells was found in overall to mineralize more than non-treated controls. This may be explained by the presence of other mineralization-inducing proteins in the exosome fraction. In conclusion, the exosomes from myeloma cells appear to promote osteoblast differentiation, but the effect may not be dependent on IL-32.

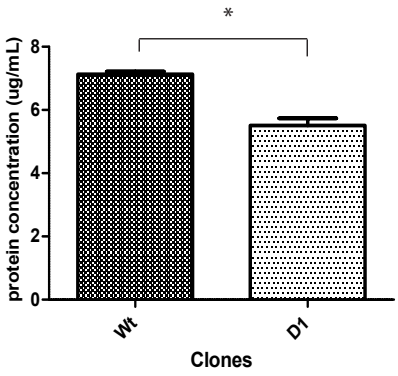

Figure 18: Protein concentration in exosome samples isolated from the JJN-3 IL 32 KO clones D1 and WT. Amount of protein were evaluated by the Bradford assay using a BSA standard as reference. *p<0.05, unpaired two-sided Student's t- test).

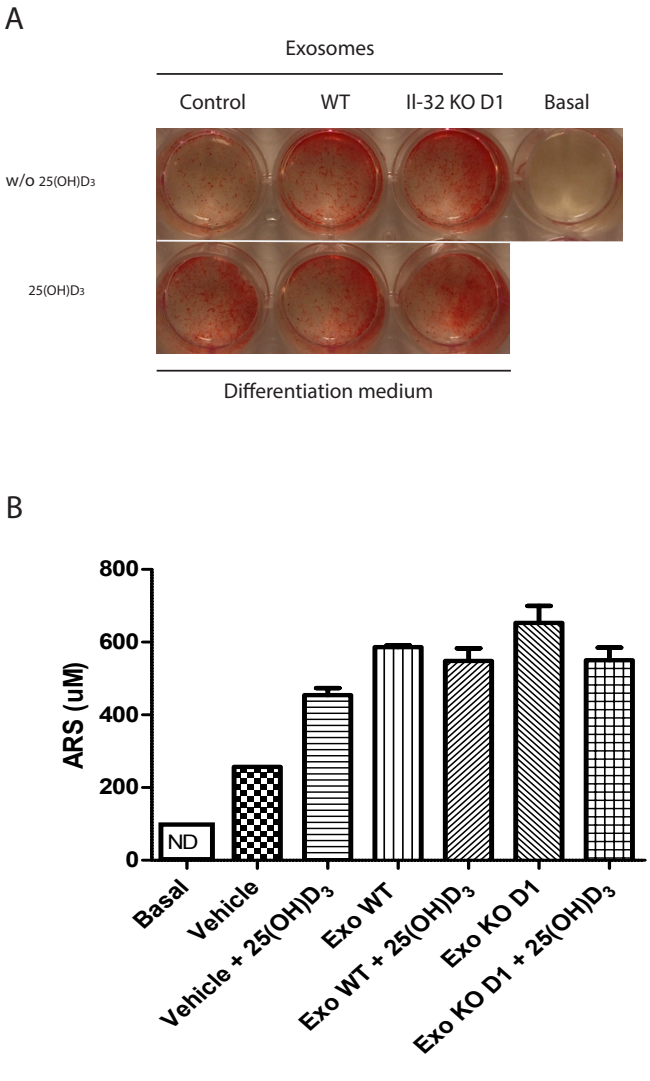

Figure 19: Mineralization in exosome treated cells. MSCs were differentiated in osteogenic direction for 15 days in media supplemented with exosomes isolated from JJN-3 IL-32 KO cells (D1) and JJN-3 KO WT cells (WT). In addition a control containing only PBS (designated vehicle), but exposed to the same isolation procedure as the exosome suspensions was treated to cells in the same manner as the WT and IL-32 KO D1 exosomes. All exosome treatments was in addition combined with 10 nM 25(OH)D_3. **A)** Visualization of mineralization by ARS-staining. **B)** Quantitation of mineralization. ARS dye was extracted from the monolayer and absorbance was measured. Concentration of ARS (uM) was determined by using an ARS standard curve.

IL-32 protein expression is absent in IL-32 KO B11 JJN-3 clone, while a truncated protein may be expressed by IL-32 KO D1 JJN-3 clone

To confirm knock-down of IL-32 in the clones, cell-lysates with Western Blot. JJN-3 KO WT and IL-32 KO cell lines B11 and D1, were harvested and the protein lysate analyzed by Western Blot using an polyclonal goat IL-32 antibody specific for all IL-32 isoforms (**Figure 20**). Strikingly, we detected IL-32 protein in the D1 IL-32 KO clone, indicating that the knock-out had not been complete or that the IL-32 expressing phenotype had recovered by clonal expansion of IL-32^{+} D1 cells. However, the detection signal was not as strong as for the WT protein sample, and the protein size was somewhat reduced in IL-32 KO D1, indicating the presence of a truncated IL-32 protein in D1, possibly a result of incomplete cleavage of the gene by the CRISPR/Cas system. However, the B11 IL-32 KO clones used in osteoclast experiments had no expression of IL-32, and therefore still regarded as complete knock-outs. Hence, as the knock-down of IL-32 in D1 clones is uncertain, we cannot conclude on the effect of IL-32 exosomes in terms of osteoblast differentiation (presented in **Figure 19**).

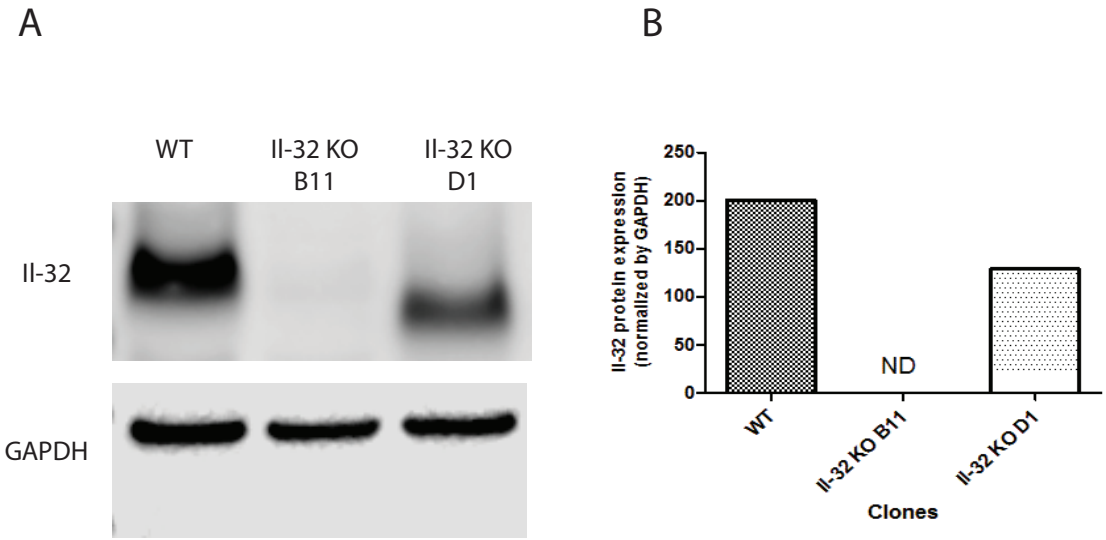

Figure 20: IL-32 protein expression in myeloma IL-32 KO cell lines. Protein lysates from JJN-3 IL-32 KO clones D1 and B11 and the JJN-3 KO WT clones were analyzed by western blotting using a polyclonal goat antibody spesific for IL-32. Results were normalized by subsequent detection of GAPDH. **A)** Protein detection on membrane by western blot. IL-32 KO D1 shows expression of IL-32 protein in reduced concentration and with lower molecular weight compared to the WT clone. No IL-32 protein expression detected in B11. **B)** Quantitative presentation of signal from western blot, normalized by GAPDH. No signal was detected in B11, while there is detection of signal for D1, although lower than for WT.

Part 3

Effect of rhIL-32 on osteoblast differentiation when combined with 25(OH)D_3

In our initial experiments, treatment with IL-32 alone showed no effects on osteoblast differentiation or function. To investigate if IL-32 exerts an 1,25$(OH)_2D_3$ -mediated effect on osteoblasts through upregulation of CYP27B1 and subsequent conversion of 25(OH)D_3 to 1,25$(OH_2)D_3$, the pro- and active form of vitamin D, respectively, we measured ALP-activity in MSCs differentiated in osteogenic direction in presence of rhIL-32 and different concentrations of 25(OH)D_3 . As previous experiments suggested that neither rhIL-32γ, nor rhIL-32α influenced osteoblast differentiation, we chose to continue our experiments with rhIL-32γ (from now on referred to as rhIL-32) as this is considered the most biologically active isoform and the isoform we suspect is secreted from the myeloma cells[165].

Initially, we examined various 25(OH)D_3 concentrations to investigate if any of them could influence osteoblast differentiation in the presence of rhIL-32. We therefore titrated 25(OH)D_3 at 1 nM, 10 nM and 100 nM against IL-32 5 ng/mL, 25 ng/ml and 100 ng/mL. As 25(OH)D_3 was reconstituted in 100 % DMSO we also treated with 1, 10 and 100 nM of DMSO. BMP-2 and MSCGM (basal) treatment was included as positive and negative control, respectively. The effects of the different concentrations were evaluated by differentiating MSCs in osteogenic direction and measure the ALP-activity at day 5 and day 7. As we had problems with DNA quantitation in wells subsequent to the ALP-assay, we measured cell viability in a similarly treated plate and determined the relative number of cells in each well by including a cell number standard in the CTG assay. These numbers were then used to adjust the total ALP-activity of each well.

The ALP-activity did not differ significantly between the groups with different concentrations of 25(OH)D_3, therefore the results is not shown (see Appendix 4, fig.2). When we normalized ALP-activity by CTG cell number measured in a corresponding plate, we found 1nM 25(OH)D_3 treated cells to be dose dependently inhibited by rhIL-32. However these results are also shown in Appendix 4 (fig. 2B), as we found the experimental approach comparing two wells from different plates as less reliable. We did not pinpoint any particular concentration of action in our titration of vitamin D, therefore we chose to continue our experiments with 10

nM concentrations as this, according to available literature, is the concentration of $1,25(OH)_2D_3$ that induced most cellular activity in osteoblasts[122,166,167].

To further examine the effect of IL-32 and vitamin D on ALP-activity we used two metabolic forms of vitamin D to stimulate the osteoblasts. By including both the pro form, $25(OH)D_3$, and the active form, $1,25(OH)_2D_3$, we were able to investigate possible inhibitory or activating effects of $1,25(OH)_2D_3$ compared to $25(OH)D_3$. In this experiment, we treated the cells with both 10 nM and 1 nM 25(OH)D3 to evaluate the dose dependent inhibition for 1 nM observed in titration experiments presented in Appendix 4. As before we combined with rhIL-32 at different concentrations, to examine if a potential effect on osteoblasts by vitamin D could be related to IL-32 doses.

MSCs were differentiated in osteogenic direction for 5 days, and cell ALP-activity was measured (**Figure 21**). When comparing the $25(OH)D_3$ and $1,25(OH)_2$ treatments with the non-treated group (w/o vit D), without regard to IL-32 doses, there was significant differences in ALP-activity (two-way ANOVA). However, the tendency for increased ALP-activity by vitamin D was most prominent for $25(OH)D_3$ (**Figure 21A**) .With regard to IL-32 there was a tendency for increased ALP-activity with increasing doses of IL-32 in both the $25(OH)D_3$ (**Figure 21A**), the $1,25(OH)_2D_3$ (**Figure 21B**) treated samples, as well as the no-vitamin D treated samples, but the difference was not significant. The statistical significance was evaluated using two-way ANOVA and Bonferroni post test. ALP-activity were also evaluated at day 6 (Appendix 4, fig.3), where $25(OH)D_3$ showed inhibitory actions, rather than the positive influence observed at day 5.

The ALP-activity was roughly two-fold higher in the $25(OH)D_3$ - treated plate (**Figure 21A**) treated compared to the $1,25(OH)_2D_3$- treated plate (**Figure 21B**), and as the corresponding increase in ALP-activity was seen in the differentiation media and IL-32-group (black bars), this was not due to vitamin D treatments. This obvious variability between experiments reduces the credibility of the results, and implies that the ALP-assay has low reproducibility and may be very sensitive to variations in the experimental conditions.

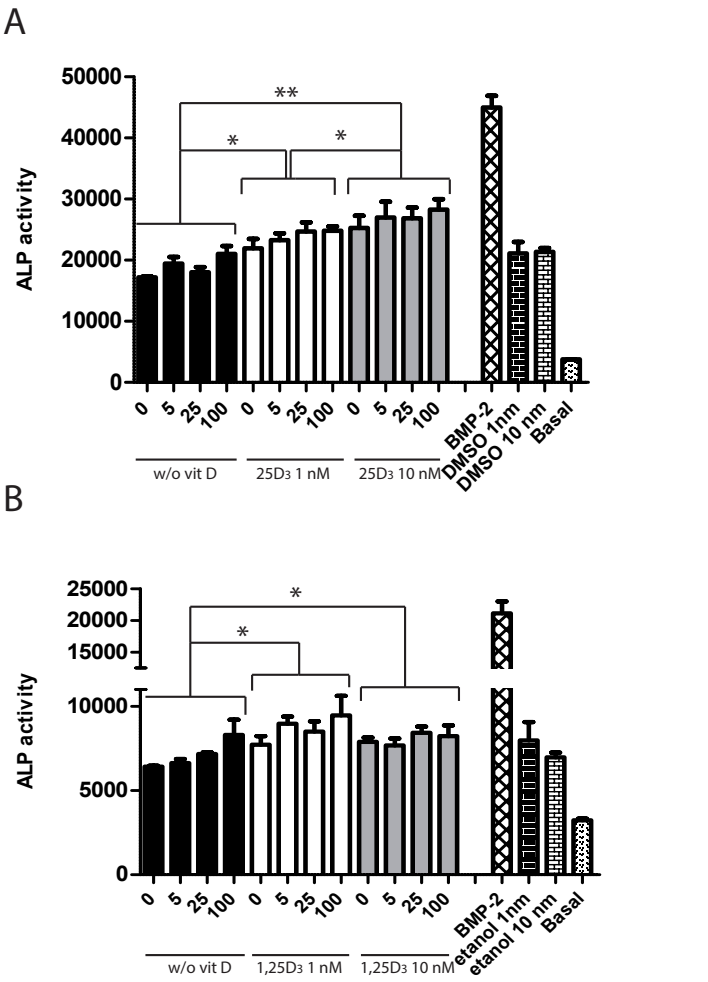

Figure 21: ALP activity at day 5. MSCs were seeded 2500 cells/well in 96-well plates and differentiated in osteogenic direction for 5 days treated with or without the active ($1,25(OH)_2D_3$) or the pro form ($25(OH)D_3$) of vitamin D at 1nM or 10 nM concentrations , together with rhIL-32γ at at concentrations (ng/mL) indicated. As controls, reconstitution reagents DMSO and etanol, for $25(OH)D_3$ and $1,25(OH)_2D_3$, respectively, were included. Positive control was BMP-2 (300ng/mL). Negative control was undifferentiated MSCs (basal) treated with MSCGM only. At day 5, ALP-activity for each well was measured. Data is reported as mean±SEM of technical replicates. *p<0.05, **p<0.01, two-way ANOVA, and Bonferroni post test. **A)** ALP-activity in cells treated with $25(OH)D_3$ ($25D_3$) for 5 days. **B)** ALP-activity in cells treated with $1,25(OH)_2D_3$ ($1,25D_3$) for 5 days.

In our later experiments, we found an accurate protocol for DNA quantitation, and were able to adjust the ALP-activity by the DNA quantity in each well to normalize for differences in cell number between samples. MSCs were differentiated in the presence of IL-32 and $25(OH)D_3$ (10 nM). As before we measured the preosteoblast ALP-activity at day 5 of differentiation (**Figure 22A**). In addition we measured ALP-activity at day 7 (**Figure 22B**). However, the adjustments for amount of DNA did not augment any significant differences between treatments. There appeared to be inhibition of ALP at day 7 for the $25(OH)D_3$-treated group, were ALP-activity was significantly lower than in untreated group. Although there was a tendency for IL-32 dose dependent reduction in ALP-activity in both $25(OH)D_3$-treated group and untreated group at day 5 and day 7, there were no significant differences between concentrations IL-32 in any of the groups (Two-way ANOVA, Bonferroni post test).

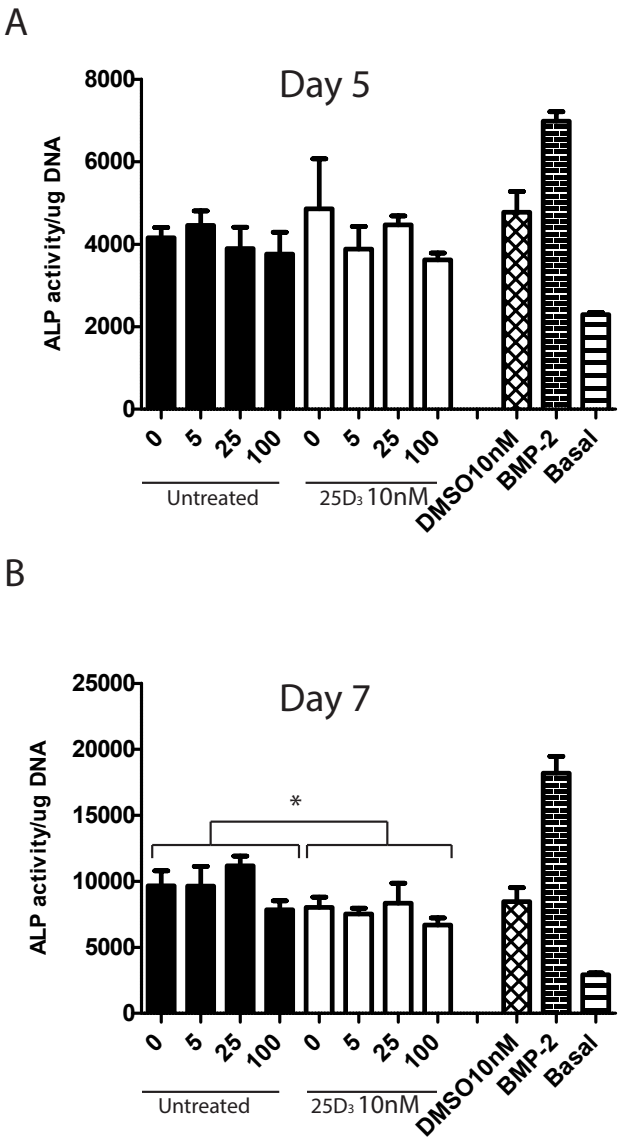

Figure 22: ALP-activity adjusted by μg DNA. MSCs were seeded 2500 cells/well in 96-well plates and cultured in differentiation media with IL-32 concentrations as indicated (ng/mL) and 10 nM 25(OH)D_3 (25D_3) for 5 and 7 days before ALP-activity was measured for each well, followed by quantitation of DNA for the same wells. The ALP results were then adjusted for µg DNA in each well. A) ALP/ µ g DNA activity in preosteoblasts at day 5. Data is reported as mean ±SEM of technical replicates. B) ALP/ µg DNA activity in preosteoblasts at day 7. Data is reported as mean ±SEM of technical replicates (*p<0.05, Two-way ANOVA).

As other studies have demonstrated an inhibitory effect of the 1,25$(OH)_2D_3$ (active vitamin D) after 10 days[168], we examined the ALP-activity in MSC-derived osteoblast treated with 25(OH)D_3 and IL-32γ at day 11. We treated cells with 1,25$(OH)_2$ D_3 to compare ALP-activity in these osteoblasts to the ALP-activity in 25(OH)D_3 treated osteoblasts, as similar effects in high dose rhIL-32 treated cells hypothetically could be related to vitamin D conversion in these cells (**Figure 23**).

1,25$(OH)_2D_3$ showed a slight inhibition of ALP-activity compared to cells treated with differentiation media only (first black bar, IL-32 0 ng/ml), however the difference were not significant (unpaired two-sided Student's t-test). No dose dependent inhibition was demonstrated by rhIL-32 in 25(OH)D_3 treated cells. IL-32 100 ng/mL deviated highly from

the other samples in the 25(OH)D_3 -treated group, and may indicate technical errors during experimental procedures. BMP-2 control is also low, introducing additional uncertainties in measurements.

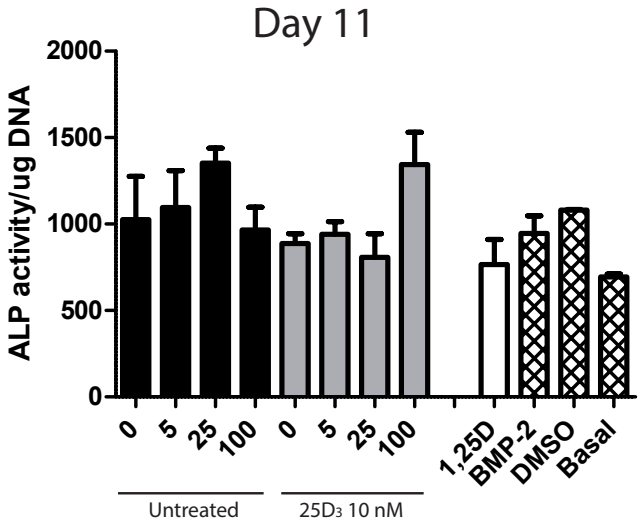

Figure 23: ALP-activity in MSC derived osteoblasts at day 11. MSCs were seeded 2500 cells/well in 96-wells plates and cultured in MSCGM in two days before differentiated into osteoblasts in differentiation media supplemented with IL-32 and IL-32 combined 10 nM 25(OH)D_3 (25D_3). IL-32 concentrations are indicated for each bar. For 1,25(OH)$_2$$D_3$ (1,25D) concentration treated was 10 nM. As controls, BMP-2 (300 ng/mL), and reconstitution reagent for 25(OH)D_3; DMSO (10 nM) were included. As negative control undifferentiated MSCs (basal) cultured in MSCGM was included. ALP-activity was measured at day 11. Data is presented as mean ±SEM of ALP/ugDNA of technical replicates. N.S differences (using Two-way ANOVA comparing groups, and unpaired two-sided Student's t-test comparing 0 ng/mL IL-32 (untreated group) and 1,25D treated sample)

Effect of rhIL-32 on osteoblast proliferation in the presence of 25(OH)D_3

We also evaluated MSC proliferation by extent of ATP-levels, when differentiated in osteogenic direction for 5 days in the presence of 25(OH)D_3 and rhIL-32 (**Figure 24**), using the same concentrations as previous experiments. Proliferation was significantly increased in groups treated with 25(OH)D_3, and the increase may also be correlated to increasing IL-32 doses, with an exception for 25 and 100 ng/mL IL-32 in the 25(OH)D_3-10 nM- group, but the difference between concentrations was not significant (Two-way ANOVA and Bonferroni post test). However, at day 6 (shown in Appendix 4, fig. 4) the ATP-level was equally high in 25(OH)D_3-groups and a even higher ATP-level was observed in the no-vitamin D treated group, indicating that the pro-proliferative effect of vitamin D was only transient.

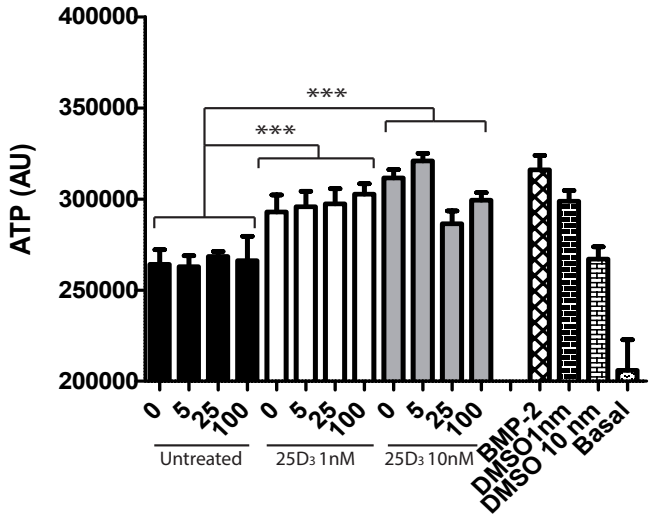

Figure 24: Preosteoblast proliferation in the presence of 25(OH)D_3 and rhIL-32. MSCs were seeded 2500 cells/well in 96-well plates and differentiated in osteogenic direction for 5 days in the presence of 25(OH)D_3 (25D_3) in concentrations 1nM and 10 nM together with IL-32gamma in concentrations as indicated for each bar(ng/mL) . Proliferation was measured at day 5 by the extent of ATP levels in each well using CTG-assay. Data is presented as mean±SD of ATP (arbitrary units) of technical replicates. *** p<0.0001 (Two-way ANOVA, comparing untreated group to vitamin D groups)

Effects of rhIL-32 short-term treatment on osteoblast-specific gene expression in the presence of 25(OH)D_3 or 1,25(OH_2)D_3

To investigate if IL-32 and vitamin D combined exerts transient effects in early stages of osteoblast differentiation, expression of osteoblast signature genes *RUNX2* and Osterix (*SP7*) were measured in preosteoblasts after 6h, 24 h and 72 h stimulation with IL-32γ combined with 25(OH)D_3 or 1,25(OH_2)D_3 (**Figure 25**).

For Runx gene expression, there was no significant difference between IL-32 treated group and the no-IL-32 treated group (unpaired two-sided Student's t-test). As for previously presented gene expression studies, Osterix mRNA was poorly detected (Ct values > 35) and the standard deviations were therefore high. Osterix mRNA were not detected in 72 h samples (not shown). If not regarding the uncertainties in measurements caused by low detection, 1,25$(OH)_2D_3$ increased Osterix gene expression in comparison to the 25(OH)D_3 and IL-32 w/o vitD treatments, indicating that the active form of vitamin D may play a role as positive regulator of Osterix gene expression in early stages of osteoblast differentiation.

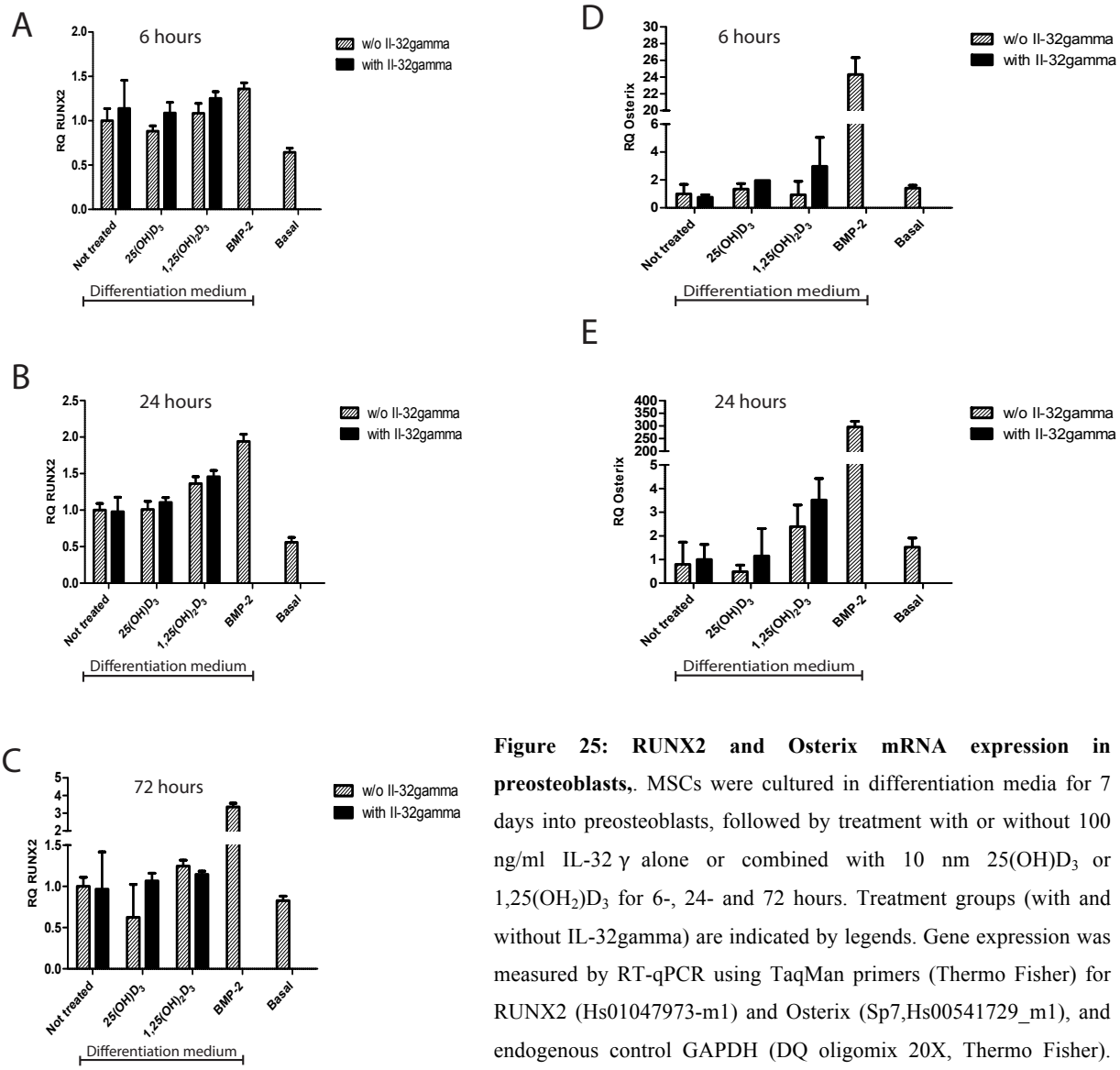

Figure 25: RUNX2 and Osterix mRNA expression in preosteoblasts,. MSCs were cultured in differentiation media for 7 days into preosteoblasts, followed by treatment with or without 100 ng/ml IL-32 γ alone or combined with 10 nm $25(OH)D_3$ or $1,25(OH_2)D_3$ for 6-, 24- and 72 hours. Treatment groups (with and without IL-32gamma) are indicated by legends. Gene expression was measured by RT-qPCR using TaqMan primers (Thermo Fisher) for RUNX2 (Hs01047973-m1) and Osterix (Sp7,Hs00541729_m1), and endogenous control GAPDH (DQ oligomix 20X, Thermo Fisher). RQ was calculated using the comparative Ct-method. **A)** RUNX2 gene expression after 6 hours. **B)** RUNX2 gene expression after 24 hours. **C)** RUNX2 gene expression after 72 hours. **D)** Osterix gene expression after 6 h. **E)** Osterix gene expression after 24 h (poorly detected with Ct values >35) Osterix was not detected at 72 hours.

We also studied regulation of osteocalcin, an osteogenic marker related to mature stages of osteoblast maturation, in response to IL-32 and vitamin D. Although its role in osteoblasts not completely clarified, osteocalcin is considered as a negative regulator of mineralization[169] and has been shown to be upregulated by $1,25(OH)D_3$[123]. We measured expression of osteocalcin (*BGLAP*) in MSC derived osteoblasts after 11 days of differentiation in the presence of IL-32 and $25(OH)D_3$ (**Figure 26**).

$1,25(OH)_2D_3$ demonstrated to be a potent inducer of osteocalcin also in our MSC/osteoblast system. However, no upregulation of BGLAP were observed in the IL-32 and $25(OH)D_3$ treated sample, indicating less or no increase in the level of the active metabolite $1,25(OH)D_3$ in this cell culture. The level of osteocalcin mRNA was equally low in all samples, except BMP-2 and $1,25(OH)D_3$, supporting our previous findings that IL-32 effects are not potentiated by $25(OH)D_3$.

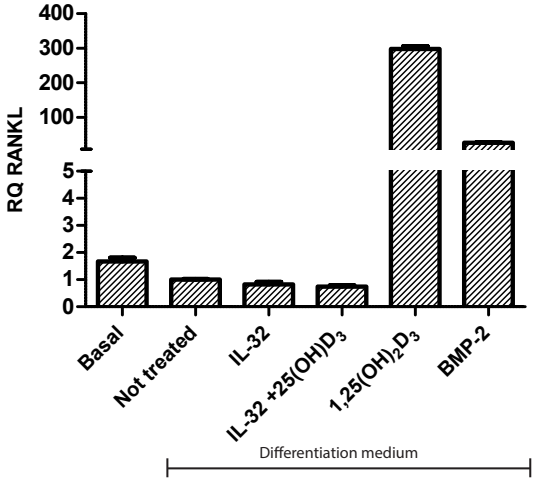

Figure 26: Osteocalcin (BGLAP) mRNA expression. MSCs were seeded 80 000 cells/well in 6-well plates and cultured in differentiation media supplemented with 100 ng/mL IL-32γ, or 100 ng/mL IL-32γ and 10 nM $25(OH)D_3$ for 11 days. As controls MSCs were cultured in MSCGM (Basal) and differentiation medium (diff) for the same time period. Also MSCs differentiated in presence of $1,25(OH)D_3$ (10 nM) and BMP-2 (300 ng/mL) were included as positive controls

Effect of rhIL-32 on CYP27B1

To examine our hypothesis that IL-32 mediates CYP27B1 dependent vitamin D conversion, we measured the CYP27B1 mRNA levels in MSCs and MSC-derived preosteoblasts after 6h stimulation with IL-32 combined with $25(OH)D_3$ or $1,25(OH)_2D_3$.

For undifferentiated MSCs treated with $25(OH)D_3$ in presence or absence of rhIL-32 (**Figure 27A**), CYP27B1 mRNA in the $25(OH)D_3$ treated group was increased in the presence of rhIL-32 in 3 out of 3 independent experiments the difference was not significant. Importantly, due to low expression (Ct values > 34 for all experiments) the standard deviations were high, and it is therefore hard to conclude on the total significance of the results.

Similarly, for the preosteoblasts (**Figure 27B**), the expression of *CYP27B1* were low and there were no significant differences in mRNA levels between rhIL-32 treated and untreated cells for the $25(OH)D_3$-group.

Similar low detection results (Ct values >35) were obtained for CYP27B1 mRNA levels for MSCs and preosteoblasts treated 24- and 72 hours (data shown in Appendix 5, fig. 1).

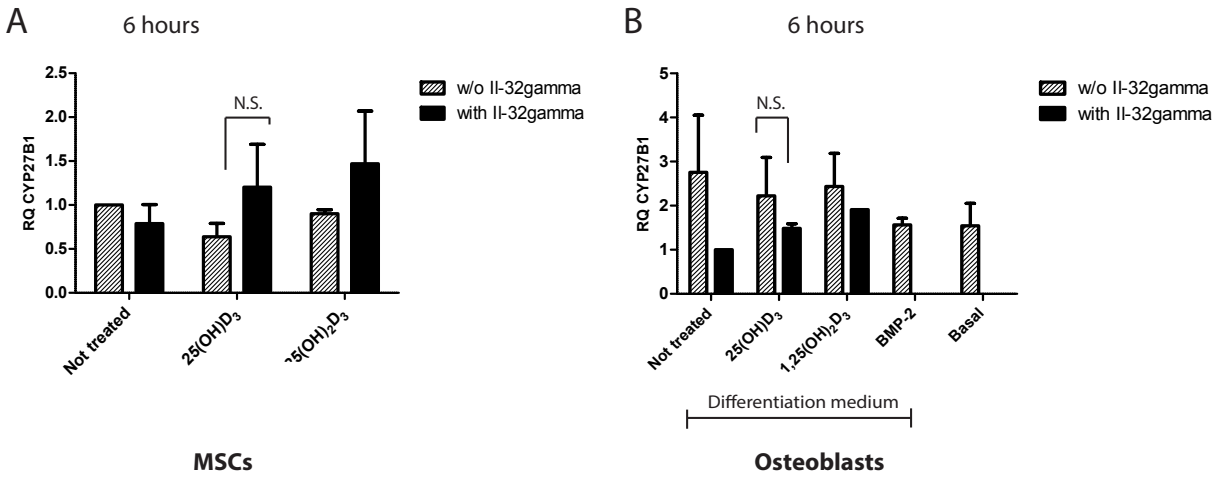

Figure 27: CYP27B1 expression in MSCs and MSC derived preosteoblasts after 6 h treatment. A) MSCs were seeded in 6-well plates (80 000 cells/well) and treated with $25(OH)D_3$ (pro vitamin D, 10 nm) with and without IL-32 (100 ng/mL) one day after seeding or after being differentiated for 7 days into pre-osteoblasts. Control groups include treatment without vitamin D (designated "not treated") and $1,25(OH)_2D_3$ treatment. Gene expression was evaluated by RT-qPCR using TaqMan primers for CYP27B1 (Hs01096154_m1, Thermo Fisher) and GAPDH (DQ oligomix 20X, Thermo Fisher). RQ was calculated using the comparative Ct-method. **A)** MSCs cultured in basal medium for 6 h with the treatment as reported above (the "not treated group is cells cultured in MSCGM). Data is reported as mean±SEM for (N=3) biological replicates. **B)** MSCs were differentiated for 7 days into preosteoblasts, before treated as reported above for 6 hours (the "not treated" group is cells cultured in diff.medium). BMP-2 (300 ng/mL) and basal (MSCGM) medium treated cells were included as controls. Data is reported as mean±SD for technical replicates. N.S.: $p>0.05$

Finally, as previous CYP27B1 gene expression studies had been limited to pre-osteoblasts exposed to short term stimulation we evaluated CYP27B1 expression in more mature osteoblasts differentiated for 11 days in continuous presence of IL-32γ and $25(OH)D_3$ (**Figure 28**). Although cells treated with differentiation media showed increased CYP27B1 mRNA levels compared to undifferentiated MSCs, rhIL-32 did not influence the expression, neither alone nor in the presence of $25(OH)D_3$. Again low expression of CYP27B1 mRNA resulted in high standard deviations between technical replicates.

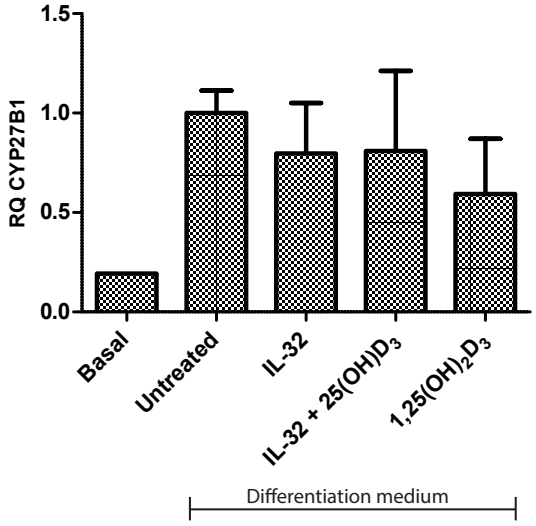

Figure 28: CYP27B1 mRNA levels in MSC-derived osteoblasts differentiated for 11 days. MSCs were seeded 80 000 cells/well in a 6-well plate and differentiated in osteogenic direction with IL-32γ and IL-32 γ + 25(OH)D_3 for 10 days. BMP-2 (300ng/mL),1,25(OH)D (10 nM) and basal and differentiation media treated cells were included as controls. CYP27B1 mRNA expression was measured by RT-qPCR using TaqMan primers for CYP27B1 (Hs01096154_m1, Thermo Fisher) and GAPDH (DQ oligomix 20X, Thermo Fisher). RQ was calculated using the comparative Ct-method. Data is presented as mean±SD of technical replicates. N.S. between differentiated samples using one-way ANOVA, and Dunnett's post test.

Effects of rhIL-32 on *CYP24A1* expression

CYP24A1 is a key enzyme in the vitamin D metabolism as it initiates the degradation of vitamin D metabolites[166]. The expression of CYP24A1 usually is low, but highly induced by 1,25(OH)$_2$D$_3$[170], therefore a high level of CYP24A1 mRNA could be an indicator of high levels of 1,25(OH)$_2$D$_3$ in cell cultures. By examine whether IL-32 and 25(OH)D$_3$ increased CYP24A1 gene expression at a level equivalent to the expression level in 1,25(OH)$_2$D$_3$-treated samples, we could indirectly evaluate the extent of IL-32-dependent vitamin D conversion. As 1,25(OH)$_2$D$_3$ effects are mostly mediated through VDR mediated gene regulation[170], we also measured VDR mRNA levels in the same experimental samples to investigate overall responsiveness to IL-32 and vitamin D treatment.

CYP24A1 expression was, as expected induced by 1,25(OH)$_2$D$_3$, both at 24 hours ($p<0.003$) and 72 hours ($p=0.0004$) (**Figure 29A** and **B**). On the other hand, rhIL-32 alone or in combination with 25(OH)D$_3$ had no effect on *CYP24A1* expression. As no significant difference in *CYP24A1* expression was found, neither between the differentiation media control (not treated) and the rhIL-32/25(OH)D$_3$ treatment, nor when comparing rhIL-32 treatment and "w/o IL-32" treatment our hypothesis of higher CYP24A1 in rhIL-32 treated

samples was disproved. All p-values were calculated from n=3 technical replicates by unpaired two-sided Student's T-test. CYP24A1 mRNA levels were found to be related to duration of treatment; the levels was almost a two-fold increased from 24 hours to 72 hours. The BMP-2 control showed induction of *CYP24A1* in both time-points, indicating that osteoblast maturation may be related to increased *CYP24A1* in cells.

To evaluate IL-32 effect on vitamin D signaling, *VDR* expression in MSCs and osteoblasts were also measured, at 6h, 24 h and 72 h treatment with $1,25(OH)_2D_3$ and $25(OH)D_3$, with or without rhIL-32 100 ng/mL. However, no overall change in CYP27B1 mRNA levels in response to IL-32 and vitamin D metabolites were observed. The results for VDR expression are presented in Appendix 5, figure 1.

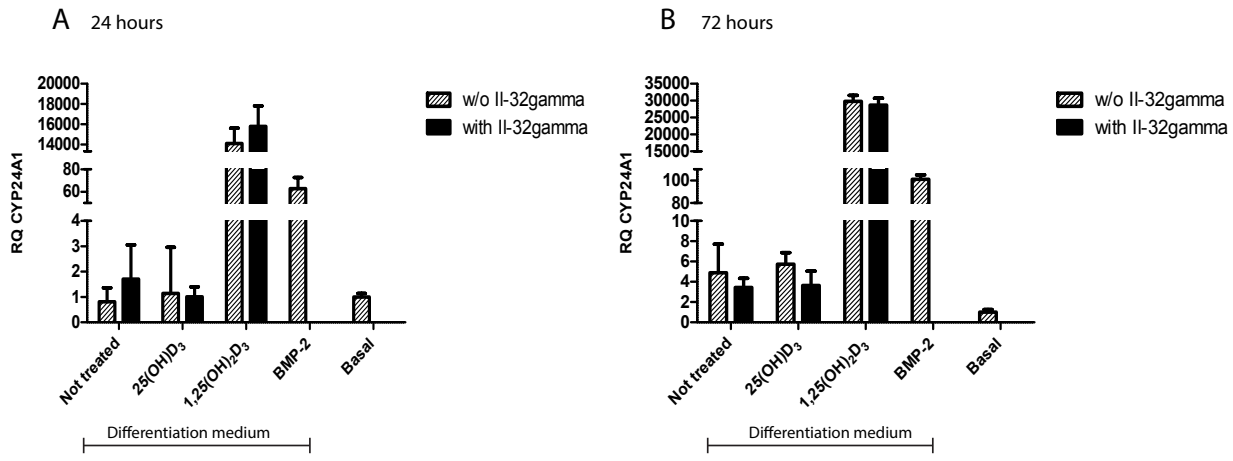

Figure 29: Relative gene expression of CYP24A1 in rhIL-32 and vitamin D treated preosteoblasts. MSCs were seeded 80 000 cells/well and differentiated in osteogenic direction for 7 days before treated 24h and 72 h with 10 nM $25(OH)D_3$, 10 nM $25(OH)D_3$, or differentiaion medium only, with or without rhIL-32 gamma (100 ng/mL). As controls PTH (10 nM), BMP-2 (300ng/mL) and basal medium (MSCGM) treated cells were included. CYP24A1 expression was evaluated by RT-qPCR, using TaqMan primers for CYP24A1 (Hs00167999_m1, Thermo Fisher) and for endogenous control, GAPDH, (DQ, oligomix 20X, Thermo Fisher). RQ values were calculated using the comparative Ct-method. Data is reported as mean±SD for technical replicates. **A)** CYP24A1 gene expression after 24 hours. **B)** CYP24A1 gene expression after 72 hours.

Effect of rhIL-32 on RANKL in the presence of 25(OH)D_3

In our previous experiments IL-32 alone did not influence RANKL. However, as 1,25$(OH)_2D_3$ has been shown to upregulate RANKL in osteoblasts,[45] we wanted to investigate if RANKL mRNA expression was increased by rhIL-32 in combination with 25$(OH)D_3$, with basis in our hypothesis about intracellular CYP27B1 dependent conversion to the active metabolite 1,25$(OH)_2D_3$. Using the cDNA from the preosteoblast short-term stimulation experiment (MSCs differentiated into osteoblasts for 7 days stimulated for 6h, 24h and 72h with IL-32 and vitamin D) we measured RANKL mRNA by qPCR (**Figure 30**).

As expected, 1,25$(OH)_2D_3$ induced RANKL mRNA at all time points (6h, 24h and 72h, **Figure 30A, B and C**) stimulated cells. In contrast, low expression of RANKL were observed in both the 25$(OH)D_3$ and the non-treated group. IL-32, in combination with 25$(OH)D_3$ increased RANKL mRNA after 24 hours (**Figure 30B**), but there was no difference at 6 hours (**Figure 30A**) or 72 hours (**Figure 30C**). Also in all samples except 1,25$(OH)_2D_3$ treated samples, the Ct-values were low, reducing the precision of measurements. Hence, our data suggest that rhIL-32 in combination with 25$(OH)D_3$ promotes a slight, transient increase in RANKL mRNA. However, further experiments are needed to conclude on this matter.

A

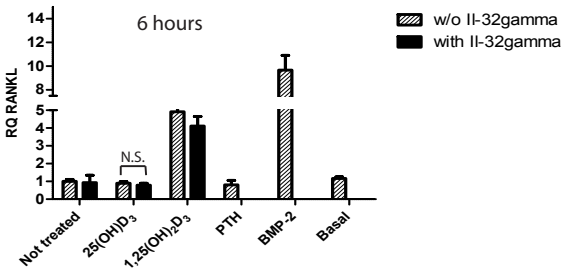

B

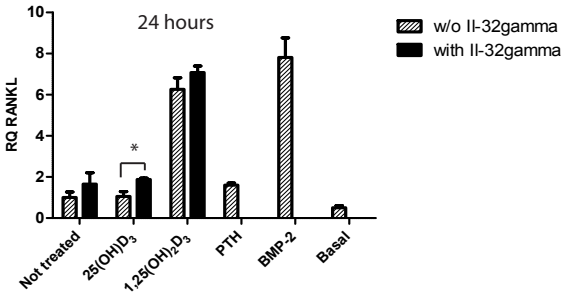

C

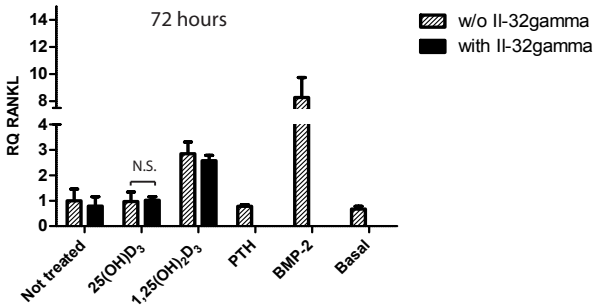

Figure 30: RANKL gene expression in preosteoblasts treated with IL-32 and 25(OH)D_3. MSCs were seeded 80 000 cells/well and differentiated in osteogenic direction for 7 days before treated 24h and 72 h with 10 nM 25(OH)D_3, 10 nM 25(OH)D_3, or differentiaion medium only (not treated), with or without IL-32 gamma (100 ng/mL). RANKL (*TNFS11*)-expression was evaluated by TaqMan based RT-qPCR (Hs00243522_m1, Thermo Fisher) using GAPDH(DQ, oligomix 20X, Thermo Fisher) as endogenous control. RQ values were calculated using the comparative Ct-method. Data is reported as mean±SD for technical replicates. *$p<0.05$, N.S.: $p>0.05$ (unpaired two-sided Student´s t-test). **A)** RANKL gene expression after 6 hours stimulation. **B)** RANKL gene expression after 24 hours stimulation **C)** RANKL gene expression after 72 hours stimulation.

Effect of rhIL-32 combined with 25(OH)D_3 on late osteoblasts differentiation evaluated by extent of matrix mineralization

As our previous results on ALP-activity and gene expression implied that there was no effect rhIL-32 either alone, nor in combination with 25(OH)D_3, we turned our attention to later differentiation stages. As earlier mentioned, matrix mineralization is a marker for mature osteoblast function. We therefore cultured MSCs in osteogenic direction in the presence of 25(OH)D_3 and rhIL-32 for 15 days and visualized mineralization by ARS-staining. The level of mineralization was also quantified by extracting the dye from the cell monolayer. Interestingly, in our initial experiment, we found that mineralization in the 25(OH)D_3 treated group was IL-32 dose dependently inhibited at day 15 (**Figure 31A and B**), but it should be noted that the mineralization also was inhibited in the control with reconstitution reagent for 25(OH)D_3, DMSO. However, also for the 1,25$(OH)_2D_3$ treated cells, mineralization was completely inhibited, supporting that the active form of vitamin D may act as an inhibitor of late osteoblast-maturation in our *in vitro* system.

To investigate whether this 25(OH)D3-dependent inhibition of mineralization was caused by conversion of 25(OH)D_3 to 1,25$(OH)_2D_3$, we measured the amount of 1,25$(OH)_2D_3$ in the conditioned cell culture media by ELISA (**Figure 31C**). Increased 1,25$(OH)_2D_3$ levels in cell media can be an indicator increased CYP27B1 activity. Importantly, there was a slight increase in 1,25$(OH)_2D_3$ with increasing concentrations of rhIL-32, supporting that IL-32 may increase CYP27B1. However, differences was almost, but not significant (p=0.072), when comparing 1,25$(OH)_2D_3$ levels in differentiation media with the 1,25$(OH)_2D_3$ levels in the rhIL-32 100 ng/mL and 25(OH)D_3 (25D_3) treated samples (indicated in **Figure 31C**). Also, the levels of 1,25$(OH)_2D_3$ were very low in all measurements, and there were found corresponding levels of 1,25$(OH)_2D_3$ in the conditioned media from samples that was not treated with 25(OH)D_3, indicating that the main proportion of 1,25$(OH)_2D_3$ measured may be accounted to unspecific detection in the 1,25$(OH)_2D_3$ ELISA assay at such low concentrations. Alternatively there was 1,25$(OH)_2D_3$ or 25(OH)D_3 present in the human serum component of the MSCGM medium used as basis for the differentiation media.

We also quantified $1,25(OH)_2D_3$ in conditioned media obtained from MSCs cultures differentiated with rhIL-32 and $25(OH)D_3$ for 7 days, before ALP-activity was measured (**Figure 31D**). We found a negative correlation between ALP-activity and the level of $1,25(OH)_2D_3$ present in the conditioned media. This also supported our hypothesis of IL-32 indirectly inhibiting osteoblast activity through $1,25(OH)_2D_3$.. However, high rhIL-32 doses did not increase the level of $1,25(OH)_2D_3$. Hence, the consensus of these results (**Figure31 C and D**) cannot be conclusive on an upregulating effect of IL-32 on CYP27B1.

Furthermore, we did not succeed in validating the mineralization results presented in **Figure 31A and B**. The experiment was repeated in total 7 times (Appendix 6) with MSCs from two different donors. IL-32 dose-dependent inhibition of mineralization in the $25(OH)D_3$ treatment group was not seen in any of the repeated experiments (one representative shown in **Figure 22 E**), while $1,25(OH)_2 D_3$ still inhibited mineralization in 4 out of 6 experiments. However, in many of the repeated experiments there was low degree of mineralization (Appendix 6). Hence, we cannot conclude nor exclude that there is an inhibitory effect of IL-32 and $25(OH)D_3$ on late osteoblast differentiation in the terms of matrix mineralization.

We also remarkably noted that there was high mineralization for etanol, the reconstitution reagent for $1,25(OH)_2 D_3$ in all experiments, indicating that etanol somehow potentiated the mineralization process. However, the inhibiting effect of $1,25(OH)_2 D_3$ mostly seemed to surpass the positive effect of the etanol present in the $1,25(OH)_2 D_3$ treated samples.

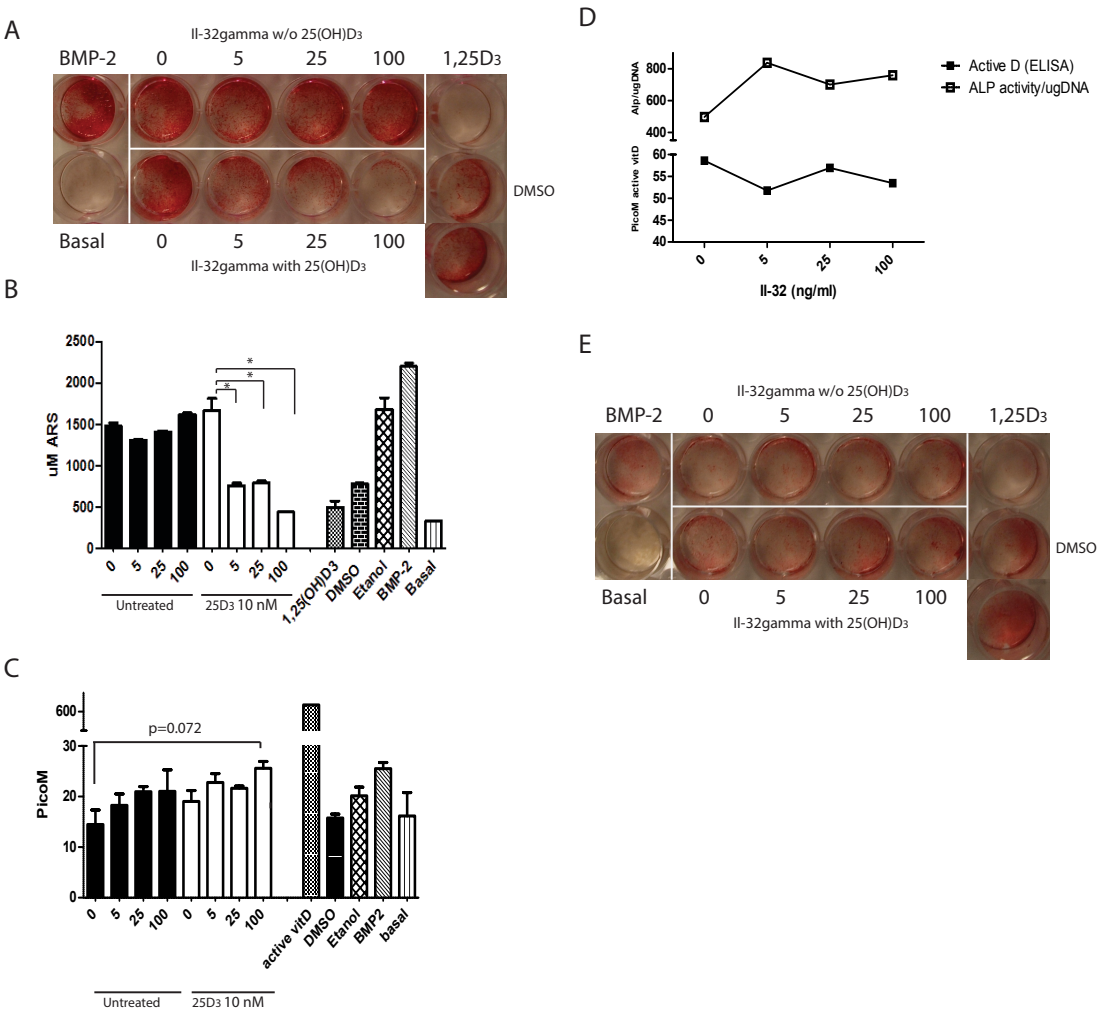

Figure 31: Osteoblast mineralization and ALP activity compared to CYP27B1 enzyme activity (quantified by the amount of 25(OH)D_3 converted to 1,25(OH)$_2D_3$ in cell culture media). MSCs were seeded at density 2500 cells/well in 96 wells plate for ALP-experiments, and 15000 cells/well in 24-wells plate for mineralization experiments. At day 2 after seeding the MSCs were differentiated in osteogenic direction in the presence of IL-32 at concentrations indicated (ng/mL), with or without 10 nM of 25(OH)D_3 (25D_3). Also for DMSO, etanol and 1,25(OH)$_2D_3$ (1,25D/active vitD) controls at 10 nM were used. BMP-2 (300 ng/mL) was used as positive control, while negative control were MSCs cultured in MSCGM (basal). **A)** Matrix mineralization by osteoblasts at day 15, visualized by ARS-staining. **B)** Quantitation of matrix mineralization (in the samples from fig. A). ARS-staining was quantified by extracting the dye from the monolayer and measure the absorbance. Concentration (uM) was determined from an ARS standard curve. Statistic significance was evaluated by unpaired two-sided Student's t-test (*P<0.05). Data is reported as mean± SEM of technical replicates. **C)** Levels of 1,25(OH)$_2D_3$ in cell culture media measured by ELISA. Cells were treated for 15 days with OB diff media and the concentrations of IL-32, vitamin D and controls as previously reported, before cell culture media was removed and assayed by 1,25(OH)$_2D_3$ EIA. Data is reported as mean± SEM of technical replicates. (p-value reported calculated by unpaired two-sided Student's t-test) **D)** Relationship between ALP activity and level of 1,25(OH)$_2D_3$ in media when treated with different IL-32 concentrations. Cells were cultured for 7 days with 25(OH)D_3 10 nM and concentrations of IL-32 as reported, before culture media were harvested and assessed by 1,25(OH)$_2D_3$ EIA, while cell ALP activity were measured in the corresponding wells. **E)** Repeat of the experiment shown in fig22 A to validate IL-32 dose dependent inhibition in 25(OH)D_3 treated group. Mineralization was visualized by ARS stain. The other repetitions are shown in Appendix 6.

Effect of 48 hours stimulation with rhIL-32 and 25(OH)D_3 on osteoblasts

A previous study demonstrated effects of 25(OH)D_3 on CYP27B1, as well as osteogenic markers after 48 hours[122]. We therefore wanted to investigate if short time stimulation of osteoblasts could reveal a more potent role of IL-32 in relation to vitamin D conversion than previous experiments. As the current study also showed that treatment with 1,25$(OH)_2D_3$ resulted in differential response in the osteoblast ALP-activity depending on which day of the differentiation process the treatment was initiated[122], we performed 48 h stimulation with rhIL-32 and 25(OH)D_3 in pre-differentiated osteoblasts and evaluated the effect by level of ALP-activity.

ALP-activity was measured at day 7 or day 9 following 48 h stimulation (**Figure 32 A and B**) and adjusted by quantitation of DNA in each well. Although not significant, ALP-activity was increased in cells in response to increasing doses of rhIL-32 in the group without vitamin D, while in the 25(OH)D_3 group, on the opposite, a tendency for reduced ALP-activity with increasing doses of IL-32 was observed. Statistical significance were evaluated using one-way ANOVA (p-values were still not found significant comparing each of the concentrations 5, 25, 100 ng/mL to the 0 ng/mL rhIL-32 using Dunnett's test). However, the BMP-2 controls was lower than expected at both day 7 and day 9, and effects seen in **Figure 32** was not reproducible when experiments were repeated (Appendix 4, fig. 5), making the certainty of measurements questionable.

We also measured matrix mineralization in pre-differentiated osteoblasts when incubating with 25$(OH)_2D_3$ for 48 h. MSCs were differentiated for 13 days, followed by incubation with 25(OH)D_3 and IL-32 gamma, and mineralization visualized (**Figure 33A**) and quantified (**Figure 33B**). No significant differences in matrix mineralization between rhIL-32 concentrations in the presence of 25$(OH)_2D_3$ was found after 48 hours stimulation (one-way ANOVA and Dunnett's test).

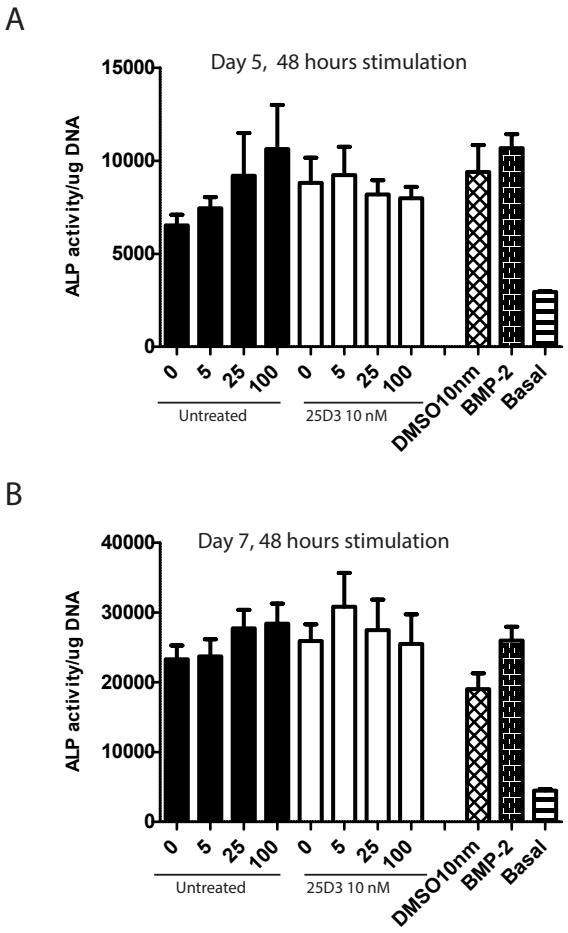

Figure 32: ALP- activity in osteoblasts after 48 hours stimulation with rhIL-32 with or without 25(OH)D_3. MSCs were seeded 2500 cells/well in 96-well plates and differentiated in osteogenic direction for 5 and 7 days before treated with IL-32 gamma (ng/mL) at concentrations indicated, and 25(OH)D_3 (pro vitamin D) for 48 h. BMP-2(300 ng/mL), DMSO (10 nM) and basal (MSCGM) treated cells were included as controls. ALP-activity was measured by ALP-assay following 48 h treatment, and adjusted by µg DNA in each well. Data is presented as mean±SEM of technical replicates. **A)** ALP-activity/ µ g DNA at day 7 following 48 h treatment. **B)** ALP-activity/ µg DNA at day 9 following 48 h treatment.

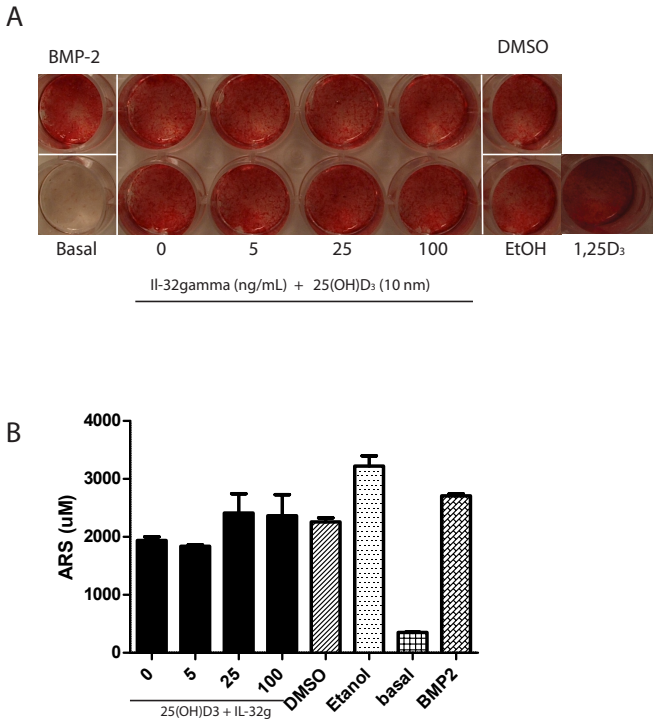

Figure 33: Osteoblast mineralization at day 15 after 48 h stimulation with IL-32 and pro vitamin D. MSCs were seeded 15000 cells/well in 24-wells plate, and differentiated for 13 days, followed by incubation with 10 nM 25(OH)D3 and IL-32 gamma (IL-32g) in concentrations as indicated (ng/mL) for 48 hours. BMP-2(300 ng/mL), DMSO (10 nM) and basal (MSCGM) treated cells were included as controls. **A)** Visualization of mineralization by ARS staining at day 15 following 48 hours stimulation. **B)** Quantitative results of ARS stain shown in A. The dye was extracted from the monolayer and absorbance was measured. Concentration (uM) was determined from an ARS standard curve.

The role of dexamethasone in osteoblast differentiation experiments with vitamin D

The glucocorticoid dexamethasone (dex), frequently used as supplement in osteoblast differentiation media to promote osteogenic differentiation, is also a part of the common osteoblast differentiation protocol in our lab. As dex also have been reported to play a role $1,25(OH)_2D_3$ signaling and transcriptional responses[171] as well as $1,25(OH)_2D_3$ bioavailability[172], we hypothesized that dex could mask or distort osteoblast vitamin D responses as well as differentiation parameters in our experiments. The consequences of removing dex from differentiation media were evaluated by ALP activity an osteoblast mineralization, with the same setup for IL-32 and vitamin D treatment as prior experiments, but this time again including both $1,25(OH)_2D_3$ and $25(OH)D_3$-treatment groups. As controls, corresponding plates were treated with differentiation media with dex, and cultures were terminated at day 5 and 8. Mineralization experiments were terminated at day 15 and assessed by ARS staining.

Excluding dexamethasone from differentiation media did not change the response to vitamin D with regard to ALP-activity (**Figure 34**). There were no significant response to increasing concentrations of IL-32 in the $25(OH)D_3$ -group at neither day 5 (**Figure 34A**). B) nor day at (**Figure 34B**), using one-way ANOVA and Dunnett's Multiple Comparison test.

ALP-activity was lower in osteoblasts differentiated without dex compared to dex-differentiated cells, especially at day 8 (**Figure 34B**), supporting the role of dexamethasone as a promoter of osteogenic differentiation. Also basal (MSCGM) control was higher than expected compared to the differentiated samples in dex-depleted differentiaton media, indicating poor overall differentiation in these experiments. In the "untreated"-group differentiated without dex, day 8, ALP activity was inversely associated to IL-32 concentration (**Figure 34B**). In contrast to previous experiments, ALP-activity was higher in $1,25(OH)_2D_3$ treated cells compared to the other treatments (indicated by grey bars), however no distinguishable change in the $1,25(OH)_2D_3$ response was seen between the no-dex and the dex treatment.

For the mineralization experiment, there were no enhancement of dose dependent responses to IL-32 alone (**Figure 35A**), nor to IL-32 when combined with $25(OH)D_3$ (**Figure 35B**), for cells differentiated in dex-depleted media. As neither the ALP-activity- nor the mineralization

results show effects that can be related directly to the exclusion of dexamethasone, we cannot conclude that dex has affected our previous osteoblast differentiation experiments with vitamin D.

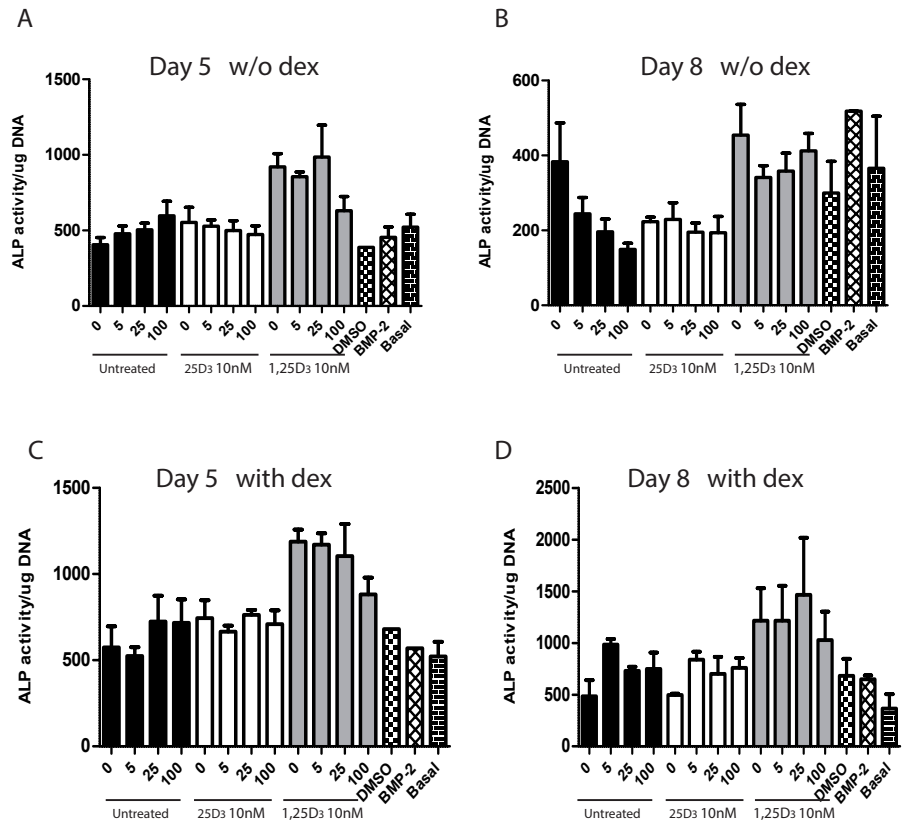

Figure 34: Excluding dex from differentiation media did not reveal any differential effect of IL-32 and vitamin D on osteoblast ALP-activity. MSCs were seeded 2500 cells/well in 96-well plates and differentiated in differentiation media with and without dex and ALP-activity was measured at day 5 and day 8. In all experiments ALP activity was adjusted by DNA quantitation for each well. Cells were treated with 25(OH)D_3 (25D_3, 10 nM), and 1,25$(OH)_2D_3$ (1,25D_3, 10 nM) with rhIL-32 gamma at concentrations (ng/mL) as indicated at the x-axis. For DMSO control 10 nM was used, for BMP-2, 300 ng/mL, and "basal" control refer to MSCGM treated cells. **A)** ALP-activity day 5, in osteoblasts treated with dex-depleted differentiation media. **B)** ALP-activity at day 8, in osteoblasts treated with dex-depleted differentiation media. **C)** ALP-activity at day 5, in osteoblasts treated with differentiation media with dex. **D)** ALP-activity at day 8, in osteoblasts treated with differentiation media with dex.

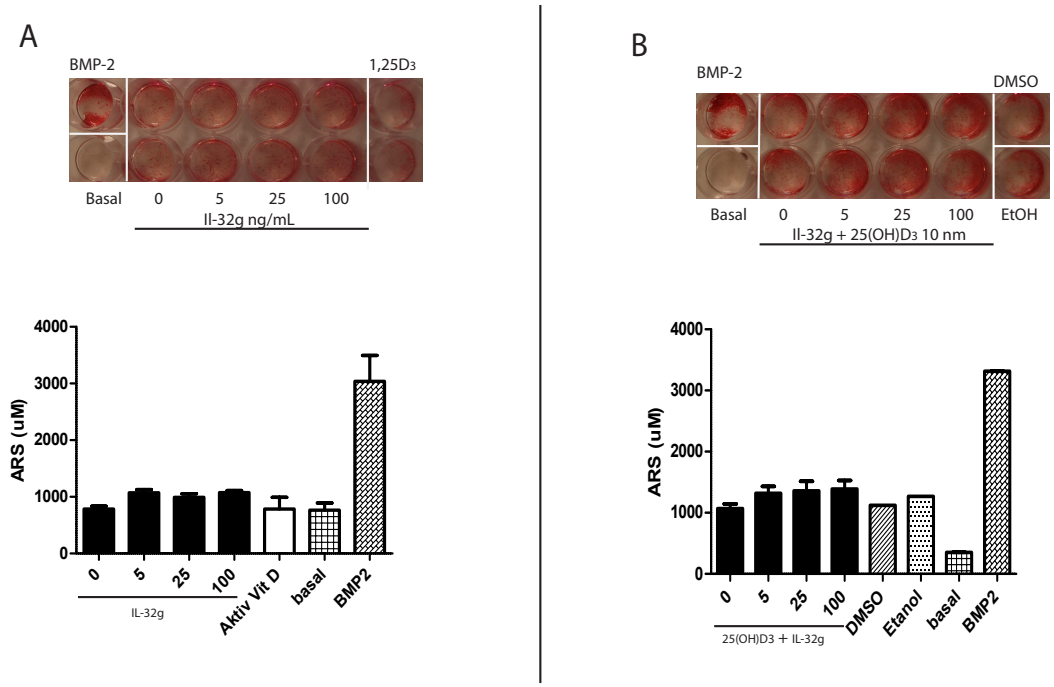

Figure 35: Mineralization in osteoblasts differentiated without dexamethasone. MSCs were differentiated in osteogenic direction with dex-depleted differentiation media. Cells were treated with 25(OH)D_3 (10 nM) and rhIL-32 gamma at concentrations (ng/mL) indicated. 1,25(OH)D_3 (active vitD 10 nM) BMP-2(300 ng/mL), DMSO (10 nM), etanol (10 nM) and basal (MSCGM) treated cells were included as controls. Mineralization in osteoblasts were visualized and quantified by ARS-staining at day 15. **A)** Mineralization in osteoblasts treated with rhIL-32γ **B)** Mineralization in osteoblasts treated with rhIL-32γ (ng/mL) and 25(OH)D_3 .

Part 3

Effect of hypoxia on bone marrow mesenchymal stromal cells

In our preliminary data we showed that IL-32 was induced in myeloma cells cultured in hypoxic conditions. IL-32 has also been related to hypoxia in recent studies on various cancer tissues, interestingly also in stromovascular fraction of adipose tissue[98,104,173]. We therefore investigated RANKL, CYP27B1 and finally, IL-32 gene expression in MSCs exposed to hypoxia for 3 days. Gene expression was measured by RT-qPCR using TATA-binding protein (TBP) as endogenous control as we found GAPDH to be differentially expressed in hypoxic conditions.

RANKL was poorly detected by qPCR, with Ct-values > 35 (**Figure 36**). However, on the basis of the mRNA levels detected, we could not find RANKL mRNA to be upregulated by hypoxia. In normoxia, rhIL-32 appeared to have a positive effect on RANKL expression, but as this was not supported by any of our previous RANKL gene expression results.

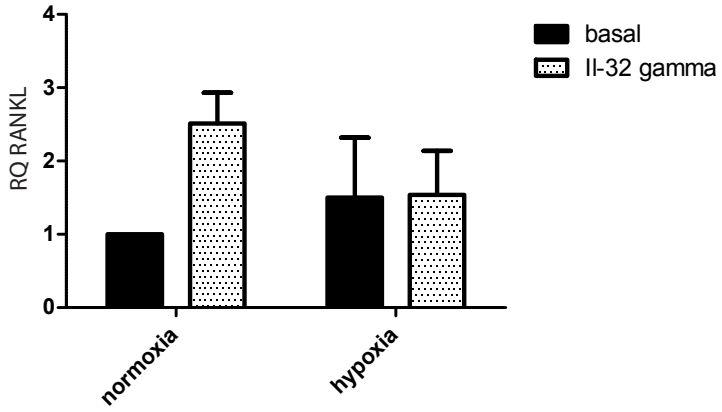

Figure 36: RANKL expression in MSCs cultured in hypoxia. MSCs were seeded 80 000 cells/well in 6-well plates and cultured for 3 days in MSCGM (basal medium) in normoxic (normal O_2 conditions; 20 % O_2 and 5%CO_2) or hypoxic (2%O_2, 5% CO_2) conditions in the presence of IL-32γ (100 ng/mL). RANKL(*TNFS11*)- expression was evaluated by TaqMan based RT-qPCR (Hs00243522_m1, Thermo Fisher) using TBP (Thermo Fisher) as endogenous control. RQ values were calculated using the comparative Ct-method (Ct values >35) Data is reported as mean±SD for technical replicates.

CYP27B1 gene expression (**Figure 37**) was measured in MSCs cultured in hypoxia or normoxia for 3 days with or without IL-32γ in the presence or absence of 25(OH)D_3. Again CYP27B1 mRNA expression were low, with Ct-values>35. For the IL-32 treated group, *CYP27B1* expression in hypoxia was significantly higher than in normoxia (p=0.048), however, an equal upregulation of *CYP27B1* was found for basal control cultured in hypoxia. For IL-32 and 25(OH)D_3 treated group, the opposite response were demonstrated; there were a significant difference (p=0.049) between normoxia and hypoxia, with reduced CYP27B1 mRNA levels in hypoxia.. (the p-values were calculated by unpaired two-sided Student's T-test).

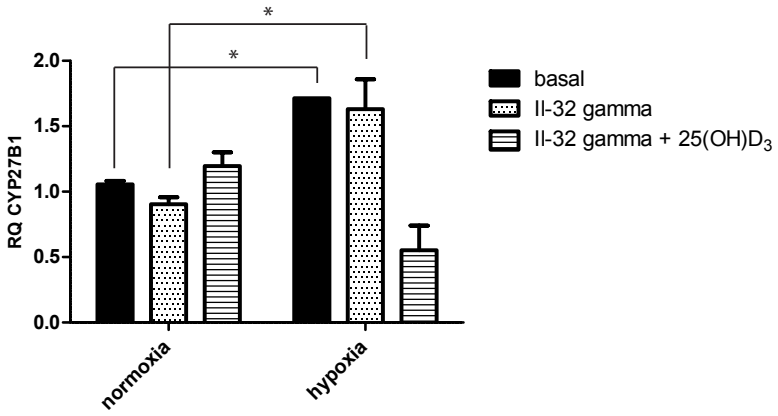

Figure 37: CYP27B1 gene expression in MSCs cultured in hypoxia. MSCs (N=2 donors) were seeded 80 000 cells/well in 6 well-plates and cultured for 3 days with 100 ng/mL IL-32γ with or without 10 nM 25(OH)D_3 in normoxic (normal O_2 conditions; 20 % O_2 and 5%CO_2) or hypoxic (2%O_2, 5% CO_2) conditions. CYP27B1 gene expression was measured by RT-qPCR using TaqMan primers for CYP27B1 (Hs01096154_m1, Thermo Fisher) and endogenous control TBP (Thermo Fisher). RQ values was calculated using the comparative Ct-method (Ct values >35, significant differences between samples therefore not reported). Data is reported as mean±SEM of relative RQ for biological replicates (for basal/hypoxia treated sample CYP27B1 expression was detected in only one donor). * P< 0.05 (p-values calculated by unpaired two-sided Student´s T-test).

IL-32 expression in MSCs was measured after 3 days exposure to hypoxia or normoxia, with or without IL-32γ (**Figure 38**). For the basal medium treated MSCs there were a significant increase in IL-32 expression in hypoxia compared to normoxia (black bars). The same significant difference was found between normoxia and hypoxia in the IL-32 treated group (white, dotted bars). Furthermore, IL-32 expression was markedly increased by rhIL-32 treatment, indicating that IL-32 may induce a positive feedback loop in the MSCs.

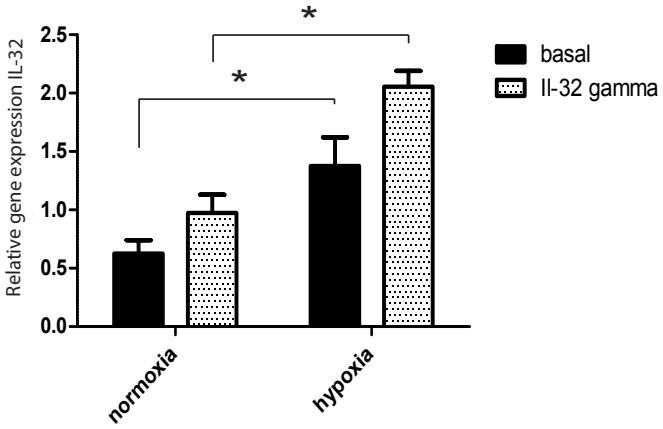

Figure 38: IL-32 expression in MSCs cultured in hypoxia. MSCs were seeded 80 000 cells/well in 6-well plates and cultured for 3 days with MSCGM (basal media) with or without IL-32γ (100 ng/mL) in hypoxic (2% O_2, 5 % CO_2) or normoxic (20% O_2, 5 % CO_2) conditions. *IL-32* expression (primer targeting all isoforms) was evaluated by TaqMan based RT-qPCR (Hs00992441_m1, Thermo Fisher) using TBP (Thermo Fisher) as endogenous control Data is reported as mean±SD of technical replicates. (* P< 0.05, p-values calculated by unpaired two-sided Student´s T-test).

Discussion

IL-32 in myeloma cell-derived exosomes promote *in vitro* osteoclast differentiation

In our preliminary data we showed that recombinant IL-32 is a potent inducer of osteoclastogenesis both *in vivo* and *in vitro* (Zahoor et al, manuscript in preparation). We also found that IL-32 is secreted from the myeloma cells into the bone marrow microenvironment in a vesicle-bound form. In a recent study it has been shown that myeloma cell-derived exosomes induced osteoclast differentiation and migration, however the exosomal factors responsible were not characterized[174]. As we hypothesized IL-32 to be an exosomal effector protein we knocked out IL-32 in JJN-3 cells; an IL-32 expressing myeloma cell line, and compared the pro-osteoclastogenic effect of exosomes from KO cells and control cells where IL-32 was still expressed. (hereafter called WT cells). The exosomes were used to stimulate primary monocytes and the degree of osteoclastogenesis in these cultures was evaluated by counting the number of TRAP-positive osteoclasts. We demonstrated that exosomes from IL-32 expressing wild-type clones was more efficient in inducing osteoclastogenesis than IL-32 depleted exosomes from IL-32 knock-out cells. This difference in osteoclastogenesis was significant in the pre-osteoclast experiments where the monocytes had been exposed to exosome treatment from day 1. However, RANKL demonstrated low osteoclast inducing effects, indicating that the monocytes in these experiments in general differentiated poorly. For the post-osteoclast experiments where exosomes were treated to already-differentiated monocytes, RANKL potently induced osteoclastogenesis. However, the difference between knock-outs and wild-type exosome treatment was less pronounced in these experiments- in fact higher osteoclast number was observed in cultures treated with the D1 KO clone compared to wild-type treated cultures. This finding was later explained by the analysis of the KO JJN-3 protein fraction, where the B11 KO clone still demonstrated complete knock-out of IL-32, while D1 KO clone showed protein expression of IL-32. Furthermore the protein detected had lower molecular weight and apparently lower expression compared to the wild-type IL-32 protein, indicating that incomplete cleavage of the gene by the CRISPR/Cas system has resulted in expression of a truncated form of IL-32. As the IL-32 KO D1 clone was found to induce osteoclastogenesis to the same extent as the WT clone, the truncated IL-32 may still be biologically active. The CRISPR/Cas protocol should not be particularly prone

to incomplete gene cleavage as it provides a mix of three plasmids, each one with a gRNA targeting an specific sequence in the gene, resulting in cleavage of three different exons of the IL-32 gene. However, as the IL-32 gene consists of 8 exons, there is a probability for one or more of the receptor binding sites to be preserved after cleavage, enabling the truncated interleukin to still activate cell-signaling pathways.

During culturing of the JJN-3 IL-32 KO clones, we observed that the KO clone-proliferation was reduced compared to the WT-IL-32 expressing clone (results not shown). As the WT clone had been exposed to the same knock-out procedure and clonal selection process, the differences in proliferation are not likely to be explained by these stress factors, implying that IL-32 may be important for myeloma cell proliferation and survival. Alternatively, truncated forms of IL-32 could interfere with normal cell function and thereby reduce cell division, supported by the fact that IL-32 KO D1 cells were the clones with less proliferative potential. However, also the complete knock-out B11 divided more slowly. Taken together these findings suggest a more diverse role of IL-32 in multiple myeloma, as not only an osteoclastogenic factor, but also as a growth factor for the cancer cell itself.

It should be emphasized that the isolation of exosomes was not specific for IL-32 containing exosomes and that also a single exosome cargo may include several signaling proteins[175]. In the pre-osteoclast experiments, the wild-type exosomes induced more osteoclastogenesis than both RANKL and recombinant IL-32, indicating that there are several osteoclastogenic factors present in the isolated exosome fraction. Still, the difference between B11 exosome-treatment and WT-treatment was highly significant; with remarkably low osteoclast numbers in B11 treated cultures, indicating that IL-32 may account for a great proportion of the total osteoclast promoting effect provided by the myeloma secretory apparatus. However, as the pre-osteoclast experiments demonstrated poor RANKL effect, and the post-osteoclast experiments showed large variation, more experiments needs to be performed before concluding there is an actual difference in osteoclastogenesis between treatments with IL-32-depleted and IL-32 containing exosomes.

Exosomes from myeloma cells may promote *in vitro* osteoblast differentiation

To test the effect of myeloma-derived exosomes on osteogenic differentiation MSCs were treated with differentiation media with exosomes and extent of mineralization was quantified. Remarkably, cells treated with exosomes showed higher mineralization than the cells treated with vehicle only, suggesting that there are pro-osteogenic factors present in the exsosomes. However, it should be noted that the cells treated with vehicle with $25(OH)D_3$ mineralized more, indicating that the pro form of vitamin D alone have promoting effects on mineralization. However, no differences were observed between Il-32 KO D1 exosome treatment and IL-32 WT exosome treatment. The lack of difference may be due to the incomplete knock-out of IL-32 in the D1 clone, and the experiment therefore needs to be repeated with another clone with proper knock out of IL-32 (for example the B11 clone). However, as rhIL-32 in general did not show any effect on osteoblasts in our experiments (further discussed below) we do not expect to see a difference in KO and WT exosomes in terms of osteoblast differentiation.

IL-32 had no apparent effect on osteoblast differentiation

To investigate if recombinant IL-32 had a direct effect on differentiation of MSCs into osteoblasts we measured RUNX2 gene expression and ALP-activity in early osteoblasts, and mineralization in late osteoblasts. Also we studied the effects on proliferation, however, no association between rhIL-32 and cell division was demonstrated. Furthermore, there was no apparent effect of rhIL-32 on any of the osteoblastic markers. We used two isoforms, rhIL-32α and rhIL-32γ, but there were no difference between the two splice variants in terms of effects on proliferation and differentiation. IL-32γ is the most characterized isoform, previously been associated to osteoclastogenesis in relation to rheumatoid arthritis in a study by Kim et al. (2010)[107]. The same authors were the first to publish data on Il-32 and osteoblasts; -in a recent study they showed that IL-32γ increased ALP-activity and mineralization in mouse calvarial osteoblasts. However these results cannot be seen as completely representative as a mouse homologue of IL-32 has still not been characterized[176]. When they in the same study evaluated the effect of Il-32 in human osteoblasts, they found reduced expression of the Wnt-pathway inhibitor DKK-1, but demonstrated no further influences on osteoblast differentiation, indicating that the effect of Il-32 on human osteoblasts still is uncertain.

IL-32 does not increase RANKL in MSCs or osteoblasts

RANKL is an important inducer of osteoclastogenesis and a marker of immature osteoblasts, which we suspected to be increased in an IL-32 rich myeloma bone marrow microenvironment. Furthermore we expected RANKL to be upregulated in hypoxia as this has been demonstrated in studies of other cell types[177,178]. Also this would compliment our findings of increased osteoclastogenesis in response to stimulation with exosomes derived from hypoxia cultured myeloma cells. We did not demonstrate an increased RANKL gene expression in osteoblasts by treating with rhIL-32, neither in normoxia nor hypoxia. However, gene expression of the antagonist OPG was not evaluated, so the RANKL:OPG ratio could potentially have been skewed in favour of RANKL by IL-32-dependent decrease in OPG. In the study by Kim et al. (2010) it was shown that IL-32γ potently skewed the RANKL:OPG ratio in fibroblast-like synviocytes, not only by increasing RANKL expression, but also by significantly reducing OPG[107]. To elucidate the total effect of IL-32 on osteoblast-osteoclast interaction the level of OPG should therefore also have been evaluated.

Osteoblasts are more responsive to IL-32 when combining with 25(OH)D_3, but there is currently not evidence for a inhibitory role of IL-32 through vitamin D metabolism

Since osteoblasts was not affected by IL-32 treatment alone, we changed the experimental approach by including 25(OH)D_3 in the further stimulation experiments. Our hypothesis that IL-32 could induce CYP27B1 expression in osteoblast and thereby mediate conversion of 25(OH)D_3 to 1,25$(OH)_2D_3$ was supported by only a minor number of experiments. Early stages of osteoblast differentiation appeared to be positively regulated by 25(OH)D_3, while there were no clear shift when combining with rhIl-32, in neither positive nor negative direction. 1,25$(OH)_2D_3$ mostly appeared to play a neutral role in early differentiation, when evaluated by extent of RUNX2 gene expression. Both neutral (**Figure 21B**) and positive effects (**Figure 34C** and **D**) of 1,25$(OH)_2D_3$ on ALP-activity was found in independent experiments with MSCs from two different donors, indicating that the effect of active vitamin D may vary slightly between individuals, or alternatively, a consequence of the experimental

variability in primary cell experiments. For Osterix expression in preosteoblasts, no effect of rhIl-32 and $25(OH)D_3$ short term treatment were demonstrated. However Osterix was slightly upregulated by $1,25(OH)_2D_3$ after 24 hours, a finding which is supported by a study by Maehata Y et al. (2007), which reported induction of Osterix by $1,25(OH)_2D_3$ in an human osteoblastic cell line[121]. Interestingly another study demonstrated that Osterix is an important positive regulator of VDR expression in primary osteoblasts from mice calvaria and that the ALP and osteocalcin expression was abrogated when interfering with the Osterix-mediated VDR signaling[179].This indicates that osterix might be important for vitamin D dependent responses in osteoblasts, as VDR is the major receptor for $1,25(OH)_2D_3$[170] in these cells. However, we found Osterix hard to detect, especially in later stages of osteoblastogenesis. The low detection could have diminished differences between samples that might have been present. Whether Osterix expression is particularly low in the osteogenic cells in our system, and this may indirectly abolish the effects of vitamin D though VDR, was not clarified.
However, taken together our findings do not support that IL-32 acts differently on osteoblasts in the presence of $25(OH)D_3$. .

Osteogenic markers are sensitive to experimental conditions and technical variations in laboratory procedures

In both the osteoclast-differentiation- and osteoblast-differentiation experiments we used primary cells. Compared to cell lines primary cells, primary cells are more sensitive to culture conditions, have a limited life span, and show greater experimental variability. However primary cells offer several advantages with regard to the understanding of *in vivo* responses, as the morphology, function and cellular markers are still maintained[180]. Our osteoblast model is derived from primary MSCs differentiated in osteogenic media. Osteoblast gene expression and function differ greatly between maturation stages. It is therefore important to evaluate the osteoblasts at the correct time point of differentiation, depending on what osteogenic marker that is to be studied. However, determining the osteoblast maturation stage of the differentiated stem cells can be a challenge.

The osteogenic markers measured in our study showed high variability between experiments, implying that these are parameters with relatively low statistical power. For example the

activity of alkaline phosphatase appeared to be highly responsive to changes in media volumes, small deviations between wells having major influences on the later measurements. Within experiments there were large variations in ALP-activity between culture plates- also when terminated at the same day. These experiences imply that the ALP-assay is sensitive to technical errors, and require careful lab procedures to be representative for the actual response to a given treatment. Also the mineralization of the MSC-derived osteoblasts appeared to be highly susceptible to changes in media volumes as well as which stage of confluence the differentiation treatment was introduced. The fact that these osteogenic parameters were so sensitive to changes in cell culture conditions reflects their biological role in the bone, which is tightly regulated to maintain bone homeostasis. This complex network of positive and negative feedback mechanisms, endocrine and autocrine signaling, and cell to cell interactions make bone a challenging research area where the *in vitro* system lack the bone marrow microenvironmental factors important for the overall response to a given treatment.

CYP27B1 expression was not induced by rhIL-32 in osteoblasts, but may transiently be upregulated in MSCs

CYP27B1 was poorly detected by qPCR, which might have been due to low expression in MSCs and early osteoblasts or because the primers were not optimally designed. With consideration to the general uncertainty of the CYP27B1 PCR results, the 6 hours stimulation of MSCs with $25(OH)D_3$ and rhIL-32 resulted in higher CYP27B1 mRNA copy number than cells treated with $25(OH)D_3$ alone in convincingly 3 out of 3 experiments. However, the *CYP27B1* promoting effect of rhIL-32 was not observed in pre-osteoblast. On the contrary, there was a tendency for reduced CYP27B1 when pre-osteoblasts were treated with rhIL-32. Although these contradictory findings could be caused by random variations, it might be due to differential regulation of CYP27B1 in MSCs and osteoblasts as other studies report that vitamin D regulation of CYP27B1 differ completely between the MSC and its osteogenic derivatives[122]. Furthermore, the initial increase in CYP27B1 by rhIL-32 in MSCs after 6 hours were only transient, - after 24 hours the positive effect of rhIL-32 were absent. This can hypothetically be explained by $25(OH)D_3$ initially inducing *CYP27B1* expression, followed by *CYP27B1* downregulation as more $25(OH)D_3$ are converted to $1,25(OH)_2D_3$. This suggestion

of internal vitamin D regulation is supported by another study by Zhou et al. (2010), describing these two processes as a feed-forward amplification mechanism and negative feedback repression respectively[181]. In summary, these studies as well as our own findings reflects the complexity of endogenous CYP27B1 regulation- still not completely characterized, and explain our difficulties in identifying an effect of Il-32 on CYP27B1 and its metabolic actions.

$1,25(OH)_2D_3$ inhibitory actions as well as CYP27B1 expression and enzymatic activity may be primarily associated with later stages of osteoblast differentiation

Our finding of $1,25(OH)_2D_3$ as an inhibitor of mineralization is both supported and contradicted by other *in vitro* studies. In most studies of human osteoblasts, $1,25(OH)_2D_3$ had a positive effect on mineralization, however, it were mainly associated with osteogenic events *before* onset of mineralization, while apparently there were no direct influence on the mineral deposition[122]. Furthermore, there are *in vivo* evidences for $1,25(OH)_2D_3$ being a negative regulator of mineral deposition and bone mass[182-184] but these studies are based on murine experimental models, and cannot be directly related to human bone cell biology Although $1,25(OH)_2D_3$ inhibited mineralization in 5 out of 7 of our experiments terminated at day 15, $25(OH)D_3$ combined with increasing concentrations of rhIL-32 only inhibited mineralization in 1 out of those 7. However, the mineralization in this experiment showed a significant rhIL-32 dose dependent reduction, which we found unlikely to occur by chance. Moreover, the cells mineralized poorly in the majority of the experiments (5 out of 7), so more experiments needs to be performed to make a definite conclusion on the role of IL-32 and $25(OH)D_3$ in the osteoblast-lineage . The fact that we demonstrated inhibitory effects of rhIl-32 and $25(OH)D_3$ as well as $1,25(OH)_2D_3$ in mature osteoblasts after onset of mineralization, but not in the earlier differentiation stages may be explained by studies showing that CYP27B1 expression peaked in the stage of osteoblasts maturation with highest mineralization[185] and that high levels of CYP27B1 mRNA were correlated with high concentrations of calcium[186]. Also our own experiment at day 11 of differentiation pointed to a higher expression of CYP27B1 in later osteogenic stages, as the MSC control demonstrated notably lower mRNA levels than the differentiated samples. These findings argue for late osteoblasts being best suited for CYP27B1 gene expression studies. However, from the results of the current study we cannot

presume any effect of Il-32 on CYP27B1 expression nor CYP27B1 mediated vitamin D conversion to be inhibitory to osteoblasts in any stages of differentiation.

Dexamethasone was required for $1,25(OH)_2D_3$ dependent inhibition of mineralization

The glucocorticoid dexamethasone (dex), is a standard component in medium used in *in vitro* osteogenic differentiation of mesenchymal stem cells, and also a part of our differentiation protocol. However, more recent research is contradictory regarding the role of dexamethasone. It has been demonstrated inhibitory effects of glucocorticoids on bone formation, mainly through negative regulation of osteoblast differentiation[187]. Antagonists of the Wnt-pathway, DKK1 and sclerostin, was upregulated by glucocorticoid treatment[187]. Also dexamethasone in particular has been shown to suppress osteoblast function through induction of BMP and Wnt antagonists[188]. Also dex has been shown to interefere with $1,25(OH)_2D_3$ and signaling and bioavailability by increased VDR expression and VDR dependent transcription[171] and by inducing CYP24A1[172], respectively. We hypothesized that removing dex could reveal previously masked or exaggerated affects of vitamin D. Curtis et al. (2014) recently showed that $1,25(OH)_2D_3$ completely inhibited mineralization when dex was excluded from the osteoblast differentiation medium, while on the opposite high level of mineralization was demonstrated when dex was present[168]. However excluding dex from the differentiation medium in our vitamin D stimulation experiments did not result in inhibition of mineralization by $1,25(OH)_2D_3$. On the opposite, $1,25(OH)_2D_3$ potently inhibited mineralization in dex-containing medium while mineralization was not reduced compared to other treatments when using dex depleted medium. Although these findings conflict with the results by Curtis et al. (2014), they are supported by other means, including the fact that dex increased VDR expression and VDR dependent transcription[171], and thereby indirectly could potentiate the effects of $1,25(OH)_2D_3$. We did not outline the reasons for $1,25(OH)_2D_3$ dependent inhibition of mineralization, however, the same study by Curtis et al. showed that the production of reactive oxygen species (ROS) was induced in $1,25(OH)_2D_3$ treated osteoblast cultures, and another study by Arai et al. (2007) demonstrated complete inhibition of mineralization by ROS in osteoblastic cells[189], indicating that induction of ROS may be a part of a negative regulatory mechanism exerted by $1,25(OH)_2D_3$ in bone cells. In our system dexamethasone may play a role in augmenting ROS production, a theory that can be both

supported and contradicted by other studies, which showed both activating[190] as well as suppressive effect of dex on cellular ROS production[191].

$1,25(OH)_2D_3$ biosynthesis was negatively associated to osteogenic markers but not dependently of rhIL-32

To quantitatively evaluate the CYP27B1 activity in response to IL-32 we measured the level of $1,25(OH)_2D_3$ biosynthesis in conditioned media from rhIL-32 and $25(OH)D_3$ treated osteoblasts. We observed a small correlation between rhIL-32 dependent inhibition of mineralization and the level of $1,25(OH)_2D_3$ in cell culture supernatant, but this relationship was only evaluated for the experiment in which we observed an IL-32 dependent inhibition, and has thereby not been further validated. Furthermore ALP-activity were slightly associated with the level of $1,25(OH)_2D_3$ detected in media from these wells, with higher $1,25(OH)_2D_3$ levels associated to lower ALP-activity. However, there were no association between $1,25(OH)_2D_3$ levels and IL-32 concentrations. Our findings thereby to some extent supported our hypothesis of increased CYP27B1-activity and higher $1,25(OH)_2D_3$ conversion by IL-32, but we outlined several weaknesses regarding our experimental approach, that if been performed in a different manner might have resulted in more interpretable data. First, we detected nearly equal levels of $1,25(OH)_2D_3$ in all our samples regardless of $25(OH)D_3$ being supplemented in medium or not. We found this unlikely to be due to unspesific binding to other metabolites or background noise, as the ELISA was highly specific towards $1,25(OH)_2D_3$ and with sensitivity for concentrations as low as 9.4 pmol/L[157]. The $25(OH)D_3$ concentration of human serum is usually 10 nM[192], we therefore suspected that $25(OH)D_3$ was present in the serum proportion of the MSC growth medium used as basis for the differentiation media. Hence, this supply of $25(OH)D_3$ could be consumed as substrate for CYP27B1 in samples that were intended as $25(OH)D_3$ depleted controls. Moreover, studies evaluating $1,25(OH)_2D_3$ biosynthesis, cultured the cells in serum free medium in the time period treating with $25(OH)D_3$, further implying that this should be the standard procedure when measuring conversion of $25(OH)D_3$ to$1,25(OH)_2D_3$ by CYP27B1.

Furthermore, activity of CYP27B1 is often represented by biosynthesized $1,25(OH)_2D_3$ /protein/hr where the cells are treated with $25(OH)D_3$ for a definite time-period and protein

concentration in each sample is evaluated subsequent to the harvest of supernatant[166,181,185]. However, since we used the supernatant from cell-cultures that were to be stained by ARS or used in ALP-assay, we could not analyze the cell-fraction of the experiment, and were therefore not able to account for differences in cell number or protein levels in cultures. By normalizing the level of $1,25(OH)_2D_3$ for protein content in each well, and defining a time-period for $25(OH)D_3$ treatment we would have achieved a more precise quantitative measure of the actual CYP27B1 activity in each sample.

Finally, in a study by Atkins et al. (2007), also evaluating the intracellular levels of $1,25(OH)_2D_3$ they interestingly found 55% of the synthesized $1,25(OH)_2D_3$ to be associated with the cell monolayer[185]. This suggests that a total quantification of $1,25(OH)_2D_3$ from cell media and cell lysates would have resulted in higher levels and more precise measurements of the active metabolite. The fact that a large proportion of the $1,25(OH)_2D_3$ remained in the cell vicinity, supports the paracrine and autocrine roles of vitamin D in osteoblast.

Bone marrow mesenchymal stromal cells express IL-32 and the expression is increased by IL-32 and by hypoxia

Preliminary data by our group showed that Il-32 expression was increased when primary cells or Il-32 expressing cell lines were cultured in hypoxic conditions, implying a connection between IL-32 expression and hypoxia. Briefly, Il-32 expression has been demonstrated in bone marrow stromal cells, but only in the context of myelodyplasmic syndromes[110,111]. We found that also mesenchymal stromal cells of our system expressed Il-32. Intriguingly, the expression was enhanced by hypoxia and an even greater effect was demonstrated by including Il-32, the latter finding suggesting an autocrine feedback loop. As the bone marrow niche is a highly hypoxic environment[193], this finding indicate that both positive feedback loops between the MSCs and myeloma cells, as well as the hypoxic nature of the microenvironment contribute to increased Il-32 production by the mesenchymal stromal cell population. The obvious role of hypoxia in Il-32 regulation demands for more experiments on osteoblasts and MSCs exposed to hypoxic conditions; although we did not find any effect of IL-32 on osteoblasts in normoxia, stimulating the cells in hypoxia might unveil novel mechanism of action. Furthermore, an interesting follow-up experiment to investigate the suggested feedback signaling mechanisms would be to co-culture MSCs and an IL-32 expressing myeloma cell line and evaluate IL-32 expression.

Taken together, these findings improves the understanding of IL-32 in the myeloma bone marrow microenvironment, convincingly suggesting that the IL-32 secreted by the malignant plasma cells accelerate production of IL-32 in the stromal cell population and thereby increase the concentration and total impact of IL-32 in the bone marrow. Whether also osteoblasts express IL-32 or if this is a property of undifferentiated cells, remains to be investigated, but from our current finding we suggest that MSCs works in concert with myeloma cells to increase osteoclastogenesis by the expression of IL-32.

CYP27B1 expression in MSCs may be increased by hypoxia

CYP27B1 gene expression were increased in response to hypoxia in non-treated and IL-32 treated samples in our study. Remarkably, on the opposite to the other treatments, CYP27B1 was downregulated in hypoxia when including 25(OH)D_3 to the treatment. The reason for this was not outlined, but may be related to intrinsic downregulation of CYP27B1 by 25(OH)D_3 in response to hypoxia, as the metabolite previously have been shown to protect cells from cellular stress, including low oxygen[194]. Apart from this, our finding of hypoxia-dependent upregulation of *CYP27B1* is supported by a gene correlation study performed by Ormsby et al. (2014) reporting a strong positive correlation between CYP27B1 and HIF1α, the master transcription factor for cellular responses to hypoxia[195]. This, taken together with our finding, propose that bone metabolism of vitamin D is affected by hypoxia and that vitamin D may play a role in cellular adaption to hypoxic condition.

The study by Ormsby et al. also found CYP27B1 expression to be correlated preferently with osteoclast resorption markers rather than osteoblastic marker genes. The evidence for CYP27B1 being mainly associated with osteoclast resorption may indicate that CYP27B1 expression in osteoclasts may be more relevant for the myeloma bone disease than CYP27B1 expression in osteoblasts. The fact that IL-32 was upregulated CYP27B1 in monocytes[1] was important for our approach in this project studying IL-32 in the context of vitamin D metabolism in osteoblasts. However, as osteoclasts are derived from monocytes there is even more likely that the IL-32 dependent upregulation of CYP27B1 could take place in the osteoclastic cells. Furthermore, CYP27B1 metabolism of 25(OH)D_3 resulted in an significant elevation of $TRAP^+$ multinucleate osteoclasts in a study by Kowaga et al. (2010)[196], suggesting that the IL-32 dependent increase in osteoclasts demonstrated in our initial

experiments may be partially explained by CYP27B1 expression and vitamin D metabolism, and that an even higher CYP27B1 gene signature may be present in hypoxic conditions.

Conclusion

In this project we evaluated the role of IL-32 in multiple myeloma bone disease, focusing on osteoclasts and osteoblasts, the cells involved in bone resorption and bone formation respectively. Preliminary results by our group (Zahoor et al.) showed that IL-32 was secreted by the myeloma cells bound to exosomal vesicles, and that recombinant IL-32 as well as myeloma-derived exosomes increased osteoclastogenesis both *in vivo* and *in vitro.* As primary cells from bone marrow aspirates demonstrated an IL-32 expressing phenotype, while only a few cell lines expressed IL-32, the production of this interleukin seemed to be dependent on BM microenvironmental factors. The importance of bone marrow environment for IL-32 expression was further supported by the finding that hypoxic conditions increased the production of IL-32 by the myeloma cells and that vesicles derived from these conditions were even more efficient in inducing osteoclastogenesis.

By using exosomes from myeloma IL-32 knock-out and wild-type cells to stimulate osteoclast and osteoblast in differentiation experiment, we found that IL-32 wild-type exosomes increased osteoclastogenesis, while knock-out exosomes had less or no ability to induce osteoclast differentiation. On the opposite, no differential effects between exosome treatments were found in osteoblasts, evaluated by extent of mineralization. However, the KO clone used in the osteoblast experiments was shown to be incomplete knockout when protein expression was re-evaluated by western blot. Worth noting was the reduced proliferation observed in Il-32 KO cells, which suggest that IL-32 may also function as growth factor for the myeloma cells.

The main objective of the project was to investigate the effect of IL-32 on osteoblasts differentiation. However our hypothesis that IL-32 would influence osteoblast maturation and function was disproved. IL-32 alone was not found to exert any effect on osteoblast alkaline phosphatase activity, osteoblast-specific gene expression, proliferation or mineralization. Combining IL-32 with the pro-form of vitamin D to investigate if the effect may be dependent on upregulation of CYP27B1 and subsequent conversion of pro to active form of vitamin D,

showed no enhanced effect of osteoblast differentiation. Although the osteoblasts seem to be more responsive to this treatment, the results were ambiguous, so it cannot be concluded that IL-32 act on osteoblasts through CYP27B1 conversion of vitamin D. Furthermore, vitamin D demonstrated both negative and positive regulatory actions on the osteoblasts of our system, a characteristic supported by most available literature; - the role of local paracrine and autocrine signaling by vitamin D is not yet completely understood.

Although IL-32 did not impair the activity of the bone forming cells, we found that the progenitors of osteoblasts, mesenchymal stromal cells, also express IL-32. Furthermore expression was increased by hypoxia and stimulation with exogenous IL-32, suggesting a myeloma-supportive role of the mesenchymal stromal cell population in the context of IL-32 in the bone marrow microenvironment.

Finally, CYP27B1 gene expression was also upregulated by hypoxia, indicating that the cell metabolism of vitamin D may be changed as a part of cellular adaption to low oxygen.

Taken together our findings argue for a role of IL-32 in myeloma bone disease as a factor inducing bone resorption, but not affecting bone formation. Instead the osteogenic progenitors may act in concert with the myeloma cells by producing IL-32, further leading to increased osteoclastogenesis and progression of bone disease. In summary, these findings contribute to a better understanding of IL-32 in the myeloma bone disease, although more extensive research needs to address the total impact of IL-32 on the myeloma bone marrow microenvironment and the mechanisms behind IL-32 effector functions.

References

1 Montoya, D. *et al.* IL-32 is a molecular marker of a host defense network in human tuberculosis. *Sci Transl Med* **6**, 250ra114, doi:10.1126/scitranslmed.3009546 (2014).

2 Bianchi, G. & Munshi, N. C. Pathogenesis beyond the cancer clone(s) in multiple myeloma. *Blood* **125**, 3049-3058, doi:10.1182/blood-2014-11-568881 (2015).

3 Palumbo, A. & Anderson, K. Multiple Myeloma. *New England Journal of Medicine* **364**, 1046-1060, doi:10.1056/NEJMra1011442 (2011).

4 Kastritis, E., Palumbo, A. & Dimopoulos, M. A. Treatment of relapsed/refractory multiple myeloma. *Seminars in hematology* **46**, 143-157, doi:10.1053/j.seminhematol.2009.01.004 (2009).

5 Kyle, R. A. & Rajkumar, S. V. Criteria for diagnosis, staging, risk stratification and response assessment of multiple myeloma. *Leukemia* **23**, 3-9, doi:10.1038/leu.2008.291 (2009).

6 Norwegian Cancer Registry https://www.kreftregisteret.no/Registrene/Kreftstatistikk/ 2014.

7 Nyenget T., "Benmargskreft", Oslo: Kreftforeningen; https://kreftforeningen.no/om-kreft/kreftformer/benmargskreft/ , 2015.

8 Smith, L. *et al.* Multiple myeloma and physical activity: a scoping review. *BMJ open* **5**, e009576, doi:10.1136/bmjopen-2015-009576 (2015).

9 Owen, J., Punt, J., Strandford, S. & Pat Jones. *Kuby Immunology*. Seventh edn, Chapter 2; p.38-39 (New York; Macmillian, 2009).

10 Prideaux, S. M., Conway O'Brien, E. & Chevassut, T. J. The genetic architecture of multiple myeloma. *Advances in hematology* **2014**, 864058, doi:10.1155/2014/864058 (2014).

11 Hideshima, T., Mitsiades, C., Tonon, G., Richardson, P. G. & Anderson, K. C. Understanding multiple myeloma pathogenesis in the bone marrow to identify new therapeutic targets. *Nature reviews. Cancer* **7**, 585-598, doi:10.1038/nrc2189 (2007).

12 Boyle, E. M., Davies, F. E., Leleu, X. & Morgan, G. J. Understanding the multiple biological aspects leading to myeloma. *Haematologica* **99**, 605-612, doi:10.3324/haematol.2013.097907 (2014).

13 Morgan, G. J., Walker, B. A. & Davies, F. E. The genetic architecture of multiple myeloma. *Nature reviews. Cancer* **12**, 335-348, doi:10.1038/nrc3257 (2012).

14 Mahindra, A. *et al.* Latest advances and current challenges in the treatment of multiple myeloma. *Nature reviews. Clinical oncology* **9**, 135-143, doi:10.1038/nrclinonc.2012.15 (2012).

15 Uttervall, K. *et al.* The use of novel drugs can effectively improve response, delay relapse and enhance overall survival in multiple myeloma patients with renal impairment. *PloS one* **9**, e101819, doi:10.1371/journal.pone.0101819 (2014).

16 Bergsagel, P. L. *et al.* Cyclin D dysregulation: an early and unifying pathogenic event in multiple myeloma. *Blood* **106**, 296-303, doi:10.1182/blood-2005-01-0034 (2005).

17 Korde, N., Kristinsson, S. Y. & Landgren, O. Monoclonal gammopathy of undetermined significance (MGUS) and smoldering multiple myeloma (SMM):

novel biological insights and development of early treatment strategies. *Blood* **117**, 5573-5581, doi:10.1182/blood-2011-01-270140 (2011).
18 Yasui, H., Hideshima, T., Richardson, P. G. & Anderson, K. C. Novel therapeutic strategies targeting growth factor signalling cascades in multiple myeloma. *British journal of haematology* **132**, 385-397, doi:10.1111/j.1365-2141.2005.05860.x (2006).
19 Roccaro, A. M. *et al.* BM mesenchymal stromal cell-derived exosomes facilitate multiple myeloma progression. *The Journal of clinical investigation* **123**, 1542-1555, doi:10.1172/jci66517 (2013).
20 Tosi, P. Diagnosis and treatment of bone disease in multiple myeloma: spotlight on spinal involvement. *Scientifica (Cairo)* **2013**, 104546, doi:10.1155/2013/104546 (2013).
21 Pearse, R. N. Wnt antagonism in multiple myeloma: a potential cause of uncoupled bone remodeling. *Clinical cancer research : an official journal of the American Association for Cancer Research* **12**, 6274s-6278s, doi:10.1158/1078-0432.ccr-06-0648 (2006).
22 Clarke, B. Normal bone anatomy and physiology. *Clinical journal of the American Society of Nephrology : CJASN* **3 Suppl 3**, S131-139, doi:10.2215/cjn.04151206 (2008).
23 Vanputte, C., Regan, J. & Russo, A. *Seeley's Essentials of Anatomy & Physiology*. Eight edn, Chapter 6; p.111-113 (New York, USA; MacGraw Hill, 2013).
24 Hadjidakis, D. J. & Androulakis, II. Bone remodeling. *Ann N Y Acad Sci* **1092**, 385-396, doi:10.1196/annals.1365.035 (2006).
25 Toscani, D., Bolzoni, M., Accardi, F., Aversa, F. & Giuliani, N. The osteoblastic niche in the context of multiple myeloma. *Ann N Y Acad Sci* **1335**, 45-62, doi:10.1111/nyas.12578 (2015).
26 Florencio-Silva, R., Sasso, G. R., Sasso-Cerri, E., Simoes, M. J. & Cerri, P. S. Biology of Bone Tissue: Structure, Function, and Factors That Influence Bone Cells. *Biomed Res Int* **2015**, 421746, doi:10.1155/2015/421746 (2015).
27 Sims, N. A. & Martin, T. J. Coupling the activities of bone formation and resorption: a multitude of signals within the basic multicellular unit. *Bonekey Rep* **3**, 481, doi:10.1038/bonekey.2013.215 (2014).
28 Sims, N. A. & Martin, T. J. Coupling Signals between the Osteoclast and Osteoblast: How are Messages Transmitted between These Temporary Visitors to the Bone Surface? *Front Endocrinol (Lausanne)* **6**, 41, doi:10.3389/fendo.2015.00041 (2015).
29 Capulli, M., Paone, R. & Rucci, N. Osteoblast and osteocyte: games without frontiers. *Arch Biochem Biophys* **561**, 3-12, doi:10.1016/j.abb.2014.05.003 (2014).
30 Liu, W. *et al.* Overexpression of Cbfa1 in osteoblasts inhibits osteoblast maturation and causes osteopenia with multiple fractures. *J Cell Biol* **155**, 157-166, doi:10.1083/jcb.200105052 (2001).
31 MacDonald, B. T., Tamai, K. & He, X. Wnt/beta-catenin signaling: components, mechanisms, and diseases. *Dev Cell* **17**, 9-26, doi:10.1016/j.devcel.2009.06.016 (2009).
32 Gong, Y. *et al.* LDL receptor-related protein 5 (LRP5) affects bone accrual and eye development. *Cell* **107**, 513-523 (2001).
33 Hartmann, C. A Wnt canon orchestrating osteoblastogenesis. *Trends Cell Biol* **16**, 151-158, doi:10.1016/j.tcb.2006.01.001 (2006).

34 Urist, M. R. & Strates, B. S. Bone morphogenetic protein. *J Dent Res* **50**, 1392-1406 (1971).
35 Vanhatupa, S., Ojansivu, M., Autio, R., Juntunen, M. & Miettinen, S. Bone Morphogenetic Protein-2 Induces Donor-Dependent Osteogenic and Adipogenic Differentiation in Human Adipose Stem Cells. *Stem Cells Transl Med* **4**, 1391-1402, doi:10.5966/sctm.2015-0042 (2015).
36 Reagan, M. R., Liaw, L., Rosen, C. J. & Ghobrial, I. M. Dynamic interplay between bone and multiple myeloma: emerging roles of the osteoblast. *Bone* **75**, 161-169, doi:10.1016/j.bone.2015.02.021 (2015).
37 Crockett, J. C., Rogers, M. J., Coxon, F. P., Hocking, L. J. & Helfrich, M. H. Bone remodelling at a glance. *J Cell Sci* **124**, 991-998, doi:10.1242/jcs.063032 (2011).
38 Feng, X. & Teitelbaum, S. L. Osteoclasts: New Insights. *Bone Res* **1**, 11-26, doi:10.4248/br201301003 (2013).
39 Boyce, B. F., Yao, Z. & Xing, L. Osteoclasts have multiple roles in bone in addition to bone resorption. *Crit Rev Eukaryot Gene Expr* **19**, 171-180 (2009).
40 Silver, I. A., Murrills, R. J. & Etherington, D. J. Microelectrode studies on the acid microenvironment beneath adherent macrophages and osteoclasts. *Experimental cell research* **175**, 266-276 (1988).
41 Delaisse, J. M. *et al.* Matrix metalloproteinases (MMP) and cathepsin K contribute differently to osteoclastic activities. *Microsc Res Tech* **61**, 504-513, doi:10.1002/jemt.10374 (2003).
42 Kohli, S. S. & Kohli, V. S. Role of RANKL-RANK/osteoprotegerin molecular complex in bone remodeling and its immunopathologic implications. *Indian J Endocrinol Metab* **15**, 175-181, doi:10.4103/2230-8210.83401 (2011).
43 Fu, Q., Manolagas, S. C. & O'Brien, C. A. Parathyroid hormone controls receptor activator of NF-kappaB ligand gene expression via a distant transcriptional enhancer. *Molecular and cellular biology* **26**, 6453-6468, doi:10.1128/mcb.00356-06 (2006).
44 Baschant, U., Lane, N. E. & Tuckermann, J. The multiple facets of glucocorticoid action in rheumatoid arthritis. *Nat Rev Rheumatol* **8**, 645-655, doi:10.1038/nrrheum.2012.166 (2012).
45 Takahashi, N., Udagawa, N. & Suda, T. Vitamin D endocrine system and osteoclasts. *Bonekey Rep* **3**, 495, doi:10.1038/bonekey.2013.229 (2014).
46 Karst, M., Gorny, G., Galvin, R. J. & Oursler, M. J. Roles of stromal cell RANKL, OPG, and M-CSF expression in biphasic TGF-beta regulation of osteoclast differentiation. *J Cell Physiol* **200**, 99-106, doi:10.1002/jcp.20036 (2004).
47 Pivonka, P. *et al.* Theoretical investigation of the role of the RANK-RANKL-OPG system in bone remodeling. *J Theor Biol* **262**, 306-316, doi:10.1016/j.jtbi.2009.09.021 (2010).
48 Hofbauer, L. C. *et al.* The roles of osteoprotegerin and osteoprotegerin ligand in the paracrine regulation of bone resorption. *J Bone Miner Res* **15**, 2-12, doi:10.1359/jbmr.2000.15.1.2 (2000).
49 Esteve, F. R. & Roodman, G. D. Pathophysiology of myeloma bone disease. *Best practice & research. Clinical haematology* **20**, 613-624, doi:10.1016/j.beha.2007.08.003 (2007).
50 Minarik, J. *et al.* Prospective study of signalling pathways in myeloma bone disease with regard to activity of the disease, extent of skeletal involvement and correlation to bone turnover markers. *European journal of haematology* **97**, 201-207, doi:10.1111/ejh.12708 (2016).

51 Yaccoby, S. Advances in the understanding of myeloma bone disease and tumour growth. *British journal of haematology* **149**, 311-321, doi:10.1111/j.1365-2141.2010.08141.x (2010).
52 Rajkumar, S. V. Evolving diagnostic criteria for multiple myeloma. *Hematology Am Soc Hematol Educ Program* **2015**, 272-278, doi:10.1182/asheducation-2015.1.272 (2015).
53 Zhan, F. *et al.* The molecular classification of multiple myeloma. *Blood* **108**, 2020-2028, doi:10.1182/blood-2005-11-013458 (2006).
54 Terpos, E., Dimopoulos, M. A. & Sezer, O. The effect of novel anti-myeloma agents on bone metabolism of patients with multiple myeloma. *Leukemia* **21**, 1875-1884, doi:10.1038/sj.leu.2404843 (2007).
55 Zangari, M., Elice, F. & Tricot, G. Immunomodulatory drugs in multiple myeloma. *Expert opinion on investigational drugs* **14**, 1411-1418, doi:10.1517/13543784.14.11.1411 (2005).
56 Pearse, R. N. *et al.* Multiple myeloma disrupts the TRANCE/ osteoprotegerin cytokine axis to trigger bone destruction and promote tumor progression. *Proceedings of the National Academy of Sciences of the United States of America* **98**, 11581-11586, doi:10.1073/pnas.201394498 (2001).
57 Choi, S. J. *et al.* Macrophage inflammatory protein 1-alpha is a potential osteoclast stimulatory factor in multiple myeloma. *Blood* **96**, 671-675 (2000).
58 Lee, J. W. *et al.* IL-3 expression by myeloma cells increases both osteoclast formation and growth of myeloma cells. *Blood* **103**, 2308-2315, doi:10.1182/blood-2003-06-1992 (2004).
59 Zannettino, A. C. *et al.* Elevated serum levels of stromal-derived factor-1alpha are associated with increased osteoclast activity and osteolytic bone disease in multiple myeloma patients. *Cancer research* **65**, 1700-1709, doi:10.1158/0008-5472.can-04-1687 (2005).
60 Westhrin, M. *et al.* Growth differentiation factor 15 (GDF15) promotes osteoclast differentiation and inhibits osteoblast differentiation and high serum GDF15 levels are associated with multiple myeloma bone disease. *Haematologica* **100**, e511-514, doi:10.3324/haematol.2015.124511 (2015).
61 Sanderson, R. D., Yang, Y., Suva, L. J. & Kelly, T. Heparan sulfate proteoglycans and heparanase--partners in osteolytic tumor growth and metastasis. *Matrix biology : journal of the International Society for Matrix Biology* **23**, 341-352, doi:10.1016/j.matbio.2004.08.004 (2004).
62 Kukreja, A., Radfar, S., Sun, B. H., Insogna, K. & Dhodapkar, M. V. Dominant role of CD47-thrombospondin-1 interactions in myeloma-induced fusion of human dendritic cells: implications for bone disease. *Blood* **114**, 3413-3421, doi:10.1182/blood-2009-03-211920 (2009).
63 Dhodapkar, K. M. *et al.* Dendritic cells mediate the induction of polyfunctional human IL17-producing cells (Th17-1 cells) enriched in the bone marrow of patients with myeloma. *Blood* **112**, 2878-2885, doi:10.1182/blood-2008-03-143222 (2008).
64 Ehrlich, L. A. & Roodman, G. D. The role of immune cells and inflammatory cytokines in Paget's disease and multiple myeloma. *Immunological reviews* **208**, 252-266, doi:10.1111/j.0105-2896.2005.00323.x (2005).
65 Atkins, G. J. *et al.* RANKL expression is related to the differentiation state of human osteoblasts. *J Bone Miner Res* **18**, 1088-1098, doi:10.1359/jbmr.2003.18.6.1088 (2003).

66 Ji, B., Genever, P. G., Patton, R. J. & Fagan, M. J. Mathematical modelling of the pathogenesis of multiple myeloma-induced bone disease. *Int J Numer Method Biomed Eng* **30**, 1085-1102, doi:10.1002/cnm.2645 (2014).
67 Gunn, W. G. *et al.* A crosstalk between myeloma cells and marrow stromal cells stimulates production of DKK1 and interleukin-6: a potential role in the development of lytic bone disease and tumor progression in multiple myeloma. *Stem cells (Dayton, Ohio)* **24**, 986-991, doi:10.1634/stemcells.2005-0220 (2006).
68 Kortesidis, A. *et al.* Stromal-derived factor-1 promotes the growth, survival, and development of human bone marrow stromal stem cells. *Blood* **105**, 3793-3801, doi:10.1182/blood-2004-11-4349 (2005).
69 Giuliani, N., Rizzoli, V. & Roodman, G. D. Multiple myeloma bone disease: Pathophysiology of osteoblast inhibition. *Blood* **108**, 3992-3996, doi:10.1182/blood-2006-05-026112 (2006).
70 Oranger, A., Carbone, C., Izzo, M. & Grano, M. Cellular mechanisms of multiple myeloma bone disease. *Clin Dev Immunol* **2013**, 289458, doi:10.1155/2013/289458 (2013).
71 Qiang, Y. W., Barlogie, B., Rudikoff, S. & Shaughnessy, J. D., Jr. Dkk1-induced inhibition of Wnt signaling in osteoblast differentiation is an underlying mechanism of bone loss in multiple myeloma. *Bone* **42**, 669-680, doi:10.1016/j.bone.2007.12.006 (2008).
72 Standal, T. *et al.* HGF inhibits BMP-induced osteoblastogenesis: possible implications for the bone disease of multiple myeloma. *Blood* **109**, 3024-3030, doi:10.1182/blood-2006-07-034884 (2007).
73 Bendre, M. S. *et al.* Interleukin-8 stimulation of osteoclastogenesis and bone resorption is a mechanism for the increased osteolysis of metastatic bone disease. *Bone* **33**, 28-37 (2003).
74 Giuliani, N. *et al.* Human myeloma cells stimulate the receptor activator of nuclear factor-kappa B ligand (RANKL) in T lymphocytes: a potential role in multiple myeloma bone disease. *Blood* **100**, 4615-4621, doi:10.1182/blood-2002-04-1121 (2002).
75 Giuliani, N. *et al.* Interleukin-3 (IL-3) is overexpressed by T lymphocytes in multiple myeloma patients. *Blood* **107**, 841-842, doi:10.1182/blood-2005-07-2719 (2006).
76 Chauhan, D. *et al.* Functional interaction of plasmacytoid dendritic cells with multiple myeloma cells: a therapeutic target. *Cancer Cell* **16**, 309-323, doi:10.1016/j.ccr.2009.08.019 (2009).
77 Terpos, E., Roodman, G. D. & Dimopoulos, M. A. Optimal use of bisphosphonates in patients with multiple myeloma. *Blood* **121**, 3325-3328, doi:10.1182/blood-2012-10-435750 (2013).
78 Luckman, S. P. *et al.* Nitrogen-containing bisphosphonates inhibit the mevalonate pathway and prevent post-translational prenylation of GTP-binding proteins, including Ras. *J Bone Miner Res* **13**, 581-589, doi:10.1359/jbmr.1998.13.4.581 (1998).
79 Rogers, M. J. *et al.* Cellular and molecular mechanisms of action of bisphosphonates. *Cancer* **88**, 2961-2978 (2000).
80 Vanderkerken, K. *et al.* Recombinant osteoprotegerin decreases tumor burden and increases survival in a murine model of multiple myeloma. *Cancer research* **63**, 287-289 (2003).

81 Yaccoby, S. *et al.* Myeloma interacts with the bone marrow microenvironment to induce osteoclastogenesis and is dependent on osteoclast activity. *British journal of haematology* **116**, 278-290 (2002).
82 Terpos, E., Confavreux, C. B. & Clezardin, P. Bone antiresorptive agents in the treatment of bone metastases associated with solid tumours or multiple myeloma. *BoneKEy Rep* **4**, doi:10.1038/bonekey.2015.113 (2015).
83 Clinical Trials.gov: Denosumab Compared to Zoledronic Acid in the Treatment of Bone Disease in Subjects With Multiple Myeloma, https://clinicaltrials.gov/ct2/show/NCT01345019. (2016).
84 Yaccoby, S. *et al.* Antibody-based inhibition of DKK1 suppresses tumor-induced bone resorption and multiple myeloma growth in vivo. *Blood* **109**, 2106-2111, doi:10.1182/blood-2006-09-047712 (2007).
85 Qiang, Y. W., Shaughnessy, J. D., Jr. & Yaccoby, S. Wnt3a signaling within bone inhibits multiple myeloma bone disease and tumor growth. *Blood* **112**, 374-382, doi:10.1182/blood-2007-10-120253 (2008).
86 Edwards, C. M. *et al.* Increasing Wnt signaling in the bone marrow microenvironment inhibits the development of myeloma bone disease and reduces tumor burden in bone in vivo. *Blood* **111**, 2833-2842, doi:10.1182/blood-2007-03-077685 (2008).
87 Yaccoby, S. *et al.* Inhibitory effects of osteoblasts and increased bone formation on myeloma in novel culture systems and a myelomatous mouse model. *Haematologica* **91**, 192-199 (2006).
88 Li, X., Pennisi, A. & Yaccoby, S. Role of decorin in the antimyeloma effects of osteoblasts. *Blood* **112**, 159-168, doi:10.1182/blood-2007-11-124164 (2008).
89 Kim, S. H., Han, S. Y., Azam, T., Yoon, D. Y. & Dinarello, C. A. Interleukin-32: a cytokine and inducer of TNFalpha. *Immunity* **22**, 131-142, doi:10.1016/j.immuni.2004.12.003 (2005).
90 Dahl, C. A., Schall, R. P., He, H. L. & Cairns, J. S. Identification of a novel gene expressed in activated natural killer cells and T cells. *Journal of immunology (Baltimore, Md. : 1950)* **148**, 597-603 (1992).
91 Mabilleau, G. & Sabokbar, A. Interleukin-32 promotes osteoclast differentiation but not osteoclast activation. *PloS one* **4**, e4173, doi:10.1371/journal.pone.0004173 (2009).
92 Netea, M. G. *et al.* Mycobacterium tuberculosis induces interleukin-32 production through a caspase- 1/IL-18/interferon-gamma-dependent mechanism. *PLoS medicine* **3**, e277, doi:10.1371/journal.pmed.0030277 (2006).
93 Khawar, M. B., Abbasi, M. H. & Sheikh, N. IL-32: A Novel Pluripotent Inflammatory Interleukin, towards Gastric Inflammation, Gastric Cancer, and Chronic Rhino Sinusitis. *Mediators of inflammation* **2016**, 8413768, doi:10.1155/2016/8413768 (2016).
94 Goda, C. *et al.* Involvement of IL-32 in activation-induced cell death in T cells. *International immunology* **18**, 233-240, doi:10.1093/intimm/dxh339 (2006).
95 Kang, J. W. *et al.* Interaction network mapping among IL-32 isoforms. *Biochimie* **101**, 248-251, doi:10.1016/j.biochi.2014.01.013 (2014).
96 Moon, Y. M. *et al.* IL-32 and IL-17 interact and have the potential to aggravate osteoclastogenesis in rheumatoid arthritis. *Arthritis research & therapy* **14**, R246, doi:10.1186/ar4089 (2012).

97 Dinarello, C. A. & Kim, S. H. IL-32, a novel cytokine with a possible role in disease. *Annals of the rheumatic diseases* **65 Suppl 3**, iii61-64, doi:10.1136/ard.2006.058511 (2006).
98 Tsai, C. Y. *et al.* Interleukin-32 increases human gastric cancer cell invasion associated with tumor progression and metastasis. *Clinical cancer research : an official journal of the American Association for Cancer Research* **20**, 2276-2288, doi:10.1158/1078-0432.ccr-13-1221 (2014).
99 Wang, S., Chen, F. & Tang, L. IL-32 promotes breast cancer cell growth and invasiveness. *Oncology letters* **9**, 305-307, doi:10.3892/ol.2014.2641 (2015).
100 Oh, J. H. *et al.* IL-32gamma inhibits cancer cell growth through inactivation of NF-kappaB and STAT3 signals. *Oncogene* **30**, 3345-3359, doi:10.1038/onc.2011.52 (2011).
101 Park, E. S. *et al.* IL-32gamma enhances TNF-alpha-induced cell death in colon cancer. *Molecular carcinogenesis* **53 Suppl 1**, E23-35, doi:10.1002/mc.21990 (2014).
102 Yang, Y. *et al.* Dysregulation of over-expressed IL-32 in colorectal cancer induces metastasis. *World journal of surgical oncology* **13**, 146, doi:10.1186/s12957-015-0552-3 (2015).
103 Lee, J. *et al.* Interleukin-32alpha induces migration of human melanoma cells through downregulation of E-cadherin. *Oncotarget*, doi:10.18632/oncotarget.11669 (2016).
104 Park, J. S. *et al.* Hypoxia-induced IL-32beta increases glycolysis in breast cancer cells. *Cancer letters* **356**, 800-808, doi:10.1016/j.canlet.2014.10.030 (2015).
105 Li, W. *et al.* IL-32: a host proinflammatory factor against influenza viral replication is upregulated by aberrant epigenetic modifications during influenza A virus infection. *Journal of immunology (Baltimore, Md. : 1950)* **185**, 5056-5065, doi:10.4049/jimmunol.0902667 (2010).
106 Shioya, M. *et al.* Epithelial overexpression of interleukin-32alpha in inflammatory bowel disease. *Clinical and experimental immunology* **149**, 480-486, doi:10.1111/j.1365-2249.2007.03439.x (2007).
107 Kim, Y. G. *et al.* Effect of interleukin-32gamma on differentiation of osteoclasts from CD14+ monocytes. *Arthritis and rheumatism* **62**, 515-523, doi:10.1002/art.27197 (2010).
108 Kim, Y. G. *et al.* The influence of interleukin-32gamma on osteoclastogenesis with a focus on fusion-related genes. *Journal of clinical immunology* **32**, 201-206, doi:10.1007/s10875-011-9611-x (2012).
109 Lee, E. J. *et al.* High level of interleukin-32 gamma in the joint of ankylosing spondylitis is associated with osteoblast differentiation. *Arthritis research & therapy* **17**, 350, doi:10.1186/s13075-015-0870-4 (2015).
110 Stirewalt, D. L. *et al.* Tumour necrosis factor-induced gene expression in human marrow stroma: clues to the pathophysiology of MDS? *British journal of haematology* **140**, 444-453, doi:10.1111/j.1365-2141.2007.06923.x (2008).
111 Marcondes, A. M. *et al.* Dysregulation of IL-32 in myelodysplastic syndrome and chronic myelomonocytic leukemia modulates apoptosis and impairs NK function. *Proceedings of the National Academy of Sciences of the United States of America* **105**, 2865-2870, doi:10.1073/pnas.0712391105 (2008).
112 van de Peppel, J. & van Leeuwen, J. P. Vitamin D and gene networks in human osteoblasts. *Frontiers in physiology* **5**, 137, doi:10.3389/fphys.2014.00137 (2014).

113 St-Arnaud, R. The direct role of vitamin D on bone homeostasis. *Arch Biochem Biophys* **473**, 225-230, doi:10.1016/j.abb.2008.03.038 (2008).
114 Christakos, S., Ajibade, D. V., Dhawan, P., Fechner, A. J. & Mady, L. J. Vitamin D: metabolism. *Endocrinology and metabolism clinics of North America* **39**, 243-253, table of contents, doi:10.1016/j.ecl.2010.02.002 (2010).
115 Geng, S., Zhou, S., Bi, Z. & Glowacki, J. Vitamin D metabolism in human bone marrow stromal (mesenchymal stem) cells. *Metabolism: clinical and experimental* **62**, 768-777, doi:10.1016/j.metabol.2013.01.003 (2013).
116 Aranow, C. Vitamin D and the immune system. *Journal of investigative medicine : the official publication of the American Federation for Clinical Research* **59**, 881-886, doi:10.2310/JIM.0b013e31821b8755 (2011).
117 Jones, G., Prosser, D. E. & Kaufmann, M. 25-Hydroxyvitamin D-24-hydroxylase (CYP24A1): its important role in the degradation of vitamin D. *Arch Biochem Biophys* **523**, 9-18, doi:10.1016/j.abb.2011.11.003 (2012).
118 Shi, Y. C. *et al.* Effects of continuous activation of vitamin D and Wnt response pathways on osteoblastic proliferation and differentiation. *Bone* **41**, 87-96, doi:10.1016/j.bone.2007.04.174 (2007).
119 Chen, Y. C. *et al.* 1alpha,25-Dihydroxyvitamin D3 inhibits osteoblastic differentiation of mouse periodontal fibroblasts. *Archives of oral biology* **57**, 453-459, doi:10.1016/j.archoralbio.2011.10.005 (2012).
120 Owen, T. A. *et al.* Pleiotropic effects of vitamin D on osteoblast gene expression are related to the proliferative and differentiated state of the bone cell phenotype: dependency upon basal levels of gene expression, duration of exposure, and bone matrix competency in normal rat osteoblast cultures. *Endocrinology* **128**, 1496-1504, doi:10.1210/endo-128-3-1496 (1991).
121 Maehata, Y. *et al.* Both direct and collagen-mediated signals are required for active vitamin D3-elicited differentiation of human osteoblastic cells: roles of osterix, an osteoblast-related transcription factor. *Matrix biology : journal of the International Society for Matrix Biology* **25**, 47-58, doi:10.1016/j.matbio.2005.09.001 (2006).
122 van Driel, M. *et al.* Evidence for auto/paracrine actions of vitamin D in bone: 1alpha-hydroxylase expression and activity in human bone cells. *FASEB journal : official publication of the Federation of American Societies for Experimental Biology* **20**, 2417-2419, doi:10.1096/fj.06-6374fje (2006).
123 Woeckel, V. J., van der Eerden, B. C., Schreuders-Koedam, M., Eijken, M. & Van Leeuwen, J. P. 1alpha,25-dihydroxyvitamin D3 stimulates activin A production to fine-tune osteoblast-induced mineralization. *J Cell Physiol* **228**, 2167-2174, doi:10.1002/jcp.24388 (2013).
124 Baldock, P. A. *et al.* Vitamin D action and regulation of bone remodeling: suppression of osteoclastogenesis by the mature osteoblast. *J Bone Miner Res* **21**, 1618-1626, doi:10.1359/jbmr.060714 (2006).
125 Kikuta, J. *et al.* Sphingosine-1-phosphate-mediated osteoclast precursor monocyte migration is a critical point of control in antibone-resorptive action of active vitamin D. *Proceedings of the National Academy of Sciences of the United States of America* **110**, 7009-7013, doi:10.1073/pnas.1218799110 (2013).
126 Deeb, K. K., Trump, D. L. & Johnson, C. S. Vitamin D signalling pathways in cancer: potential for anticancer therapeutics. *Nature reviews. Cancer* **7**, 684-700, doi:http://www.nature.com/nrc/journal/v7/n9/suppinfo/nrc2196_S1.html (2007).

127 Harada, K. *et al.* Polyphosphate-mediated inhibition of tartrate-resistant acid phosphatase and suppression of bone resorption of osteoclasts. *PloS one* **8**, e78612, doi:10.1371/journal.pone.0078612 (2013).
128 Hayman, A. R. Tartrate-resistant acid phosphatase (TRAP) and the osteoclast/immune cell dichotomy. *Autoimmunity* **41**, 218-223, doi:10.1080/08916930701694667 (2008).
129 Filgueira, L. Fluorescence-based staining for tartrate-resistant acidic phosphatase (TRAP) in osteoclasts combined with other fluorescent dyes and protocols. *The journal of histochemistry and cytochemistry : official journal of the Histochemistry Society* **52**, 411-414 (2004).
130 Acid Phosphatase Leukocyte Procedure No.387, Sigma Aldrich; https://www.sigmaaldrich.com/content/dam/sigma-aldrich/docs/Sigma/General_Information/1/387.pdf. .
131 Azo Coupling, Organic-chemistry.org, http://www.organic-chemistry.org/namedreactions/azo-coupling.shtm.
132 Livshits, M. A. *et al.* Isolation of exosomes by differential centrifugation: Theoretical analysis of a commonly used protocol. *Sci Rep* **5**, 17319, doi:10.1038/srep17319 (2015).
133 Clark, D. P. *Molecular Biology*. 2nd edn, (USA: Academic Press., 2013).
134 Western Blotting, Principles and Methods, Handsbooks from GE Healthcare; https://www.sigmaaldrich.com/content/dam/sigma-aldrich/docs/Sigma-Aldrich/General_Information/1/ge-western-blotting.pdf. .
135 Penna, A. & Cahalan, M. Western Blotting using the Invitrogen NuPage Novex Bis Tris minigels. *Journal of visualized experiments : JoVE*, 264, doi:10.3791/264 (2007).
136 Degasperi, A. *et al.* Evaluating strategies to normalise biological replicates of Western blot data. *PloS one* **9**, e87293, doi:10.1371/journal.pone.0087293 (2014).
137 Real Time PCR Handbook; 2012, Life Technologies. (http://www3.appliedbiosystems.com/cms/groups/mcb_marketing/documents/generaldocuments/cms_039996.pdf). .
138 Guide to Performing Relative Quantitation of Gene Expression Using Real-Time Quantitative PCR, 2008; Applied Biosystems. http://www3.appliedbiosystems.com/cms/groups/mcb_support/documents/generaldocuments/cms_042380.pdf.
139 Perez, S. *et al.* Identifying the most suitable endogenous control for determining gene expression in hearts from organ donors. *BMC molecular biology* **8**, 114, doi:10.1186/1471-2199-8-114 (2007).
140 Zhong, H. & Simons, J. W. Direct comparison of GAPDH, beta-actin, cyclophilin, and 28S rRNA as internal standards for quantifying RNA levels under hypoxia. *Biochemical and biophysical research communications* **259**, 523-526, doi:10.1006/bbrc.1999.0815 (1999).
141 Tan, S. C. & Yiap, B. C. DNA, RNA, and Protein Extraction: The Past and The Present. *Journal of Biomedicine and Biotechnology* **2009**, doi:10.1155/2009/574398 (2009).
142 High Pure RNA Isolation Kit, Roche Diagnostics. https://lifescience.roche.com/shop/products/high-pure-rna-isolation-kit.
143 Guide to the Disruption of Biological Samples, Part IV: Chemical Disruption Methods, 2012; OPS Diagnostics.

http://www.opsdiagnostics.com/applications/samplehomogenization/homogenizationguidepart4.html.
144 Reverse Transcription and cDNA synthesis; Thermo Fisher. https://www.thermofisher.com/no/en/home/life-science/pcr/elevate-pcr-research/reverse-transcription-essentials.html - 1.
145 TaqMan® Chemistry vs. SYBR® Chemistry for Real-Time PCR, Thermo Fisher; https://www.thermofisher.com/no/en/home/life-science/pcr/real-time-pcr/qpcr-education/taqman-assays-vs-sybr-green-dye-for-qpcr.html - taqman.
146 Pennings, J. L. *et al.* Degradable dU-based DNA template as a standard in real-time PCR quantitation. *Leukemia* **15**, 1962-1965 (2001).
147 TaqMan® Gene Expression Master Mix, Protocol, 2007; Applied Biosystems.

http://www3.appliedbiosystems.com/cms/groups/mcb_support/documents/generaldocuments/cms_039284.pdf.
148 User Guide TaqMan® Universal PCR Master Mix, 2014, Life Technologies by Applied Biosystems, http://tools.thermofisher.com/content/sfs/manuals/4304449_taqmanpcrmm_ug.pdf.
149 Orimo, H. The mechanism of mineralization and the role of alkaline phosphatase in health and disease. *Journal of Nippon Medical School = Nippon Ika Daigaku zasshi* **77**, 4-12 (2010).
150 Becker, K. L. *Principles and Practice of Endocrinology and Metabolism*. (Hagerstown, Maryland, USA: Lippincott Williams and Wilkins,, 1990).
151 Graneli, C. *et al.* Novel markers of osteogenic and adipogenic differentiation of human bone marrow stromal cells identified using a quantitative proteomics approach. *Stem cell research* **12**, 153-165, doi:10.1016/j.scr.2013.09.009 (2014).
152 Leggate, J., Allain, R., Isaac, L. & Blais, B. W. Microplate fluorescence assay for the quantification of double stranded DNA using SYBR Green I dye. *Biotechnology letters* **28**, 1587-1594, doi:10.1007/s10529-006-9128-1 (2006).
153 Technical Bulletin, CellTiter-Glo® Luminescent Cell Viability Assay; Promega. https://www.promega.com/-/media/files/resources/protocols/technical-bulletins/0/celltiter-glo-luminescent-cell-viability-assay-protocol.pdf.
154 Alberts, B. *Molecular Biology of the Cell*. 5th edn, (New York: Garland Science, 2008).
155 Gregory, C. A., Gunn, W. G., Peister, A. & Prockop, D. J. An Alizarin red-based assay of mineralization by adherent cells in culture: comparison with cetylpyridinium chloride extraction. *Analytical biochemistry* **329**, 77-84, doi:10.1016/j.ab.2004.02.002 (2004).
156 Moriguchi, T., Yano, K., Nakagawa, S. & Kaji, F. Elucidation of adsorption mechanism of bone-staining agent alizarin red S on hydroxyapatite by FT-IR microspectroscopy. *Journal of colloid and interface science* **260**, 19-25 (2003).
157 Seiden-Long, I. & Vieth, R. Evaluation of a 1,25-dihydroxyvitamin D enzyme immunoassay. *Clin Chem* **53**, 1104-1108, doi:10.1373/clinchem.2006.077560 (2007).
158 Aydin, S. A short history, principles, and types of ELISA, and our laboratory experience with peptide/protein analyses using ELISA. *Peptides* **72**, 4-15, doi:10.1016/j.peptides.2015.04.012 (2015).
159 Palma, B. D. *et al.* Osteolytic lesions, cytogenetic features and bone marrow levels of cytokines and chemokines in multiple myeloma patients: Role of chemokine (C-C motif) ligand 20. *Leukemia* **30**, 409-416, doi:10.1038/leu.2015.259 (2016).

160 Heinhuis, B. *et al.* Inflammation-dependent secretion and splicing of IL-32{gamma} in rheumatoid arthritis. *Proceedings of the National Academy of Sciences of the United States of America* **108**, 4962-4967, doi:10.1073/pnas.1016005108 (2011).
161 Tang, W., Li, Y., Osimiri, L. & Zhang, C. Osteoblast-specific transcription factor Osterix (Osx) is an upstream regulator of Satb2 during bone formation. *J Biol Chem* **286**, 32995-33002, doi:10.1074/jbc.M111.244236 (2011).
162 Turner, M. D., Nedjai, B., Hurst, T. & Pennington, D. J. Cytokines and chemokines: At the crossroads of cell signalling and inflammatory disease. *Biochimica et biophysica acta* **1843**, 2563-2582, doi:10.1016/j.bbamcr.2014.05.014 (2014).
163 Krisher, T. & Bar-Shavit, Z. Regulation of osteoclastogenesis by integrated signals from toll-like receptors. *J Cell Biochem* **115**, 2146-2154, doi:10.1002/jcb.24891 (2014).
164 Huang, J. C. *et al.* PTH differentially regulates expression of RANKL and OPG. *J Bone Miner Res* **19**, 235-244, doi:10.1359/jbmr.0301226 (2004).
165 Choi, J. D. *et al.* Identification of the most active interleukin-32 isoform. *Immunology* **126**, 535-542, doi:10.1111/j.1365-2567.2008.02917.x (2009).
166 Geng, S., Zhou, S. & Glowacki, J. Effects of 25-hydroxyvitamin D(3) on proliferation and osteoblast differentiation of human marrow stromal cells require CYP27B1/1alpha-hydroxylase. *J Bone Miner Res* **26**, 1145-1153, doi:10.1002/jbmr.298 (2011).
167 Beresford, J. N., Joyner, C. J., Devlin, C. & Triffitt, J. T. The effects of dexamethasone and 1,25-dihydroxyvitamin D3 on osteogenic differentiation of human marrow stromal cells in vitro. *Archives of oral biology* **39**, 941-947 (1994).
168 Curtis, K. M., Aenlle, K. K., Roos, B. A. & Howard, G. A. 24R,25-dihydroxyvitamin D3 promotes the osteoblastic differentiation of human mesenchymal stem cells. *Molecular endocrinology (Baltimore, Md.)* **28**, 644-658, doi:10.1210/me.2013-1241 (2014).
169 Hunter, G. K., Hauschka, P. V., Poole, A. R., Rosenberg, L. C. & Goldberg, H. A. Nucleation and inhibition of hydroxyapatite formation by mineralized tissue proteins. *The Biochemical journal* **317 (Pt 1)**, 59-64 (1996).
170 van Driel, M. & van Leeuwen, J. P. Vitamin D endocrine system and osteoblasts. *Bonekey Rep* **3**, 493, doi:10.1038/bonekey.2013.227 (2014).
171 Hidalgo, A. A., Deeb, K. K., Pike, J. W., Johnson, C. S. & Trump, D. L. Dexamethasone enhances 1alpha,25-dihydroxyvitamin D3 effects by increasing vitamin D receptor transcription. *J Biol Chem* **286**, 36228-36237, doi:10.1074/jbc.M111.244061 (2011).
172 Dhawan, P. & Christakos, S. Novel regulation of 25-hydroxyvitamin D3 24-hydroxylase (24(OH)ase) transcription by glucocorticoids: cooperative effects of the glucocorticoid receptor, C/EBP beta, and the Vitamin D receptor in 24(OH)ase transcription. *J Cell Biochem* **110**, 1314-1323, doi:10.1002/jcb.22645 (2010).
173 Catalan, V. *et al.* Increased IL-32 Levels in Obesity Promote Adipose Tissue Inflammation and Extracellular Matrix Remodeling. Effect of Weight Loss. *Diabetes*, doi:10.2337/db16-0287 (2016).
174 Raimondi, L. *et al.* Involvement of multiple myeloma cell-derived exosomes in osteoclast differentiation. *Oncotarget* **6**, 13772-13789, doi:10.18632/oncotarget.3830 (2015).

175 Gutierrez-Vazquez, C., Villarroya-Beltri, C., Mittelbrunn, M. & Sanchez-Madrid, F. Transfer of extracellular vesicles during immune cell-cell interactions. *Immunological reviews* **251**, 125-142, doi:10.1111/imr.12013 (2013).
176 Bai, X. *et al.* Human IL-32 expression protects mice against a hypervirulent strain of Mycobacterium tuberculosis. *Proceedings of the National Academy of Sciences of the United States of America* **112**, 5111-5116, doi:10.1073/pnas.1424302112 (2015).
177 Tang, Z. N., Zhang, F., Tang, P., Qi, X. W. & Jiang, J. Hypoxia induces RANK and RANKL expression by activating HIF-1alpha in breast cancer cells. *Biochemical and biophysical research communications* **408**, 411-416, doi:10.1016/j.bbrc.2011.04.035 (2011).
178 Yu, X. J. *et al.* Effect of hypoxia on the expression of RANKL/OPG in human periodontal ligament cells in vitro. *International journal of clinical and experimental pathology* **8**, 12929-12935 (2015).
179 Zhang, C. *et al.* Osteoblast-specific transcription factor Osterix increases vitamin D receptor gene expression in osteoblasts. *PloS one* **6**, e26504, doi:10.1371/journal.pone.0026504 (2011).
180 Kaur, G. & Dufour, J. M. Cell lines: Valuable tools or useless artifacts. *Spermatogenesis* **2**, 1-5, doi:10.4161/spmg.19885 (2012).
181 Zhou, S., LeBoff, M. S. & Glowacki, J. Vitamin D metabolism and action in human bone marrow stromal cells. *Endocrinology* **151**, 14-22, doi:10.1210/en.2009-0969 (2010).
182 Wronski, T. J., Halloran, B. P., Bikle, D. D., Globus, R. K. & Morey-Holton, E. R. Chronic administration of 1,25-dihydroxyvitamin D3: increased bone but impaired mineralization. *Endocrinology* **119**, 2580-2585, doi:10.1210/endo-119-6-2580 (1986).
183 Lieben, L. *et al.* Normocalcemia is maintained in mice under conditions of calcium malabsorption by vitamin D-induced inhibition of bone mineralization. *The Journal of clinical investigation* **122**, 1803-1815, doi:10.1172/jci45890 (2012).
184 Yamamoto, Y. *et al.* Vitamin D receptor in osteoblasts is a negative regulator of bone mass control. *Endocrinology* **154**, 1008-1020, doi:10.1210/en.2012-1542 (2013).
185 Atkins, G. J. *et al.* Metabolism of vitamin D3 in human osteoblasts: evidence for autocrine and paracrine activities of 1 alpha,25-dihydroxyvitamin D3. *Bone* **40**, 1517-1528, doi:10.1016/j.bone.2007.02.024 (2007).
186 van der Meijden, K. *et al.* Regulation of CYP27B1 mRNA Expression in Primary Human Osteoblasts. *Calcified tissue international* **99**, 164-173, doi:10.1007/s00223-016-0131-9 (2016).
187 Rizzoli, R. & Biver, E. Glucocorticoid-induced osteoporosis: who to treat with what agent? *Nat Rev Rheumatol* **11**, 98-109, doi:10.1038/nrrheum.2014.188 (2015).
188 Hayashi, K. *et al.* BMP/Wnt antagonists are upregulated by dexamethasone in osteoblasts and reversed by alendronate and PTH: potential therapeutic targets for glucocorticoid-induced osteoporosis. *Biochemical and biophysical research communications* **379**, 261-266, doi:10.1016/j.bbrc.2008.12.035 (2009).
189 Arai, M., Shibata, Y., Pugdee, K., Abiko, Y. & Ogata, Y. Effects of reactive oxygen species (ROS) on antioxidant system and osteoblastic differentiation in MC3T3-E1 cells. *IUBMB life* **59**, 27-33, doi:10.1080/15216540601156188 (2007).

190 Kraaij, M. D. *et al.* Dexamethasone increases ROS production and T cell suppressive capacity by anti-inflammatory macrophages. *Molecular immunology* **49**, 549-557, doi:10.1016/j.molimm.2011.10.002 (2011).
191 Huo, Y., Rangarajan, P., Ling, E. A. & Dheen, S. T. Dexamethasone inhibits the Nox-dependent ROS production via suppression of MKP-1-dependent MAPK pathways in activated microglia. *BMC neuroscience* **12**, 49, doi:10.1186/1471-2202-12-49 (2011).
192 Bouillon, R., van Baelen, H. & de Moor, P. The measurement of the vitamin D-binding protein in human serum. *J Clin Endocrinol Metab* **45**, 225-231, doi:10.1210/jcem-45-2-225 (1977).
193 Spencer, J. A. *et al.* Direct measurement of local oxygen concentration in the bone marrow of live animals. *Nature* **508**, 269-273, doi:10.1038/nature13034 (2014).
194 Peng, X. *et al.* Protection against cellular stress by 25-hydroxyvitamin D3 in breast epithelial cells. *J Cell Biochem* **110**, 1324-1333, doi:10.1002/jcb.22646 (2010).
195 Ormsby, R. T. *et al.* Analysis of vitamin D metabolism gene expression in human bone: evidence for autocrine control of bone remodelling. *The Journal of steroid biochemistry and molecular biology* **144 Pt A**, 110-113, doi:10.1016/j.jsbmb.2013.09.016 (2014).
196 Kogawa, M., Anderson, P. H., Findlay, D. M., Morris, H. A. & Atkins, G. J. The metabolism of 25-(OH)vitamin D3 by osteoclasts and their precursors regulates the differentiation of osteoclasts. *The Journal of steroid biochemistry and molecular biology* **121**, 277-280, doi:10.1016/j.jsbmb.2010.03.048 (2010).

Appendices

APPENDIX 1

The principle of PBMC isolation

The PBMC fraction can be isolated from a blood sample using a Ficoll- gradient (Lymphoprep™, STEMCELL™ Technologies). This method, developed by Bøyum et al. in 1968, is based on mixing the blood with a polymeric compound that in one centrifugation step separate different cell types based on their density[1]. Lymphoprep™ is a reagent containing sodium diatrizoate and a branched polysaccharide[1]. When diluted blood is added onto the lymphoprep the different cell types will migrate to form different layers during centrifugation. The polysaccharide induces aggregation of erythrocytes which then sediment at the bottom layer of the gradient following centrifugation. Lymphoprep has a higher density than platelets, lymphocytes and monocytes, which will settle on the top, while the aggregated erythrocytes and granulocytes will pass through and sediment in the bottom of the centrifuge tube[1,2] . The PBMC fraction can then be collected from the interface between the lymphoprep and the upper plasma layer

Procedure PBMC isolation

Buffycoat (from Blood Bank, NTNU) were diluted with an equal volume (1:1) of DPBS (Thermo Fisher). The Lymphoprep was placed in a centrifuge tube, and an equal volume of diluted sample was added on top, carefully not to mix. Following 20 minutes centrifugation, the PBMCs fraction was harvested by pipetting the white band at the interface between the plasma and the Lymphoprep. The isolated cells were then resuspended in Hank's Balanced Salt Solution (HANKS) (Sigma Aldrich) and centrifuged for 10 min, 250 × g, in RT. The supernatant was removed, and the pellet was resuspended in 20 ml HANKS followed by centrifugation at 300×g for 8 minutes. The wash step was repeated in total 4 times.

The principle of monocyte plastic adheration

The ability of monocytes to adhere to glass or plastic through the $\beta 2$ integrin CD11c/CD18 is exploited in monocyte adherence isolation[2]. By seeding PBMCs, briefly allowing them to settle and then expose the culture to repeated washes, the other cells are removed, while the adhering monocytes are left behind. The method is quick and cheap, but the adheration is considered as an activating event, which may induce changes in osteoclast gene expression and protein secretion[2]. Also, OC isolation by the adheration method is prone to lymphocyte contamination[2].

Procedure for adheration

For isolation of monocytes by adheration PBMCs were cultured in osteoclast media (as previously reported) for 1 hour and followed by a wash of un-attached cells using HANKS. The wash step was repeated in total 3 times. The cells left was considered monocytes.

The principle of CD14 isolation

Human CD14 MicroBeads (Miltenyi Biotec) were used to isolate CD14 positive cells from the PBMC fraction. CD14 is a receptor of the innate immune system that is preferentially expressed on monocytes and macrophages and is therefore useful as marker in isolation of these cell types[3]. In CD14 isolation cells are magnetically labeled with CD14 binding beads. The beads are superparamagnetic 50 nm particles conjugated to monoclonal anti- human CD14 antibodies (isotype: mouse IgG2a) that allow binding to the CD14 receptor on expressing cells[4]. The suspension of labeled cell is loaded onto a column with a matrix composed of ferromagnetic spheres[4]. When the column is placed on a magnetic separator, the magnetically labeled cells are retained in the column as a result of the magnetic gradient, while the other cells are washed through[4]. Then the column is removed from the magnetic field and the purified CD14+ cell fraction can be eluted into a collection tube (MACS miltenyi Biotec, CD14 Microbeads Human protocol). The MicroBeads are so small that they neither activate cells nor saturate surface epitopes[4]. As there is no disturbance of the biological function of the monocytes, there is no need for removal of beads after isolation.

Procedure for CD14 isolation

Prior to CD14 isolation the PBMCs isolated from the Ficoll-gradient were counted using the Cell-Coulter (Beckman) and the cell number was adjusted to get the desired amount of CD14 positive cells (about 10 % of the PBMCs are CD14+). In total 10^7 cells were used for labeling. The appropriate number of PBMCs was resuspended in 80 uL buffer (Miltenyi Biotec), and 20 uL of CD14 MicroBeads (Miltenyi Biotec) was added to cell suspension which then was mixed and incubated for 15 minutes in 2-8˚C. Further on the cells were washed by adding 1-2 ml buffer and centrifuge at 300×g, 10 min, followed by resuspension in 500 ul buffer. The solution was transferred to a LS MACS column installed in a MACS Separator (Miltenyi Biotec). The column was prepared by rinsing with 3 mL buffer, and cell suspension was loaded into the column. The column content was then washed 3 times using 3 mL buffer, each time making sure the column was emptied between each wash. The column was removed from the separator and placed in a collection tube, where elution of the CD14 labeled cells were performed by adding 5 mL buffer and immediately after pushing a plunger into the column. The viability and number of isolated cells were then evaluated on a Countess Automated Cell Counter (Invitrogen).

Reagents used in CD14 isolation

All reagents were purchased from Miltenyi Biotec, Germany. 2 mL CD14 human MicroBeads were supplied in each isolation kit. A buffer containing PBS (pH 7.2) supplemented with bovine serum albumin (BSA; 0.5 %), and EDTA (2 mM) was prepared by diluting MACS BSA Stock Solution 1:20 with autoMACS™ Rinsing Solution according to manufacturers recommendations.

The procedure of TRAP-staining

The monocytes were seeded in 96 well plates (8000 cells/well) and cultured in 9-6 days following the culture conditions as previously reported. After 3 days of stimulation the cells were washed with 200 ul PBS per well, and then fixated with 100 ul PFA (4 %) and incubated in RT for 15 minutes. Fast Garnet GBC base solution and sodium nitrite solution were mixed in an eppendorf tube for 30 sec and left to rest for 2 min. The solution was then added to a

corresponding amount of water and mixed thoroughly. Proportional amounts of Napthol AS-BI Phosphoric acid solution, acetate and tartrate were added according to manufacturers instructions. Following removal of PFA from the sample wells, cells were washed twice with 200 ul PBS per well. Then the 100 ul TRAP solution was added to each well and the plates were incubated for 1-2 h. The cells were frequently evaluated to ensure incubation was terminated before cells were over-stained. Imaging of stained cells was performed using EVOS FL Auto Cell Imaging System (Thermo Fisher) and the cells were counted manually using the program NIS Elements Microscope Imaging Software (Nikon Instruments). The counting was performed without knowledge of experimental setup, and criteria for osteoclasts were TRAP stained cells with three or more nuclei.

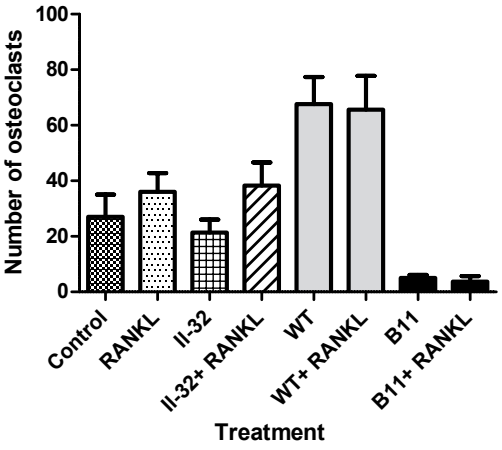

Pre-osteoclast experiment 2

Number of pre-osteoclasts in cultures treated with IL-32 WT derived and IL-32 KO derived exosomes. Primary monocytes were seeded 8000 cells/well in 96-well plates and differentiated for 5-6 days with modified differentiation media, containing only MCS-F (30 ng/mL), including 5 ul exosomes/150 ul medium, with or without rhIL-32γ (25 ng/mL) and RANKL (50 ng/mL). The data is presented as the mean+SEM of technical replicates.

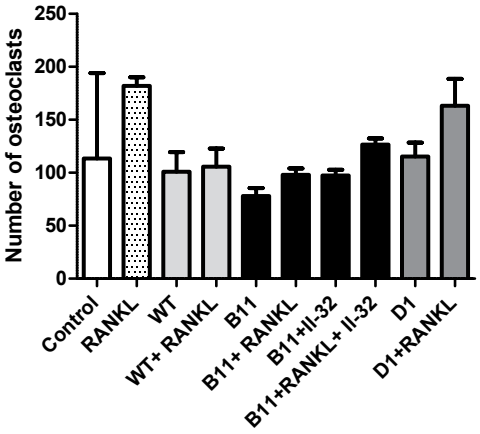

Post-osteoclast experiment 2:

Total number of osteoclasts in cultures treated with IL-32 WT derived and IL-32 KO derived exosomes. Primary monocytes were seeded 8000cells/well in 96-well plates and differentiated into preosteoclasts with MCS-F (30 ng/mL) TGF-β (1ng/mL) and RANKL (10 ng/mL) before treated with 5 ul exosomes/150 ul medium, with or without rhIL-32γ (25 ng/mL) and RANKL (50 ng/mL). The data is presented as the mean+SEM of technical replicates.

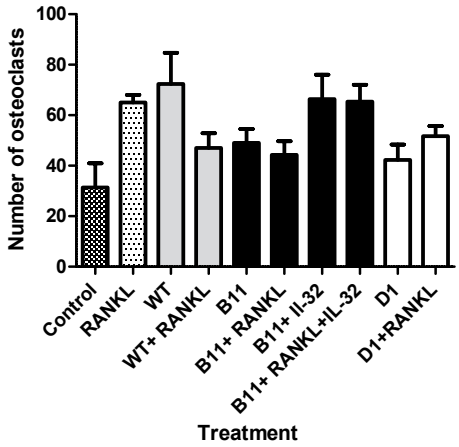

Post-osteoclast experiment 3

Total number of osteoclasts in cultures treated with IL-32 WT derived and IL-32 KO derived exosomes. Primary monocytes were seeded 8000cells/well in 96-well plates and differentiated into preosteoclasts with MCS-F (30 ng/mL) TGF-β (1ng/mL) and RANKL (10 ng/mL) before treated with 5 ul exosomes/150 ul medium, with or without rhIL-32γ (25 ng/mL) and RANKL (50 ng/mL). The data is presented as the mean+SEM of technical replicates.

APPENDIX 2

Procedure for 1,25 dihydroxyvitamin D ELISA

To measure the concentration of $1,25(OH)_2D_3$, 250 ul sample were used. To prepare the samples for ELISA, 25 μl delipidation reagent was added to each sample, followed by vortexing and centrifugation at 10 000×g, 10 minutes.

Immunoextraction

Two immunocapsules for each sample and control were prepared by vortexing and then placed upright to allow the solid phase to settle. 100 μl of delipidated samples and controls were added to the immunocapsules, which then were placed in a rotator mixer and left to rotate end over end for 5-20 revolutions per min in 90 minutes (RT).

Afterwards, the immunocapsules were placed upright in 5 minutes to allow a gel to settle, each of them was tapped to remove gel adhering to the screw caps. Then the screw caps were removed and the bottom stopper were broken off and the capsules placed in plastic tubes, followed by a centrifugation step at low speed (750×g, 1 min) to remove sample. Deionized water (500 μl) was carefully added to each capsule and the tubes were centrifuged at 750×g, in 1 minute to wash the immunoextraction gel. This step was repeated further two times before the capsules were transferred to polystyrene tubes. 150 μl elution reagent were added and allowed to soak for 1-2 minutes, followed by centrifugation at 750×g for 1 min. The elution step was repeated further two times, so the total elution volume collected for each sample was 450 μl. The immunocapsules were discarded and the elution tubes were placed in a water bath (40˚C). A gentle flow of nitrogen was used to evaporate the eluates, ensuring that no liquid was left in the tubes. 100 μl assay buffer were den added to the tubes followed by vortexing to dissolve the remaining solid residues.

ELISA assay procedure

Calibrators were prepared in polystyrene tubes in duplicate, 100 μl in each tube. 100 μl primary antibody solution were added to all tubes, including sample tubes. Following careful vortexing, all tubes where incubated overnight in 2˚C.

The next day, 150 μl of samples and calibrators were pipetted into the anti-sheep coated plate, leaving to wells empty for substrate blanks. The plate was covered and incubated on a orbital shaker at 500 rpm for 90 minutes. Subsequently 100 μl 1,25D Biotin solution were added to

all wells except substrate blanks, the plate covered and left on the orbital shaker (500 rpm, RT) for 60 minutes. The plate was then washed manually using 250 μl wash solution per well. The wash was repeated twice and to remove excess wash solution the plate was tapped firmly against tissue paper. Enzyme conjugate solution was added, 250 μl per well (except substrate blanks), and incubated in RT for 30 minutes. Then the plate was washed, by repeating the former wash procedure. 200 μl TMB substrate was added to each well including blanks, the plate was covered and incubated for 15-30 minutes. When an appropriate level of color was present, adding stop solution terminated the reaction. The absorbance was measured shortly after at 450 nm (reference 650 nm) using iMark™ Microplate Absorbance Reader from BioRad.

APPENDIX 3

The CRISPR-Cas system

CRISPR stands *for clustered regularly interspaced short palindromic repeats*, and was originally identified as an antiviral defense system present in many prokaryotes and most archaeal species[5]. The "spacer DNA" interspersed between the palindromic repeats were shown to be viral genome fragments derived from previous infections[6]. Further investigation revealed that when encountering second infection, this "genetic record" could be transcribed into small RNAs that then would guide endogenous nucleases to target complementary sequences of the invading nucleic acids[6]. The nucleases involved the CRISPR pathway are transcribed from the *Cas* genes that typically flank the CRISPR-loci[6]. The CRISPR type II-/Cas9 system has due to its favorable properties been implemented as an application in genetic engineering. The simplistic set up, including only Cas9 and a single guide RNA enables the induction of double strand breaks and highly specific gene editing, a process that by old methods posed great challenges[7]. CRISPR/Cas9 technology is now the basis for many commercial gene-editing applications. There are many approaches for delivery of Cas9 and sgRNA to the cell, including plasmids as well as expression cassettes and lentiviral vectors[7]. In this case a plasmid containing both Cas9 and the sgRNA specific for IL-32 was used. The CRISPR/Cas9 IL-32 Knockout (KO) Plasmids from Santa Cruz Biotechnology are for maximum knock-out efficiency supplied as a mix of three plasmids, all encoding the components necessary for gene-knockout, including Cas9 (pyrogene) downstream a CBh- promoter, the gRNA specific for the IL-32 gene downstream for an U6- promoter, a nuclear localization signal and Green Fluorescent Protein (GFP) for verifying transfection[8]. Following transfection into the cell the plasmids are transcribed and the Cas9/gRNA complexes translocate to the nucleus where they bind to proto-spacer adjacent motif (PAM) sites that allow unwinding of the DNA[8]. The IL-32 specific 20 nucleotide sequence of the gRNA facilitate binding to the target locus 5' of the PAM sequence followed by Cas9 cleavage[8]. By using three plasmids, three exons are disrupted, ensuring full knockout of the gene[8].

Procedure for Crispr/Cas gene knockout

JJN-3 cells were cultured in low density for 24 hours prior to transfection. $5x10^6$ cells were electroporated with 1.5µg of IL-32 Crisper/Cas9 KO Plasmid (h) (Santa Cruz Biotechnology), using Cell Line Nucleofector® Solution R from Amaxa® Cell Line Nucleofector® Kit R (Lonza) and program T-001 on Nucleofector™ Device (Lonza). The cells were then cultured in JJN3 conditioned media for 24 hours and sorting of transfected cells were done by selection of GFP positive cells using fluorescence-activated cell sorting (FACS). Clonal propagation was performed on this subpopulation. To confirm knock out of the IL-32 gene, cells were tested by Flow Cytometric Analysis.

APPENDIX 4

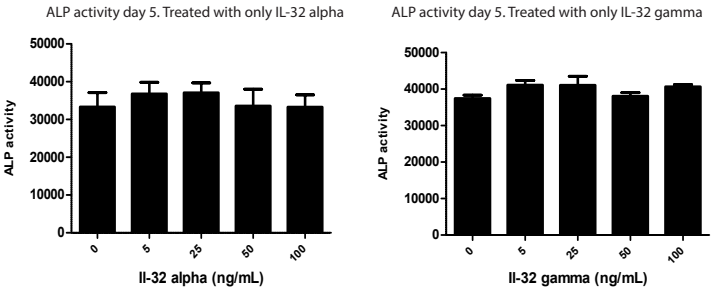

Fig. 1: ALP-activity in osteoblast treated for 5 days with rhIL-32. MSCs were seeded 5000 cells/well in 96-well plates and the day after differentiated in osteogenic direction in the presence of rhIL-32 γ or rhIL-32 α (concentrations indicated in figure). MSCGM (basal)-cultured cells were included as negative control. ALP-activity was measured after 5 days treatment, using ALP-assay. Data is reported as mean ± SEM of technical replicates.

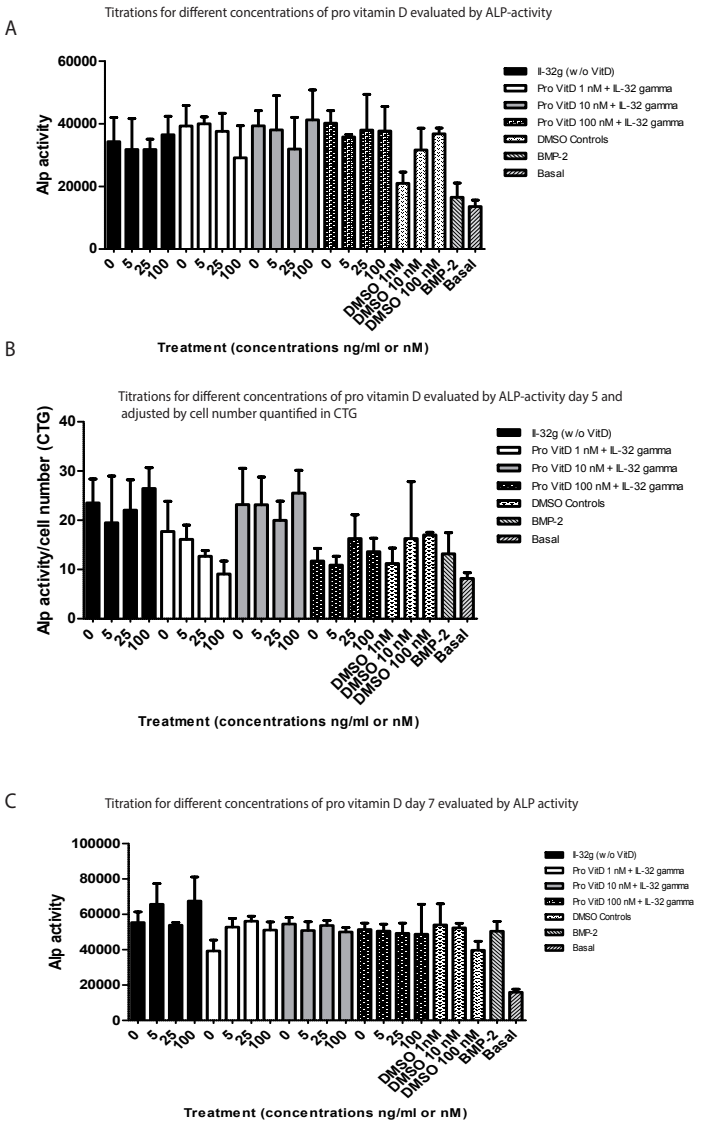

Fig. 2: Titration of pro vitamin D: MSCs were seeded 2500 cells/well in 96-well plates and differentiated in osteogenic direction for 5 and 7 days in the presence of IL-32gamma 0/5/25/100 ng/mL combined with 1, 10 or 100 nM $25(OH)D_3$ (pro vitamin D). As controls treatment with the same concentrations of the vitamin D reconstitution reagent DMSO was included. BMP-2 control was treated with 300 ng/mL and basal control was non-differentiated MSCs cultured in MSCGM. Responsiveness to different concentrations of vitamin D was evaluated by extent of ALP-activity using ALP-assay. Data is reported as mean±SEM of technical replicates. **A)** ALP-activity day 5. **B)** ALP activity, day 5 (same plate as A) adjusted by relative cell number quantified by CTG, using a cell number standard (ALP and CTG performed on two different plates with the same setup. **C)** ALP-activity at day 7.

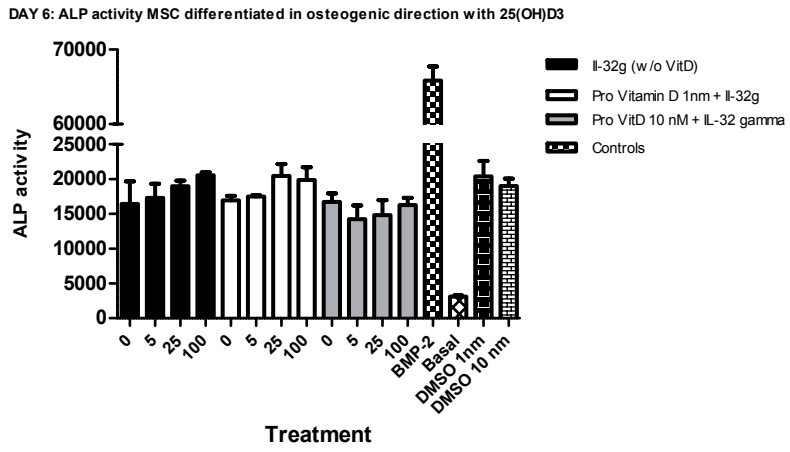

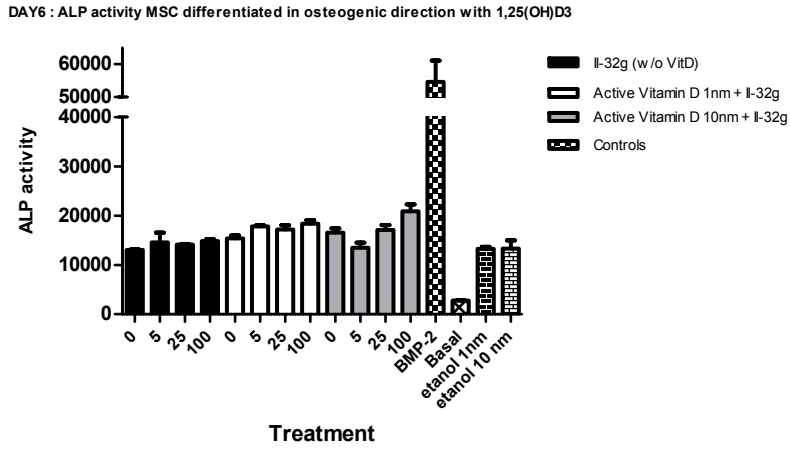

Fig. 3: ALP- activity at day 6. MSCs were seeded 2500 cells/well in 96-well plates and differentiated in osteogenic direction for 6 days treated with or without the active ($1,25(OH)_2D_3$) or the pro form ($25(OH)D_3$) of vitamin D at 1nM or 10 nM concentrations , together with rhIL-32γ at at concentrations (ng/mL) indicated. As controls, reconstitution reagents DMSO and etanol, for $25(OH)D_3$ and $1,25(OH)_2D_3$, respectively, were included. Positive control was BMP-2 (300ng/mL). Negative control was undifferentiated MSCs (basal) treated with MSCGM only. At day 6, ALP-activity for each well was measured. Data is reported as mean±SEM of technical replicates.. **A)** ALP-activity in cells treated with **$25(OH)D_3$ ($25D_3$)** for 6 days. **B)** ALP-activity in cells treated with **$1,25(OH)_2D_3$ ($1,25D_3$)** for 6 days.

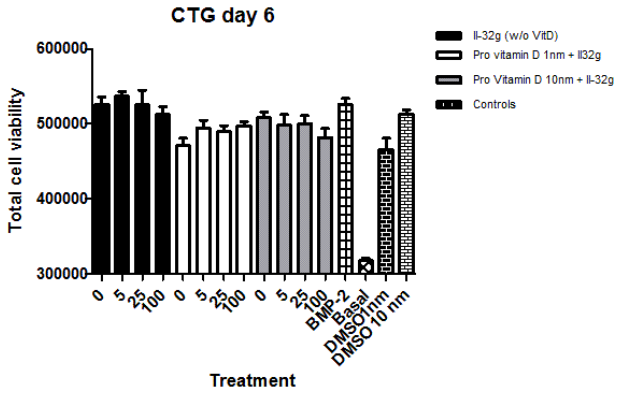

Fig. 4: Preosteoblast proliferation in the presence of $25(OH)D_3$ and rhIL-32. MSCs were seeded 2500 cells/well in 96-well plates and differentiated in osteogenic direction for 6 days in the presence of $25(OH)D_3$ ($25D_3$) in concentrations 1nM and 10 nM together with IL-32gamma in concentrations as indicated for each bar(ng/mL) . Proliferation was measured at day 6 by the extent of ATP levels in each well using CTG-assay. Data is presented as mean±SD of ATP (arbitrary units) of technical replicates.

A

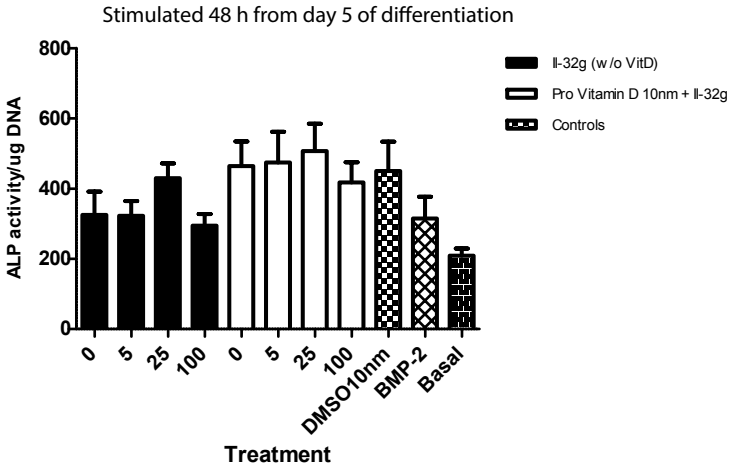

B

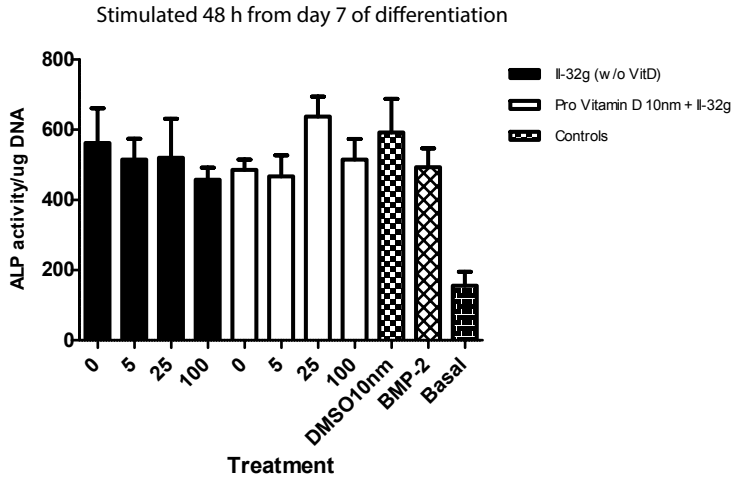

Fig. 5: ALP- activity in osteoblasts after 48 hours stimulation with rhIL-32 with or without 25(OH)D_3. MSCs were seeded 2500 cells/well in 96-well plates and differentiated in osteogenic direction for 5 and 7 days before treated with IL-32 (0/5/25/100 ng/mL) and 25(OH)D_3 (pro vitamin D) for 48 h. BMP-2(300 ng/mL), DMSO (10 nM) and basal (MSCGM) treated cells were included as controls. ALP-activity was measured by ALP-assay following 48 h treatment, and adjusted by µg DNA in each well. Data is presented as mean±SEM of technical replicates. **A)** ALP-activity/ µg DNA at day 7 following 48 h treatment. **B)** ALP-activity/ µ g DNA at day 9 following 48 h treatment.

APPENDIX 5

Calculation of RQ by the comparative C_t-method.

The comparative C_t method uses the mean C_t value and the standard deviation of the sample replicates. The difference between the average C_t of each target and its associated endogenous control C_t value is calculated (ΔC_t)[9]. Then the standard deviation of the ΔC_t value is calculated from the standard deviations of target and endogenous control[9]. Further on the $\Delta\Delta C_t$ value is calculated from the ΔC_t values of test sample and the chosen reference sample. Finally the standard deviations of $\Delta\Delta C_t$ values are calculated and incorporated into the fold-difference which is given by $2^{-\Delta\Delta Ct}$ [10].

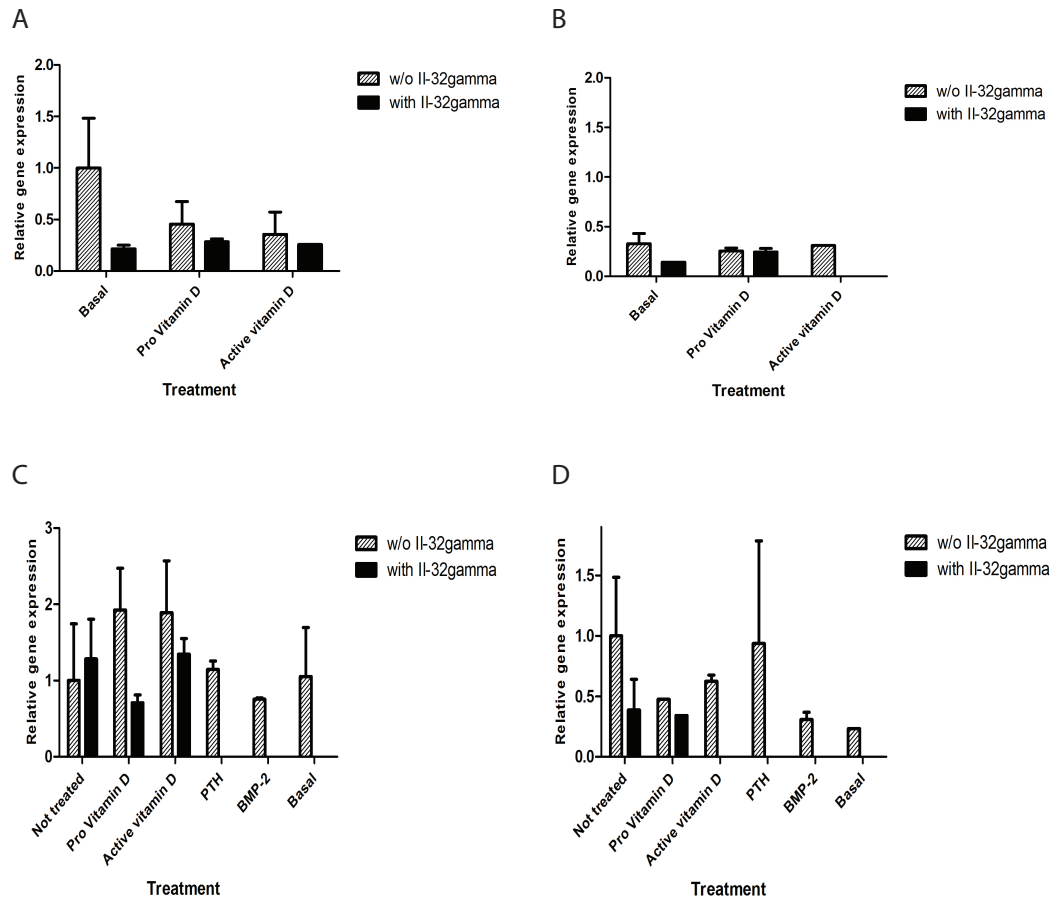

Figure 1: CYP27B1-expression after short-term stimulation with rhIL-32 and 25(OH)D_3: MSCs were seeded in 6-well plates (80 000 cells/well) and treated with 25(OH)D_3 (pro vitamin D, 10 nm) with and without IL-32 (100 ng/mL) one day after seeding or after being differentiated for 7 days into preosteoblasts. Control groups include treatment without vitamin D (designated "not treated") and 1,25$(OH)_2D_3$ treatment. Gene expression was evaluated by RT-qPCR using TaqMan primers for CYP27B1 (Hs01096154_m1, Thermo Fisher) and GAPDH (DQ oligomix 20X, Thermo Fisher). RQ was calculated using the comparative Ct-method. **A)** MSCs cultured in basal medium for 24 h with the treatment as reported above (the "not treated group is cells cultured in MSCGM only). Data is reported as mean±SD for technical replicates. **B)** MSCs cultured in basal medium for 72 h with the treatment as reported above (the "not treated group is cells cultured in MSCGM only). Data is reported as mean±SD for technical replicates. **C)** MSCs were differentiated for 7 days into preosteoblasts, before treated as reported above for 24 hours (the "not treated" group is cells cultured in diff.medium). BMP-2 (300 ng/mL) and basal (MSCGM) medium treated cells were included as controls. Data is reported as mean±SD for technical replicates. **C)** MSCs were differentiated for 7 days into preosteoblasts, before treated as reported above for 72 hours (the "not treated" group is cells cultured in diff.medium). BMP-2 (300 ng/mL) and basal (MSCGM) medium treated cells were included as controls. Data is reported as mean±SD for technical replicates.

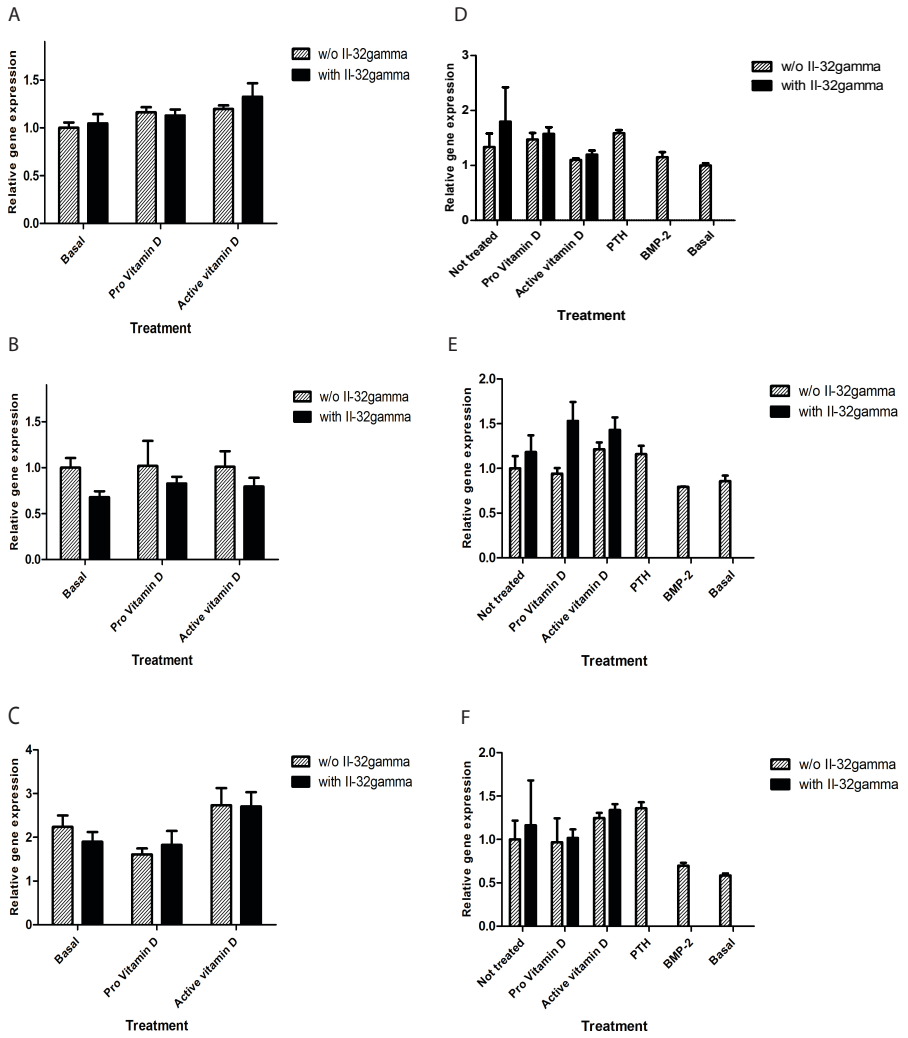

Figure 2: VDR- expression after short-term stimulation with rhIL-32 and 25(OH)D_3: MSCs were seeded in 6-well plates (80 000 cells/well) and treated with 25(OH)D_3 (pro vitamin D, 10 nM) with and without IL-32 (100 ng/mL) one day after seeding, or after being differentiated for 7 days into preosteoblasts. Control groups include treatment without vitamin D (designated "not treated") and 1,25$(OH)_2D_3$ treatment. Gene expression was evaluated by RT-qPCR using TaqMan primers for VDR (Hs00172113_m1, Thermo Fisher) and GAPDH (DQ oligomix 20X, Thermo Fisher). RQ was calculated using the comparative Ct-method. Data is reported as mean±SD for technical replicates. **A)** VDR mRNA levels in MSCs cultured in basal medium for 6 h with the treatment as reported above (the "not treated group is cells cultured in MSCGM only). **B)** VDR mRNA levels in MSCs cultured in basal medium for 24 h with the treatment as reported above (the "not treated group is cells cultured in MSCGM only). **C)** VDR mRNA levels in MSCs cultured in basal medium for 72 h with the treatment as reported above (the "not treated group is cells cultured in MSCGM only). **D)** VDR mRNA levels in MSCs were differentiated for 7 days into preosteoblasts, before treated as reported above for 6 hours (the "not treated" group is cells cultured in diff.medium). BMP-2 (300 ng/mL) and basal (MSCGM) medium treated cells were included as controls. **E)** VDR mRNA levels in MSCs were differentiated for 7 days into preosteoblasts, before treated as reported above for 24 hours (the "not treated" group is cells cultured in diff.medium). BMP-2 (300 ng/mL) and basal (MSCGM) medium treated cells were included as controls. **D)** VDR mRNA levels in MSCs were differentiated for 7 days into preosteoblasts, before treated as reported above for 24 hours (the "not treated" group is cells cultured in diff.medium). BMP-2 (300 ng/mL) and basal (MSCGM) medium treated cells were included as controls.

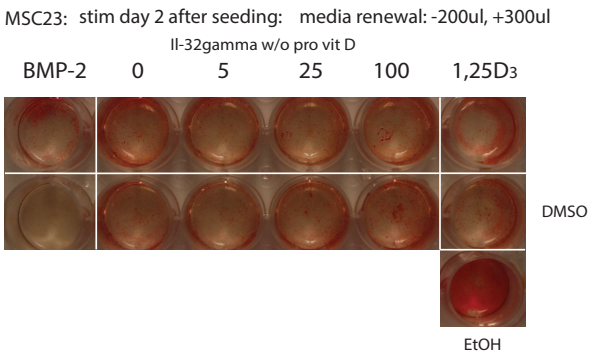

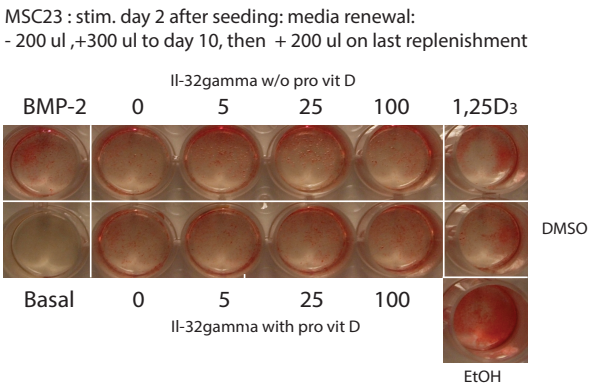

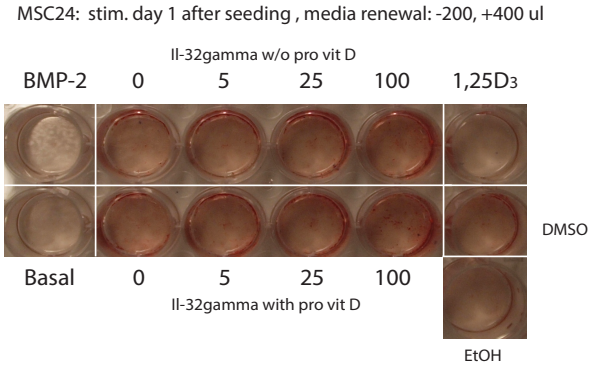

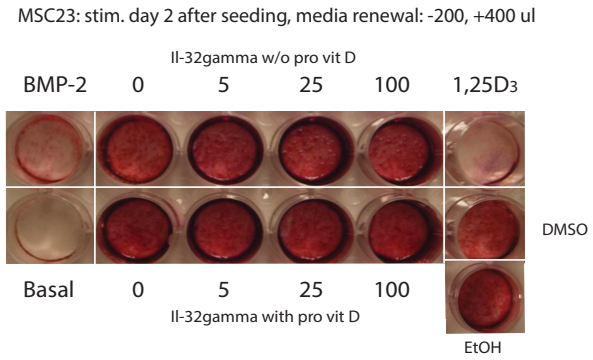

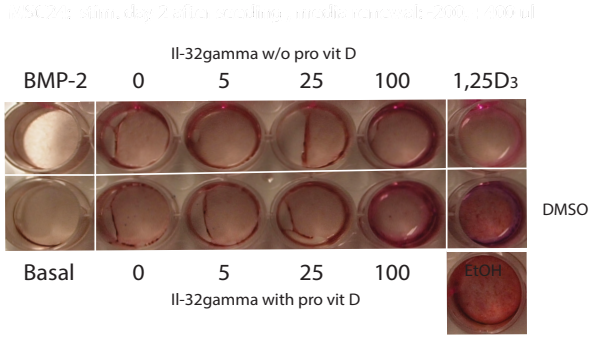

APPENDIX 6

Matrix mineralization at day 15 visualized by ARS-staining. Experiments were repeated to validate IL-32 dose dependent inhibition of mineralization in osteoblasts at day 15 (**fig. 31, Results**) in presence of pro vitamin D. In all experiments, cells were seeded in 24-well plates, 15000 cells/well. MSCs from two different donors were used (MSC23 or MSC24). Which donor used is indicated for each experiment. MSCs were stimulated with differentiation media and IL-32 either at day 1 or 2 after seeding (indicated for each plate). Also we varied the media renewal protocol, removing and adding different volumes of old and new media respectively. The volumes removed and added are indicated for each plate.

APPENDIX 7

Table shows actual reagents, manufacturer and catalogue number.

Kit/reagent	Manufacturer	Catalogue no
Cell culturing		
Dulbecco's Phosphate-Buffered Saline	Thermo Fisher Scientific Waltham, MA, USA	D8537
Fetal bovine (calf) serum	Invitrogen, Carlsbad, CA, USA	10082147
MEM-alpha medium (1X)	Life Technologies, Thermo Fisher Scientific, Waltham, MA, USA	22571-020
Gentamicin/gensumycin	SANOFI, Surrey, UK	15N0030
L-Glutamine	Sigma Aldrich, St.Louis, MO, USA	G7513
RPMI 1640	Sigma Aldrich, St.Louis, MO, USA	R8758
MSCGM	Lonza Inc, Walkerswille, MD	PT-3238
Monocyte isolation and osteoclast differentiation		
Lymphoprep™	STEMCELL Technologies, Vancouver, Canada	07861
Hanks Buffered Salt Solution	Sigma-Aldrich, St Louis, MO	H9269
autoMACS® Rinsing Solution	Milteniy Biotec GmbH, Bergisch Gladbach, Germany	130-091 -222
MACS BSA Stock Solution	Milteniy Biotec GmbH, Bergisch Gladbach, Germany	130- 091-376
RANKL	Peprotech, Rocky Hill, USA	310-01
MCS-F	Peprotech, Rocky Hill, USA	300-25
TGF- β	Peprotech, Rocky Hill, USA	100-21
Paraformaldehyde	Alfa Aesar, Thermo Fisher Scientific, Waltham, MA, USA	43368
TRAP Staining		
Leukocyte Acid Phosphatase Kit	Sigma-Aldrich, St Louis, MO, USA	387A
Osteoblast differentiation and stimulation		
Dexamethasone	Sigma Aldrich, St.Louis, MO, USA	D2915
L-ascorbic acid	Sigma Aldrich, St.Louis, MO, USA	A92902
β-glycerophosphate	Sigma Aldrich, St.Louis, MO, USA	50020
Recombinant human Il-32 γ	R&D Systems, Minneapolis, MN, USA	P24001
Recombinant human Il-32α	R&D Systems, Minneapolis, MN, USA	AAS80146
25-hydroxyvitamin D_3 monohydrate	Sigma Aldrich, St.Louis, MO, USA	17938
1,25-dihydroxyvitamin D_3	Sigma Aldrich, St.Louis, MO,USA	D1530
BMP-2	R&D Systems, Minneapolis, MN, USA	P12643
Poly (I:C)	Amersham Life Science, Little Chalfont, UK	27-4732-01
LPS-B4	InvivoGen, SanDiego, California	tlrl-eblps
ALP-assay		
ELF® 97 Endogenous	Molecular Probes™, Carlsbad, CA	E6601
Proteinase-K	Sigma Aldrich, St.Louis, MO, USA	P4850

Deoxyribonucleic Acid	Sigma Aldrich, St.Louis, MO, USA	D7290
Tween 20	Sigma Aldrich, St.Louis, MO, USA	P1379
PBS Dulbecco A tablets (10 tablets/1 L dH_2O)	Oxoid Limited, Hampshire, UK	BR0014
SYBR®green I	Molecular Probes™ Eugene, OR	S-7563
Paraformaldehyde	Alfa Aesar, Thermo Fisher Scientific Waltham, MA, USA	43368
Alizarin Red-staining		
Alizarin Red S	Sigma Aldrich, St.Louis, MO, USA	A5533
Cetylpyridinium chloride	Sigma Aldrich, St.Louis, MO, USA	C0732
NaCl 0.9 %	Braun, Melsungen, Germany	0123
RT-qPCR		
High Pure RNA Isolation Kit	Roche Diagnostics, Mannheim, Germany	11828665001
TaqMan Universal PCR Master Mix	Applied Biosystems Inc, Foster City, CA, USA	4304437
High Capacity RNA-to-cDNA kit	Applied Biosystems Inc, Foster City, CA, USA	4387406
SP7 (Osterix)	Thermo Fisher Scientific Waltham, MA, USA	Hs00541729_m1
RUNX2	Thermo Fisher Scientific Waltham, MA, USA	Hs01047973_m1
CYP27B1	Thermo Fisher Scientific Waltham, MA, USA	Hs01096154_m1
TNFS11 (RANKL)	Thermo Fisher Scientific Waltham, MA, USA	Hs00243522_m1
IL-32	Thermo Fisher Scientific Waltham, MA, USA	Hs00992441_m1
CYP24A1	Thermo Fisher Scientific Waltham, MA, USA	Hs0016799_m1
VDR	Thermo Fisher Scientific Waltham, MA, USA	Hs00172113_m1
GAPDH DQ Oligomix (20X)	Thermo Fisher Scientific Waltham, MA, USA	4332649
TBP	Thermo Fisher Scientific Waltham, MA, USA	333769F
Cell Titer Glo- assay		
Cell Titer Glo	Promega, Madison, Wisconsin, USA	G7573
Il-32 gene knockout		
IL-32 CRISPR/Cas9 KO Plasmid (h)	Santa Cruz Biotechnology, Inc, Dallas, TX, USA	sc-406489
Amaxa® Cell Line Nucleofector® Kit R	Lonza Inc, Walkerswille, Maryland, USA	VCA-1001
ELISA		
1,25-dihydroxy VitaminD EIA	Immunodiagnostic Systems, Boldons, UK	32010
Western Blot		
Bradford Reagent	Sigma Aldrich, St.Louis, MO, USA	B6916
Albumin Standard (BSA)	Thermo Fisher Scientific Waltham, MA, USA	23209

NuPAGE® LDS Sample Buffer (4X)	Invitrogen, Carlsbad, CA, USA	NP0007
NuPAGE™ 10mm×10well 4-4-12% Bis-Tris Gel	Invitrogen, Carlsbad, CA, USA Invitrogen, Carlsbad, CA, USA	BN2111BX10
1 M DTT solution	PanReach AppliChem, Darmstadt, Germany	A3668-0050
Nonidet P40 (NP40)	ThermoFisher Scientific, Waltham, MA, USA	FNN0021
Sodium orthovanadate ($Na_3VO_{4)}$	Sigma Aldrich, St.Louis, MO, USA	450243
HCl-Tris	Sigma Aldrich, St.Louis, MO, USA	T5941
Mini, EDTA-free Protease Inhibitor Cocktail	Sigma Aldrich, St.Louis, MO, USA	11836170001
SeeBlue® Plus2 Pre-stained Protein Standard	Invitrogen, Carlsbad, CA, USA	LC5925
MagicMark™ XP Western Protein Standard	Invitrogen, Carlsbad, CA, USA	LC5602
Goat Polyclonal Human IL-32 α Antibody	R&D Systems, Minneapolis, MN, USA	AF3040
Polyclonal Rabbit Anti-goat Immunoglobulins /HRP)	Daco, Glostrup, Denmark	P0449
iBlot® 2NC Mini Stacks	Invitrogen, Carlsbad, CA, USA	IB23002
Mouse monoclonal GAPDH antibody	Abcam, Cambridge, UK	ab8245
Polyclonal goat anti-mouse antibody/HRP	ThermoFisher Scientific, Waltham, MA, USA	31430
Super Signal® West Femto	ThermoFisher Scientific, Waltham, MA, USA	34095

References Appendices

1 Lymphoprep™ Isolation of human mononuclear cells; Axis Shield. http://www.axis-shield-density-gradient-media.com/Leaflet Lymphoprep.pdf.

2 de Almeida, M. C., Silva, A. C., Barral, A. & Barral Netto, M. A simple method for human peripheral blood monocyte isolation. *Memorias do Instituto Oswaldo Cruz* **95**, 221-223 (2000).

3 Jersmann, H. P. Time to abandon dogma: CD14 is expressed by non-myeloid lineage cells. *Immunology and cell biology* **83**, 462-467, doi:10.1111/j.1440-1711.2005.01370.x (2005).

4 MACS Technology Microbeads, Miltenyi Biotec. http://www.miltenyibiotec.com/en/products-and-services/macs-cell-separation/macs-technology/microbeads_dp.aspx.

5 Jiang, F. & Doudna, J. A. The structural biology of CRISPR-Cas systems. *Current opinion in structural biology* **30**, 100-111, doi:10.1016/j.sbi.2015.02.002 (2015).

6 Sternberg, S. H. & Doudna, J. A. Expanding the Biologist's Toolkit with CRISPR-Cas9. *Molecular cell* **58**, 568-574, doi:10.1016/j.molcel.2015.02.032 (2015).

7 Ran, F. A. *et al.* Genome engineering using the CRISPR-Cas9 system. *Nature protocols* **8**, 2281-2308, doi:10.1038/nprot.2013.143 (2013).

8 CRISPR Systems, Santa Cruz Biotechnology. https://www3.scbt.com/scbt/whats-new/crispr-systems.

9 Vanhatupa, S., Ojansivu, M., Autio, R., Juntunen, M. & Miettinen, S. Bone Morphogenetic Protein-2 Induces Donor-Dependent Osteogenic and Adipogenic Differentiation in Human Adipose Stem Cells. *Stem Cells Transl Med* **4**, 1391-1402, doi:10.5966/sctm.2015-0042 (2015).

10 Guide to Performing Relative Quantitation of Gene Expression Using Real-Time Quantitative PCR, 2008; Applied Biosystems. http://www3.appliedbiosystems.com/cms/groups/mcb_support/documents/generaldocuments/cms_042380.pdf.